Behavior of Laterally Loaded Shafts Constructed Behind the Face of a Mechanically Stabilized Earth Block Wall

BY

Matthew Pierson

Submitted to the graduate degree program in Civil Engineering and Graduate Faculty of the University of Kansas in partial fulfillment of the requirements for the degree of Master of Science

_____
Chairperson

Committee Members _____

_____

Date defended: _____

The Thesis Committee for Matthew Pierson Certifies that
this is the approved Version of the following thesis:

Behavior of Laterally Loaded Shafts Constructed Behind the Face of a Mechanically Stabilized Earth Block Wall

_____
Chairperson

Committee Members _____

_____

Date approved: _____

List of Figures:

List of Figures (cont.):

List of Figures (cont.):

List of Tables:

Acknowledgements:

I would like to extend a special thanks to all people that play an important role in not only my studies and this thesis, but also in my life. This must begin with my advisor Dr. Robert Parsons who, by allowing me to work on this project, has given me one of the greatest opportunities of my life. I must thank Dr. Jie Han, who has also served as a great resource for my studies, activities, and research. The University of Kansas, for the outstanding support that they have provided for my education and research.

The Kansas Department of Transportation deserves special thanks, without them none of this would have been possible. James Brennan, whose diligence in maintaining a high level of expectation was invaluable. Peter Wiehe along with the entire KDOT maintenance crew proved to be exceptional craftsmen, as well as very committed employees.

I would like to thank Tensar International for the commitment of expertise, materials, and man hours. I would like to especially thank Christina Vulova, Andy Anderson, and Joe Kerrigan who I had personal contact with and proved to be true professionals.

Dr. Dan Brown, and Robert Thompson from Dan Brown and Associates, as well all of the people from Applied Foundation Testing deserve many thanks. They were integral in planning, load testing, and analysis of the test shafts.

I owe my parents, Jay and Gayle Pierson the greatest praise and thanks. They have given me the tools to be successful and the support to use them. My wife to be Toni Bishop, whose guidance, understanding, and passion are just a few of the things for which I am thankful.

Abstract:

Current practice for designing laterally loaded columns that pass through an MSE Wall involves isolating the column from the MSE mass and anchoring the column into rock with a rock socket. A sizeable cost and time savings could be realized, while still maintaining reliability, if a method were available to evaluate the lateral load capacity of a column that is supported by the MSE mass with no rock socket.

This report describes the construction, instrumentation, and testing of eight different 36" diameter columns solely supported by an MSE mass as well as a brief discussion of the results and recommendations for future testing and analysis. Instrumentation includes 24 pressure cells, 16 inclinometer locations, 112 strain gages, 20 tell tales, 84 photo measurements of the wall facing, and load cells and LVDTs associated with lateral load and response.

Chapter One

Introduction

Mechanically stabilized earth (MSE) walls are an inexpensive and aesthetically attractive means of retaining soil. While the design principles for MSE structures have been accepted for several decades, space restrictions at MSE wall sites have led to new demands on MSE wall structures for which there are no well developed design procedures. The specific area of research addressed in this thesis is to develop estimates of the capacity of MSE structures to resist additional lateral loads applied to the MSE structure by concrete columns, commonly referred to as drilled shafts, constructed within the MSE mass. Developing an effective understanding of the lateral load capacity of the wall and shafts will be of significant value for designing structures with significant lateral loads that must be constructed on top of MSE structures, such as sound walls. Current design procedures are by necessity based on very conservative design assumptions due to the lack of test data. The research described in this thesis addresses this lack of data through full scale testing of drilled shafts constructed within a laterally loaded MSE wall backfill.

Mechanically stabilized earth structures have been constructed since ancient times, but only relatively recently, with the advent of many synthetic materials, has this technology gained wide spread use as an alternative to traditional concrete retaining walls. These MSE walls typically use a high-density polyethylene or steel reinforcement material with patterns of various types to transfer the load of the soil from the active zone behind the wall face to much more stable material further from the wall. The result is a

stable, reinforced soil mass that typically has a masonry block, panel or welded wire and fabric facing to prevent raveling or erosion of soil at the face and to enhance the aesthetic value of the wall.

MSE walls must be designed with appropriate resistance factors or factors of safety for all the failure mechanisms of conventional retaining walls. In addition, MSE walls must be designed for modes of failure unique to MSE walls. Failure of an MSE wall can occur several ways: sliding of layers, pullout of the reinforcement, elongation or breakage of the reinforcement, and bulging of the facing. The entire mass must be check for external stability. As with conventional walls, sliding, overturning, bearing capacity, and deep seated stability, must be checked. Settlement issues are less of a problem with an MSE wall then with a traditional concrete retaining wall, but must still be within a reasonable limit.

Construction of a block MSE wall can be done with personnel with less skill than a conventional wall due to the type of construction. Items requiring special care include making sure each block is level, and aligned with the next block before the next course of blocks can be placed on top. The geogrid must be placed into tension in order to prevent excessive wall movement to mobilize strength in the geogrid. .

A 20 foot tall, 140 foot long MSE block wall was built using the Mesa system developed by Tensar International. The wall supports eight 36 inch diameter vertical shafts four different distances from the back of the facing to the center of the shaft. These shafts were then loaded toward the wall facing using a displacement control method. During this test, load and shaft deflection and inclination were monitored as

well as pressure behind the wall facing, strain in the geogrid layers, and wall facing deflection.

The rest of this document will describe previous work, and design procedures for MSE walls. It will also discuss construction and instrumentation of the project leading up to testing. The testing method and procedure as well as the results will be discussed in one section. Conclusions from this work related to design and recommendations for future testing will also be addressed.

Chapter 2

Literature Review

Currently there is little published guidance for designing laterally loaded shafts supported within an MSE Wall. However there are complete design procedures for each item individually. These will be reviewed, as well as two other research projects that study the combined uses of MSE Walls to support bridge abutments.

2.1 MSE Wall Design (FHWA)

An MSE wall uses inclusions that are placed within a soil mass to help distribute tensile loads and prevent slope failure. One type of MSE structure not discussed here, Reinforced Soil Slopes (RSS), incorporate planar reinforcing elements in constructed earth-sloped structures with face inclinations of less then 70 degrees (FHWA, 1996). MSE Walls use the same planar reinforcing and typically require a facing to retain the soil within the structure. "Some common facings include precast concrete panels, dry cast modular blocks, metal sheets and plates, gabions, welded wire mesh, shotcrete, wood lagging and panels, and wrapped sheets of geosynthetics" (FHWA, 1996). Most MSE systems use either a galvanized or epoxy coated steel reinforcement, or synthetic reinforcement like high density polyethylene (HDPE), polypropylene, or polyester yarn. The wall system used for this project is called The Mesa System developed by Tensar International (See Figure 2.1). It utilizes dry cast modular blocks and HDPE reinforcement.

According to FHWA (FHWA, 1996) branches and other different types of reinforcement have been used for at least 1000 years. Beginning in the early 1960's reinforced soils began to be used in engineering by the French architect and engineer

Henri Vidal who developed Reinforced Earth™. In 1972 the first wall to use this technology was built in California.

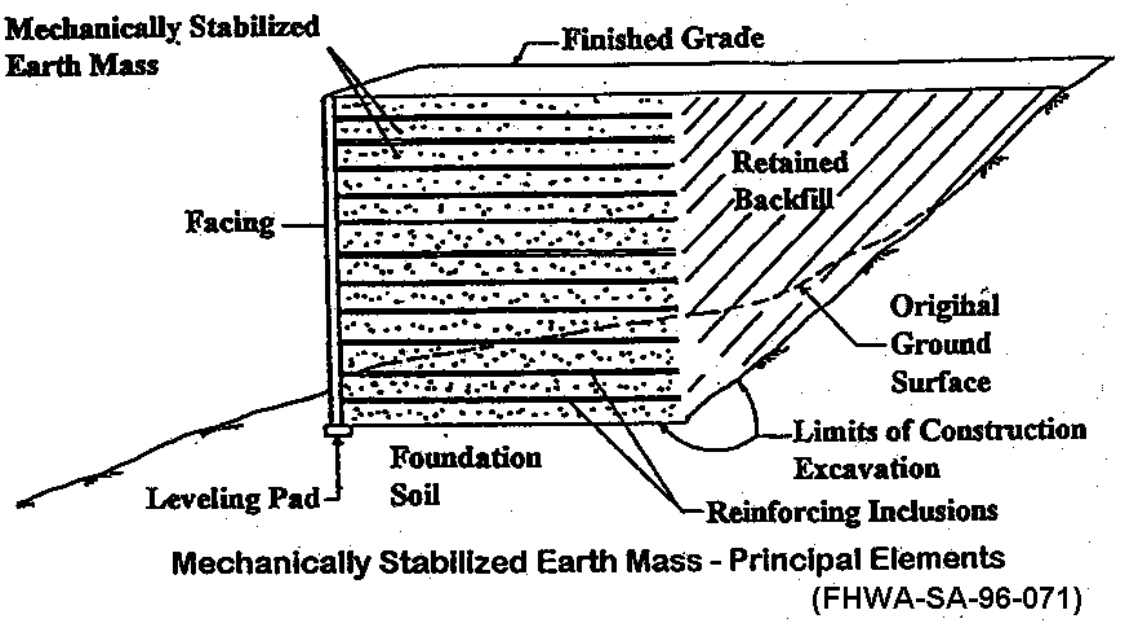

Figure 2.1 Cutaway of typical MSE wall

Some of the advantages of the MSE structure over a conventional concrete gravity retaining wall system reported by FHWA include:

- Simple and rapid construction procedures and do not require large construction equipment.
- Do not require experienced craftsmen with special skills for construction.
- Require less site preparation then other alternatives.
- Need less space in front of the structure for construction operations.
- Do not need rigid, unyielding foundation support because MSE structures are tolerant to deformations.
- Cost effectiveness.
- Are technically feasible to heights in excess of 25 meters.

When designing an MSE Wall structure there are several different failure modes that must be checked. Design should consist of checking these modes of failure using one or more of the following; working stress analysis, limit equilibrium analysis, and deformation evaluations (FHWA). The first potential mode of failure is external stability. This involves treating the entire reinforced mass as an internally stable block and checking conventional failure modes for gravity wall systems. Possible failure mechanisms include, sliding, overturning, bearing capacity, and deep seated stability. Internal stability pertains to the reinforced soil mass. The reinforcement has two failure types, elongation or breakage and reinforcement pullout. Bulging is a possibility consisting of failure of the facing material. This could be a problem if the reinforcement locations are not spaced close enough to prevent the lateral movement of individual blocks. The step by step internal design process is as follows: (FHWA, 97)

- Select a reinforcement type
- Select the location of the critical failure surface.
- Select a reinforcement spacing compatible with the facing connections and to prevent bulging.
- Calculate the maximum tensile force at each reinforcement level, static and dynamic.
- Calculate the maximum tensile force at the connection to the facing.
- Calculate the pullout capacity at each reinforcement level.

Some additional issues may need to be addressed in design depending on the situation. Traffic barriers are designed to take impact forces. Drainage should be considered as well as the corrosion resistance of metal reinforcement. Utilities may need

to pass through the reinforced soil mass. Differential settlement with cast in place structures must be considered. Surcharges as a result of road construction can increase demand placed on the reinforcement. Rapid drawdown conditions may need to be considered if tide or river fluctuations are possible. Obstructions in the reinforced soil zone, such as drainage inlets, must be considered also.

2.2 Design of Laterally Loaded Shafts

When horizontal loads are being designed for drilled shafts the most common method for analysis is the P-Y curve method. "This involves modeling the soil-structure interaction as a nonlinear beam on elastic foundation. The model assumes that the soil is continuous, isotropic, and elastic medium. The drilled shaft is divided into equally spaced sections and the soil response is modeled by a series of closely spaced discrete springs called Winkler's springs" (Johnson, 2006). This model allows for the slope, moment, shear, soil reaction, and deflection to be found for all sections along the drilled shaft. The initial curves were found by doing full scale lateral load tests. The initial tests were performed in soft and stiff clay, sand, loess, and limestone. These lateral load tests are the most accurate, but also the most expensive way to find the soil structure P-Y response. There are programs that are available (LPILE) to predict P-Y curves based on shaft geometry and soil conditions. Using engineering judgment it is possible to take the site materials and use computer programs to generate predicted P-Y curves without doing expensive lateral load testing. However, there are currently no programs that will account for shafts supported by an MSE wall. One assumption made in each program is that soil is modeled as a homogeneous half space. For the MSE wall the soil is

homogeneous but has discrete strips of reinforcement with different properties within it, and the mass is not a half space, it is a wall or slightly larger than a quarter space.

2.3 Topics related to MSE Wall interaction with Bridges

> "There are two types of MSE abutments, true and mixed. In a true MSE abutment the bridge load is placed directly on the MSE structure (See Figure 2.2). To prevent overstressing the soil of a true abutment, the beam seat is sized so the centerline of the bearing is at least 3 feet behind the MSE wall face and the bearing pressure on the reinforced soil is no more then four kips per square foot…A mixed abutment has piles or shafts supporting the bridge seat (See Figure 2.3), with the MSE walls retaining the fill beneath and adjacent to the end of the bridge. In some cases a portion of the lateral load on the pile-supported seat is transmitted to the MSE fill. This load can be resisted by MSE reinforcements in the wall or by reinforcements extending from the back wall of the seat." (Anderson, 2005)

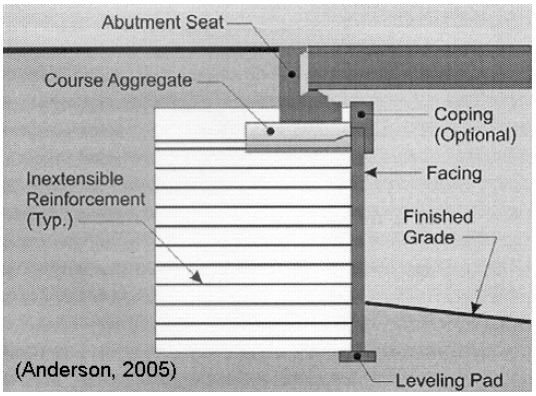

Figure 2.2 True MSE abutment

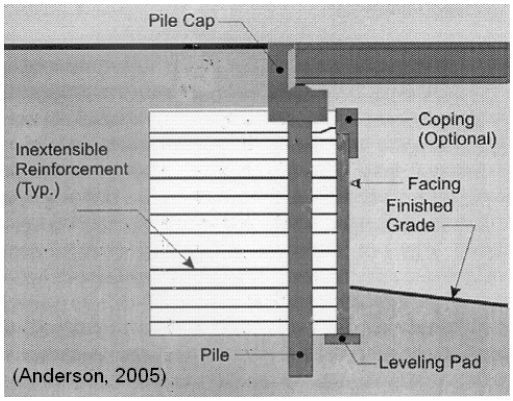

Figure 2.3 Mixed MSE abutment

For FHWA funded projects the design should follow FHWA details on the use of integral abutments. There is no provision in the FHWA manual for shafts that are laterally supported solely within an MSE Wall.

Constructability tests were performed on pile driving through HDPE geogrid reinforced soil fill by Tensar International. A section of E-470 in Colorado contained several mixed abutment type bridges. It was found that driving piles as close as four feet from the facing caused no negative performance of the MSE structure. In addition to the pile driving investigation one of the shafts was pushed over with a D9 bulldozer. It was found that with three inches of pile movement only ¼" of facing movement occurred.

Clearly there are many areas of research that can be explored. The rest of this document will describe the construction and testing of lateral load tests on shafts constructed within an MSE fill in close proximity to the facing.

Chapter 3

Scope of Research

This chapter contains a description of the testing and initial analysis conducted in association with this research. It includes a detailed discussion of the site investigation, design, construction, instrumentation, and testing of the laterally loaded MSE test wall. An accurate understanding of the load-deflection behavior is important for designing any deep foundation for lateral loads. This behavior was monitored for eight shafts within an MSE fill by conducting a series of full scale load tests. Also monitored during this time was strain in four reinforcement layers, deformations within the fill using tell tales, pressure at the face of the wall directly in front of each shaft at three elevations, and the deflection of the facing at 82 points as a result of each loading step.

3.1 Site Investigation

The site inside the southwest clover of the I-435/Leavenworth road interchange in Kansas (Figure 3.1.1) was chosen for its access to a good limestone footing to found the wall and the reaction shafts. All site investigation was performed by KDOT. Borings, sampling, and in-situ testing were conducted. This was done to define the strata present at the site in both elevation, and physical and mechanical properties, such as unconfined compressive strength of the rock, or grain size distribution of the soil. The proposed MSE wall and subsurface profile are shown in Figure 3.1.2. A typical boring log can be found in the Appendix.

A)

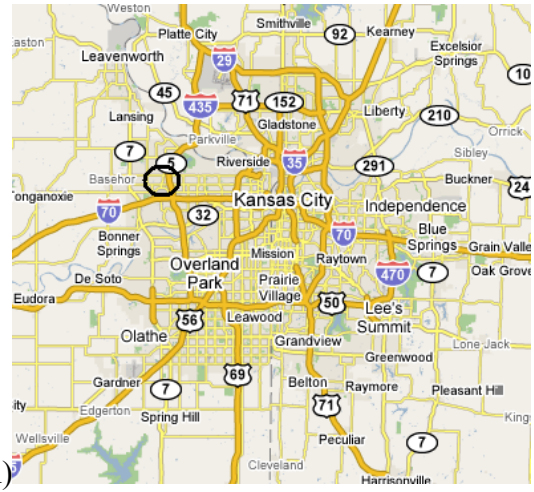

B)

C)

Figure 3.1.1 A) Regional map, B) Local map, C) Site map

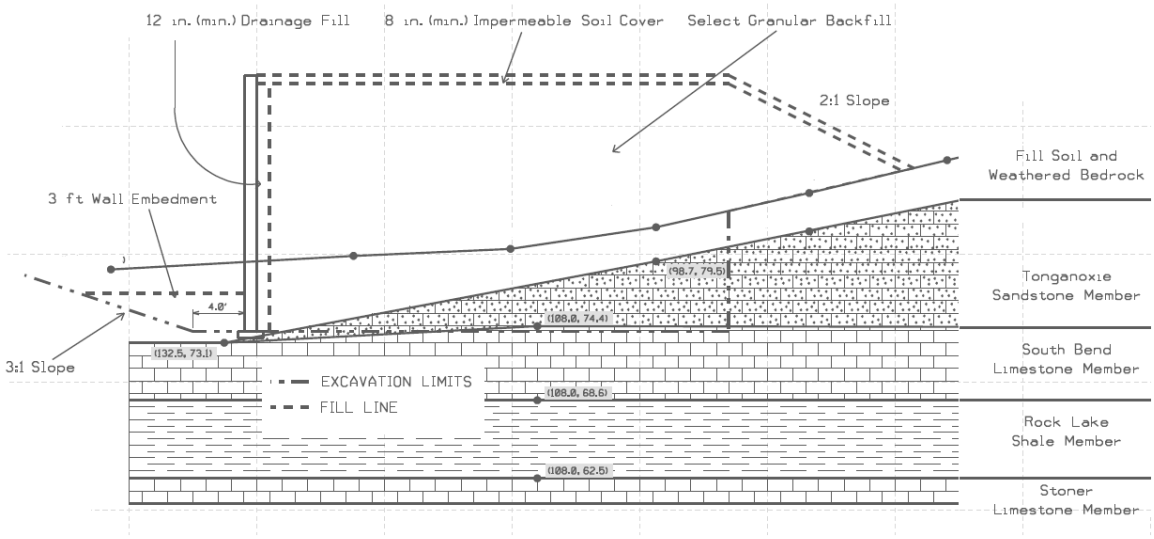

Figure 3.1.2 Proposed cross section of MSE wall and subsurface (KDOT, 2007)

3.2 Construction

A mechanically stabilized earth wall 140ft x 20ft was constructed using blocks and geogrid provided by Tensar International. Eight test shafts 36" in diameter were constructed at distances of one, two, three, and four diameters from the back of the wall. One shaft was embedded 15 feet in the reinforced fill, all others were 20 feet. Three identical shafts two diameters from the wall were tested as a group to determine if a group effect was significant. The test shaft spacing was 15', and the shaft layout is shown in Figure 3.2.1. A reference section of wall without any shafts was also constructed (see fig. 3.2.1). Six reaction shafts were rock socketed into limestone six feet and 27' behind the facing for use in loading the test shafts. The group reacted against two 48" diameter shafts. Each remaining shaft had its own 36" diameter reaction shaft except for D. Loading of D was accomplished by spanning the reaction shafts used to test A and B (see fig 3.2.1).

Tensar International, Inc. provided materials and technology from the Mesa Retaining Wall System. This consisted of design, advising, Mesa units, welded wire baskets, UX1400 and UX1500 geogrid, and connectors. Using a KDOT aggregate

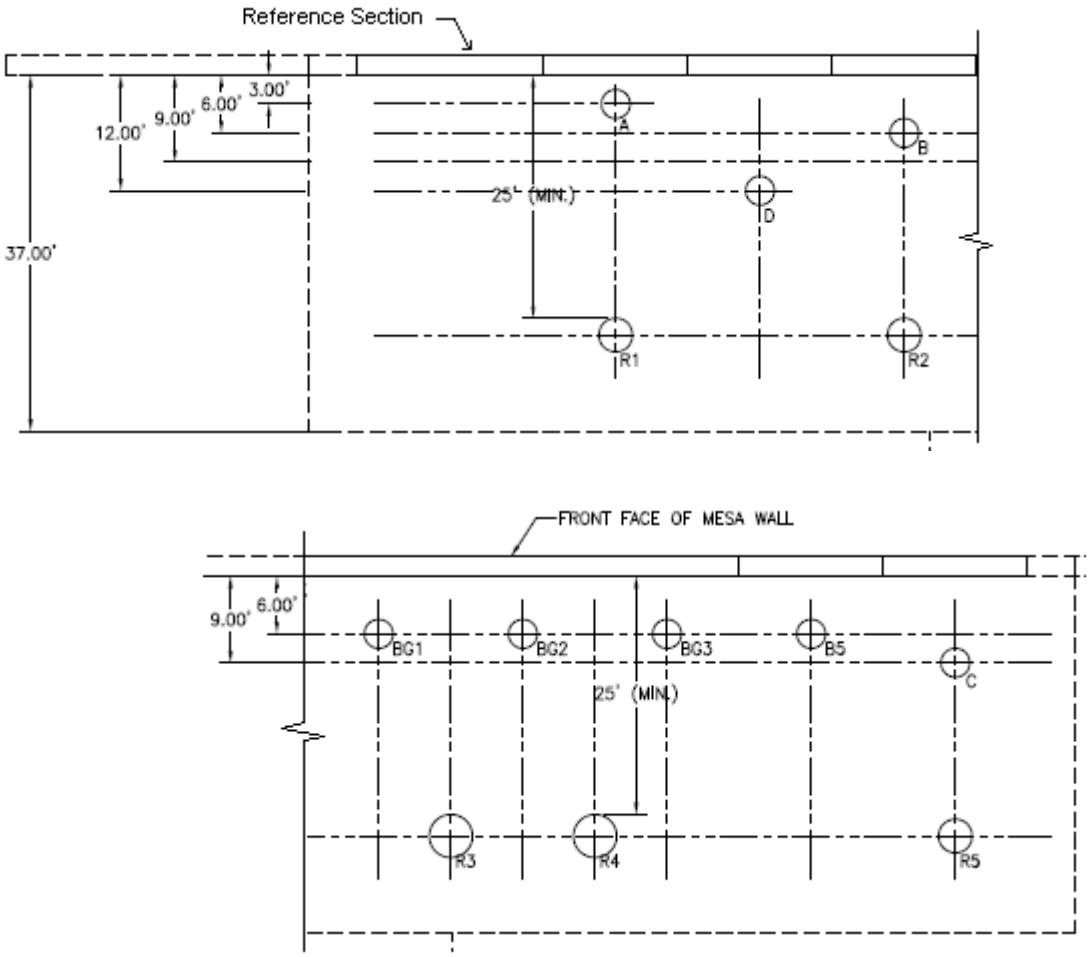

Figure 3.2.1 Plan view of MSE test wall and shafts (Tensar, 2007)

specification for clean aggregate backfill (CA-5), it was decided to use a two foot spacing (three blocks) for geogrid courses, and a geogrid length of 14' (0.7 x H, H= height of MSE Wall) from the facing. The UX1500 was used for the bottom four layers and UX1400 was used for the top six. Wing walls with a welded wire basket design were constructed at each end of the test wall. For the wing walls UX1400 was used at a 1.5' spacing for the first four layers, and a three foot spacing for the top five layers of

reinforcement (see fig. 3.2.2). Vertical slip joints were designed into the wall to minimize interaction of separate test shafts. These were located symmetrically on either side of each test section at 7.5' distance from the centerline of the shaft.

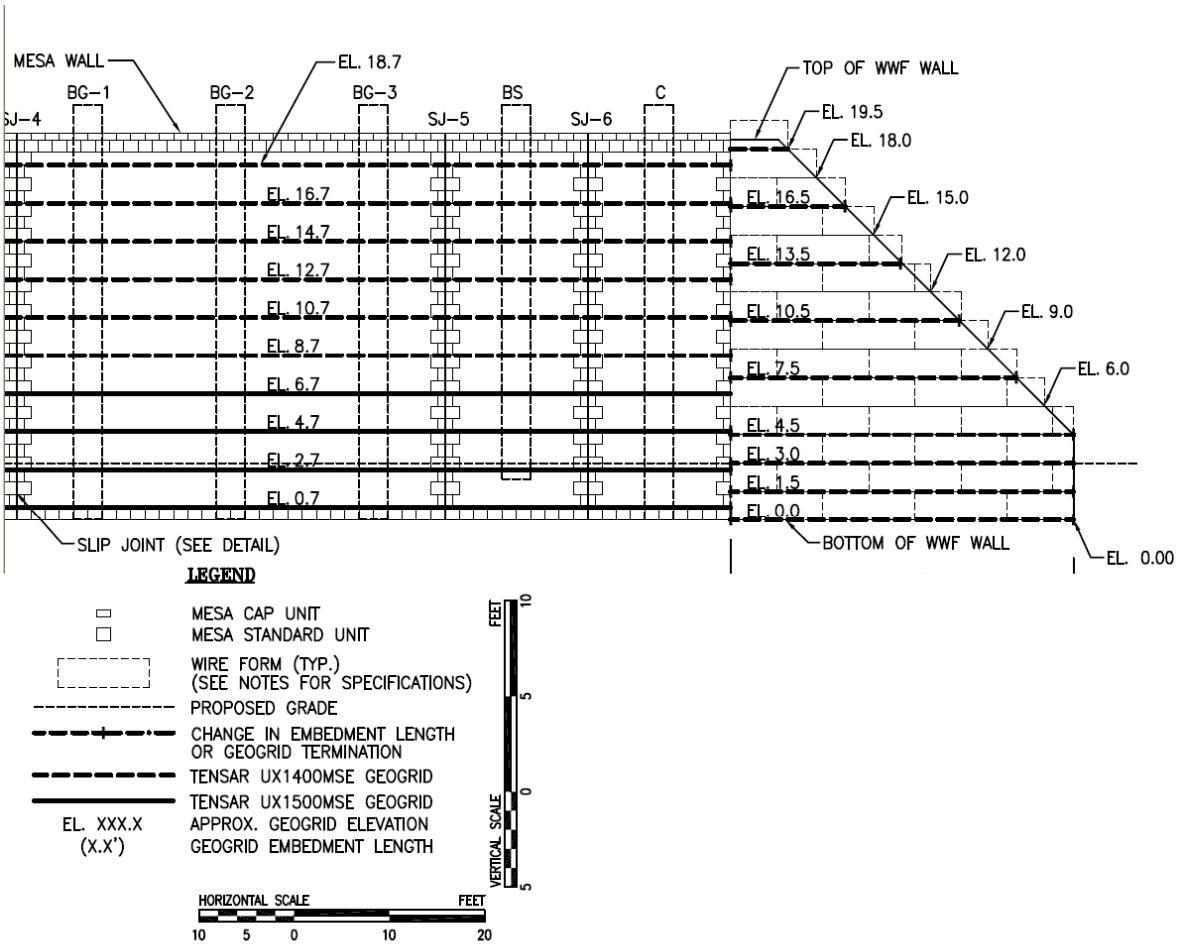

Figure 3.2.2 Wall facing layout (Tensar, 2007)

The site was excavated to limestone to provide a strong foundation for the walls and shafts. At the same time the steel reinforcement cages were tied for each shaft. (Figure 3.2.3) Each cage was composed of 12 # 11 bars evenly spaced around the radius, and #5 hoops spaced at one half foot for the top three feet, and one foot for the rest. The hoop diameter for all 36" shafts was 30" and the hoop diameter for the 48"

reaction shafts was 42”. Each cage length was such that steel reinforcement ran from the very bottom of each shaft up to 2.8’ above the top of the wall. Shaft spacers were snapped onto the cage to center the cage with three inches of concrete cover. Rock sockets were

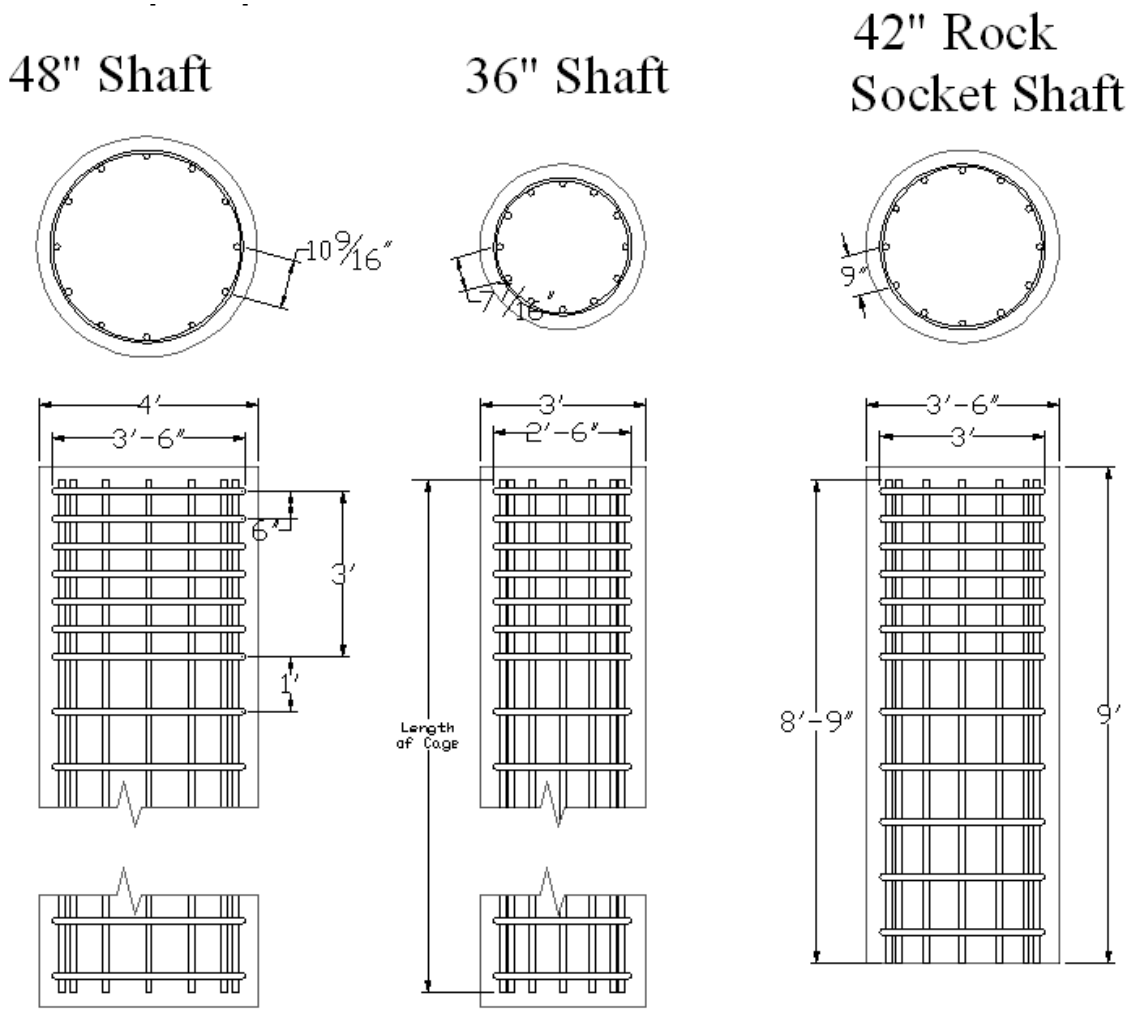

Figure 3.2.3 Typical steel configuration

drilled to a depth of six feet. The 36” diameter reaction shafts had a socket diameter of 36”, and the 48” diameter reaction shafts were drilled to a diameter of 52”. Difficulty of

extracting the rock from two holes lead to some over drilling with the deepest going one foot over for a total depth of 7'. This resulted in adding some steel reinforcement to the top of the shafts in order to maintain proper reinforcement.

Concrete for the drilled shafts was specified by KDOT to have a 9" slump and that it was to be used for drilled shafts. The ready mix plant had an existing mix design that was used. The results for slump and average compressive strength were 8 ½" and 6500psi respectively. For complete results see the Appendix.

Corrugated metal pipe (CMP) was used as a concrete form for the section of the shafts contained within the crushed stone fill. The first sections were set using the hoist truck, and legs were welded to the bottom of the CMP to maintain alignment. Next the reinforcement cages were lowered into place, and plumbed using the hoist truck. Concrete was then poured into the reaction shafts rock sockets and the first few feet of the CMP. The hoist truck was left in place overnight to allow time for the concrete to setup and hold the cages plumb.

Construction of a concrete leveling pad was required to serve as a base for the Mesa block wall. This was two feet in width and had a minimum thickness of four inches and a maximum thickness determined by the change in elevation of the limestone base across the leveling pad. Number five bars were doweled into the limestone on either side of the foundation to support the formwork. Concrete was placed and finished, and the forms were left in place.

The CMP forms for the test shafts were set using the hoist truck and welded in place to vertical dowels anchored in limestone. The CMP was positioned, plumbed and then welded to the dowels for support for the first few feet of fill. As wall height

increased the upper section of CMP was added. This was done by first placing the CMP with the hoist truck, and plumbing. The two CMP's were then welded together, and a band clamp was then tightened around the joint for added strength. The final height of the CMP was cut off at 20' of elevation. (Figure 3.2.4)

Figure 3.2.4 Extension of CMP concrete form

Crushed stone was brought up around the base of each shaft to the elevation of the top of the leveling pad. Crushed stone was placed by dumping directly out of the haul trucks, and spread using either of two large wheeled loaders, or either of two skid loaders. After a level surface was achieved, compaction was performed using a combination steel wheel/pneumatic tire roller where possible, and a walk behind tamper in front of the shafts up to one foot from the blocks. (Figure 3.2.5) Each lift was about eight inches compacted, and density measurements were performed along the wall during construction.

Blocks were placed one course at a time and aligned. Each block was checked for level, and if necessary leveled using thin strips of HDPE cut from the grid. If the thickness of the HDPE was not sufficient then asphalt shingle pieces were used to level the blocks. Each block had either two standard connectors or one DOT connector. The DOT connectors were used to secure each layer of geogrid. All connectors also served as

Figure 3.2.5 Backfilling operation

a centering device for subsequent block courses. Each end of the wall was treated with corner blocks that use no connectors.

Geogrid was placed every two feet of elevation starting at 0.7' of elevation above the leveling pad. The grid was attached by first placing the grid over the appropriate

block. The DOT connector was inserted through the grid and into the block with light hammer blows. The grid was tensioned using pitch forks prior to completely driving.

Each subsequent course of blocks was then added aligned and leveled. Back filling over geogrid was done by using a pitch fork to tension the grid and placing a small amount of crushed stone over the end of the grid to hold it in tension. Additional fill was then placed on tensioned grid. Crushed stone was spread while moving away from the facing to ensure tension in the grid. Finally, compaction was carried out using the same technique as the rest of the fill.

Slip joints were installed between each shaft to limit movement into neighboring shafts. They were constructed by putting an end or corner treatment to the blocks. This meant cutting every other block in the vertical direction and adding nonwoven geo-textile matte to the middle of the slip joint.

In front of the wall 3.3' of fill was placed to and lightly compacted. This fill was soil from on site and consisted of broken up pieces of loosely cemented silty sand stone, as well as top soil.

The top of the wall was capped with smaller architectural blocks. Crushed stone fill was brought up to no greater then elevation 19.2' and the final height of 20' was achieved using a low permeability soil cover. Each shaft was capped with a roughly cubical block of concrete. These blocks were formed to be one inch wider then the shaft each would cap. Concrete was added to each shaft to reach the final elevation 23' above the leveling pad.

3.3 Instrumentation

Tensar and KU attached many strain gauges to the geogrid in 5 locations (Table 3.3.1), and 4 different courses of grid. Pairs of strain gauges were located on the top and on the bottom of the geogrid, at up to six different distances from the wall facing. For protection the wires were run away from the grid locations in small flexible tubing toward each slip joint. From the slip joint the wires were encased in PVC pipe, and run from the slip joint to the data logger.

Table 3.3.1 Geogrid Instrumentation

	Instrumented Geogrid Layers at Shafts A, B, BG-1, BG-2		Instrumented Geogrid Layers at CONTROL Section				Distance between Gage Location and Back of Wall Facing	
Layer Elevation	El. 6.7	El. 14.7	El. 2.7	El. 6.7	El. 10.7	El. 14.7	(in)	(ft)
Strain Gage Location								
	Aperture 1	Aperture 1	Aperture 1	Aperture 1	Aperture 1	Aperture 1	7	0.6
	CMD Bar 2	CMD Bar 2	CMD Bar 2	CMD Bar 2	CMD Bar 2	CMD Bar 2	16	1.3
	Aperture 3		Aperture 3	Aperture 3			45	3.8
	CMD Bar 4		CMD Bar 4	CMD Bar 4			52	4.3
			Aperture 4		Aperture 4	Aperture 4	61	5.1
			Aperture 5	Aperture 5	Aperture 5		79	6.6
		Aperture 6			Aperture 6	Aperture 6	97	8.1
		CMD Bar 7			CMD Bar 7	CMD Bar 7	106	8.8
				Aperture 7			115	9.6
						Aperture 9	151	12.6
Strain Gages Per Layer	8	8	12	12	12	12		

Earth pressure cells (EPC) were also located on the back of the wall, directly in front of each shaft at 7.7, 13.7, and 17.7' elevation. These EPC wires were also run through the slip joints but did not require protection, and so were run directly to the data logger. All but three cells were recessed in a concrete backer block to provide a solid

surface for the back of each cell. Each cell had a sand bag in front to protect the surface from damage due to rocks. The bag was made of non-woven geotextile, folded in half and stapled. The goal was to have one inch of sand in front of the pressure cell to distribute load to the pressure cell plate more evenly. This was achieved by placing the empty bag in front the cell, and placing crushed stone next to the bag. (Figure 3.3.1) The bags were filled with a small amount of sand, and compacted to reach the one inch thickness. This process was repeated until each block was covered with crushed stone.

Figure 3.3.1 Right: Covered earth pressure cell Center: Pressure cell and protective sand bag

Wall facing was monitored with photogrammetry. The facing of 84 blocks had a target attached. Each target has a black center that is six inches long, with white on either end to help distinguish the target. Target layout was based on the centerline of each shaft, and also a horizontal line at 17.7' elevation (Figure 3.3.2). A tripod was fixed with a 10 megapixel digital single lens reflex (SLR) camera to capture the images of the wall

facing targets, and several tell-tales. These images were then rastered into AutoCAD. Using each target's six inch scale, lines were drawn to establish the scale of each target within AutoCAD. From the beginning to the end of the test each picture was rastered and the movement from the beginning of the test to the current picture was measured (Figure 3.3.3). This data was then used to show the amount of movement at the wall facing throughout the test.

Figure 3.3.2 Photo target locations (Highlighted in Red)

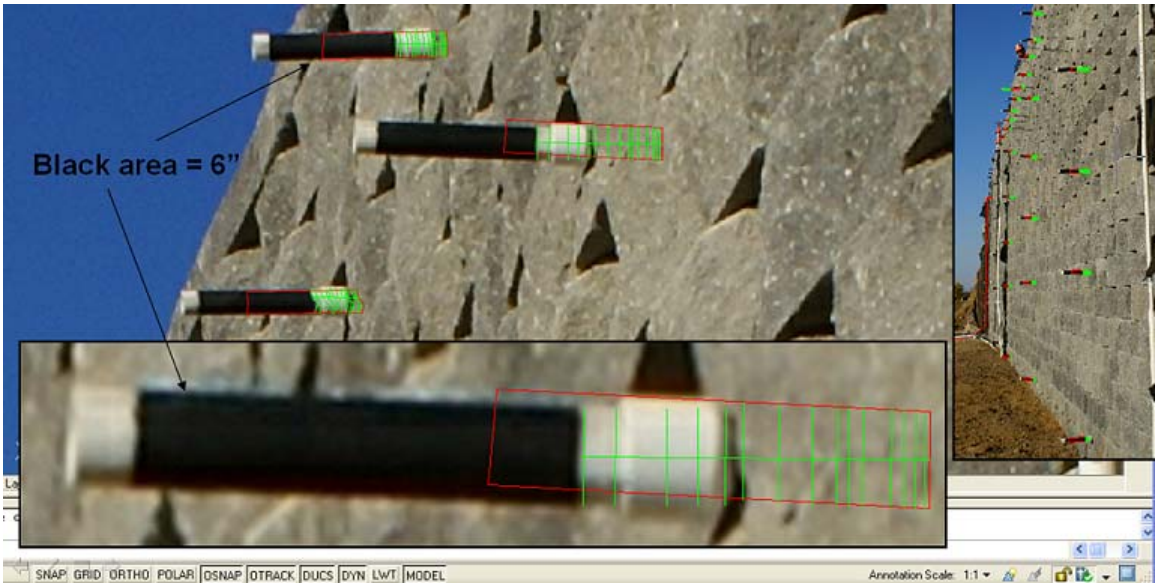

Figure 3.3.3 Screen shots taken from AutoCadd during analysis

Tell-tales were installed at various locations and attached to the geogrid. Others were placed directly in the fill, and both sets protruded through the face. These were monitored with the same technique as the wall targets.

A data logger provided by Applied Foundation Testing was used to monitor hydraulic pressure, load cells, and LVDT's. The pressure was monitored directly from the hydraulic manifold. On all but the group test, load cells were attached in line with the hydraulic jacks (Figure 3.3.4). For the group, each of two hydraulic jacks had a load cell placed directly inline. Also on the group a single load cell was placed between shaft BG2 and the loading beam. During all but the group test, each test and reaction shaft were fitted with two LVDT's at different elevations to produce an initial slope. During the group test each reaction shaft, and each of the two hydraulic jacks, were fitted with an LVDT. Two LVDTs were also fitted to the loading beam to describe its movements. All LVDTs that were not fitted to a hydraulic jack were supported by a reference beam. Each beam was placed near the location of measurement and supported on either end at a

distance believed to be great enough to prevent any movement of the reference beam. This distance proved to be insufficient to prevent movement during the group loading and corrections were applied to the measurements as described in chapter 4.

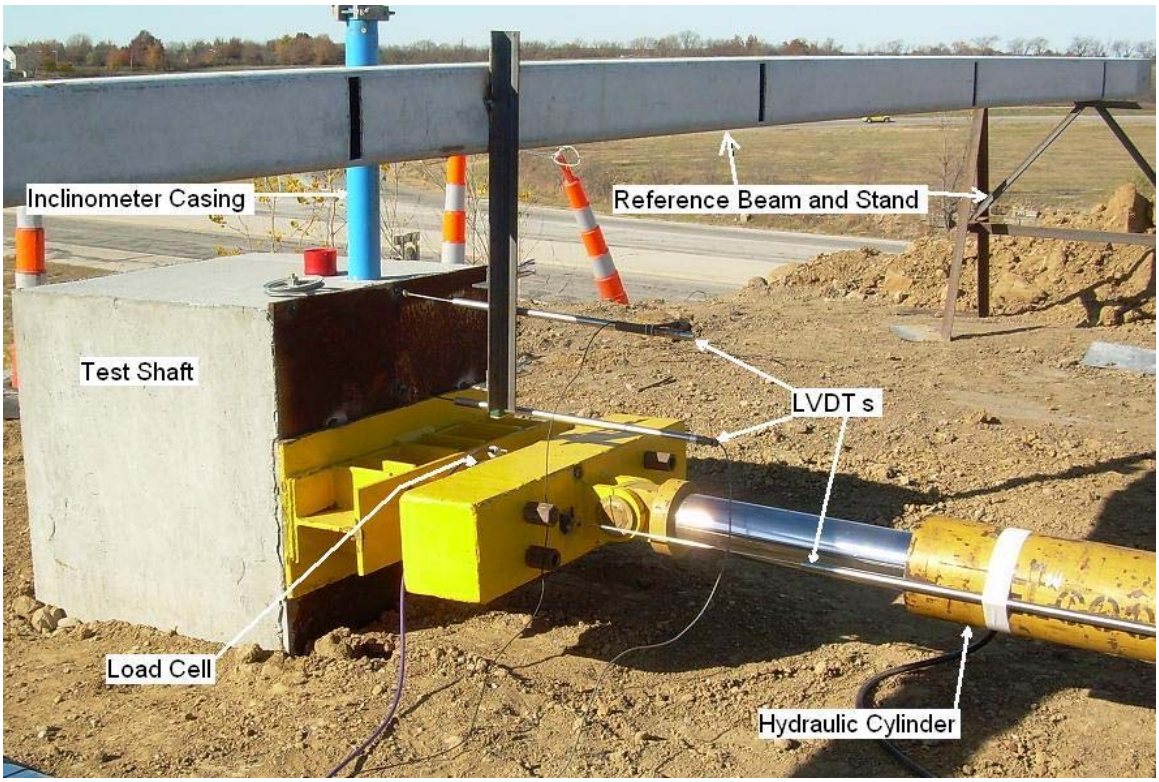

Figure 3.3.4 Typical test setup for single shafts

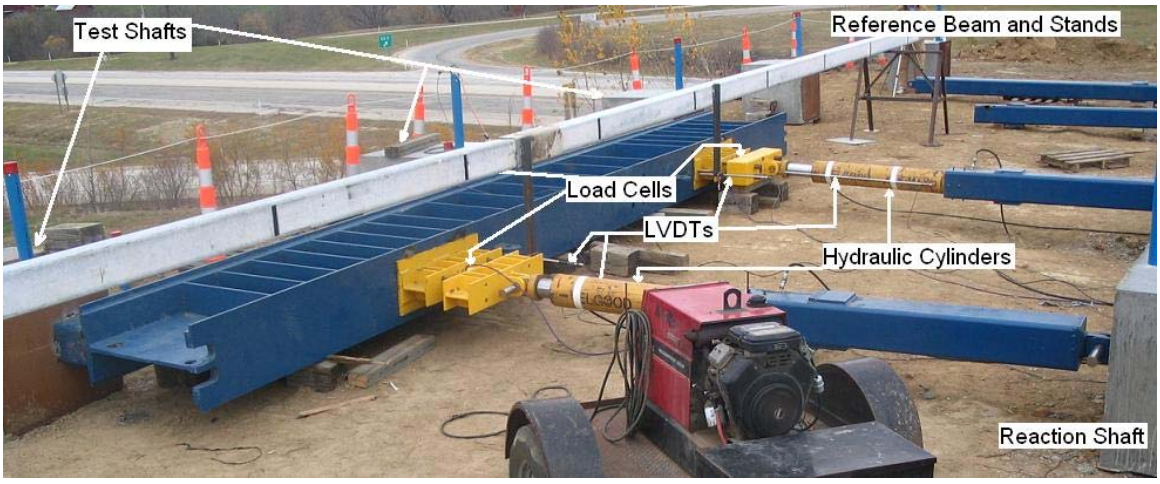

Figure 3.3.5 Group test setup

During each test inclinometers were lowered into the test shafts during every other load step. Readings were also taken after the final loading and the unloaded steps on the reaction shafts. For the group test two inclinometer casing were also placed right behind the face of the wall. These were spaced evenly between the three test shaft centerlines. Inclination readings were taken during every other interval at these locations as well to describe the wall movement during loading and unloading.

3.4 Test Procedures

Inclinometer baselines were obtained the week before all testing began. The initial setup consisted of welding the loading blocks that held each load cell into place, positioning the reference beams and LVDT mounting points, and initial setup of the hydraulics. First the hydraulic jacks were placed in the general position with cribbing for support. The cribbing was leveled and the jacks were extended to make contact with the shafts. Next the contact points were welded to support the loading block and the hydraulics. The reference beams were made of used box guard rail and supported with either oil drums or steel horses at the ends. This guard rail had angle iron welded to it to mount the LVDTs. For the group test as well as shaft D a loading beam was required so this also needed to be moved into place. The camera that was used to record wall movement was setup below and 22.5' from the centerline of the shaft to be tested. Before testing could begin all of the LVDTs and load cells were wired to the data collection system. Walkie-talkie communication was established between the testing setup on top of the wall and the cameraman monitoring the movement of the facing.

Testing began with a communication of "ready to test" this was the signal to take the initial picture. Loading began and was carried out until the desired deflection was

achieved. At that point loading stopped and the hydraulic cylinders were locked into position and held for five minutes or until inclinometer readings were finished. During that time pictures were taken immediately after loading and then every 1.25 minutes until it was time to load again. The loading procedure was repeated until the final loading step. After the last load was applied and locked off, inclinometer readings were made on all shafts or casing associated with that test, and then the entire setup was completely unloaded. Finally another complete set of inclinometer readings were made at the unloaded positions.

During construction, testing, and test analysis lab tests were run to obtain properties of the CA-5 clean aggregate backfill. These tests consisted of sieve analyses, triaxial compression tests, and large direct shear tests. The results of these tests are contained in the next chapter.

Chapter 4

Test Results and Analysis

Results of the full scale lateral load testing, as well as laboratory tests used to determine the properties of the aggregate backfill, are presented in this chapter. Results of site investigation tests are presented in Appendix.

4.1 Laboratory Results and Analysis

The University of Kansas performed large direct shear, triaxial compression, and sieve analysis tests on the Clean Aggregate backfill (CA-5). Samples were collected from several different loads of aggregate during construction of the wall.

Sieve analysis was performed using both a small sieving machine with an eight inch diameter sieve, and large sieving machine with an area of 15 x 23 in.^{2} Both tests yield similar results, and the results of three large sieve analyses were averaged and presented in Figure 4.1.1.

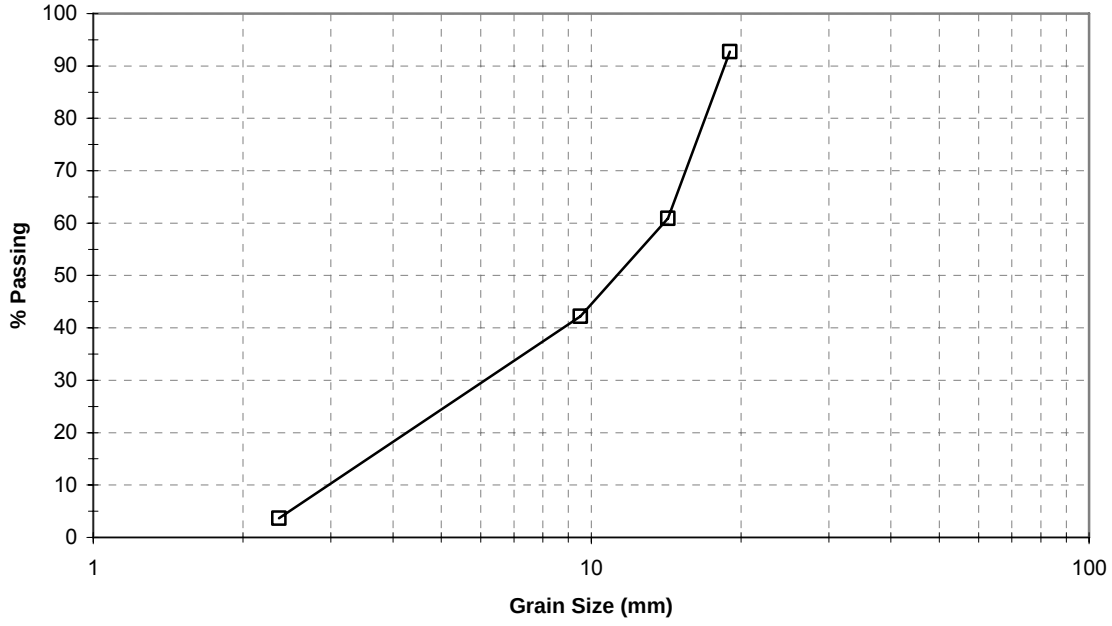

Figure 4.1.1 Large sieve analysis results

4.1.1 Large Direct Shear Box

The large direct shear box measures 12” x 16” with a 4” deep upper and 4” deep lower portion. This shear box has several different ways to apply vertical pressure; pneumatic bladder, pneumatic plate, and dead weight. The height of the gap between the two halves of the box is adjustable from less then 1/8inches to more than an inch of gap.

During testing using the pneumatic bladder loading mechanism it was apparent that the results for the clean aggregate backfill (CA-5) were inaccurate. Poor results with the bladder lead to testing with the pneumatic plate, as well as dead weight. Reasonable results were obtained when dead weight loading was used. Unfortunately due to limitations on the amount of dead weight that could be used it was not possible to use enough weight safely to reach the same target confining pressure as with the pneumatic systems. Results can be found in Figure 4.1.2.

Figure 4.1.2 Large direct shear results

4.1.2 Triaxial Testing

Triaxial compression tests were also conducted. The triaxial cell was capable of supporting samples up to 4.0 inches diameter and 8.5 inches tall. This was large enough to conduct tests consistent with ASTM specifications based on the maximum aggregate size. These tests produced a friction angle, φ of 51˚. The results of these tests can be found in Figure 4.1.3. and the Appendix.

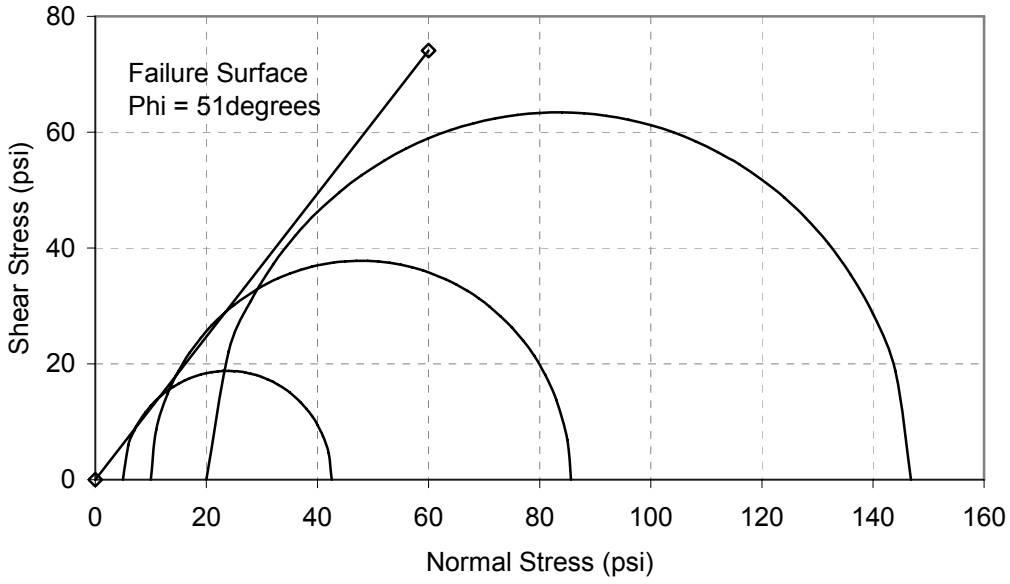

Figure 4.1.3 Mohr's circle at failure for 5, 10, and 20 psi confining pressure

4.2 Field Test Results and Analysis

Testing occurred from November 08, 2007 to November 16, 2007. Monitoring of the control section was ongoing during construction. Five lateral load tests were performed on individual shafts, one lateral load test was performed a group of three shafts, and one lateral load test was performed on the two large 48 inch diameter reaction shafts, for a total of 8 tests. The results of the tests on the test shafts are presented in this

document. Loads and deflections associated with a shaft were measured at one foot above the ground surface

Figure 4.2.1 illustrates a typical graph for loading of a single test shaft. This graph shows deflection and load versus time. Testing of the shafts was considered to be displacement controlled. The process began with increasing hydraulic pressure until movement began, and then maintaining movement until a desired deflection was achieved. At this point the hydraulic fluid valves were closed, preventing load cylinder movement and maintaining the deflection for the greater of five minutes or until inclinometer measurements were competed. During the holding time deflection was nearly constant and load decreased.

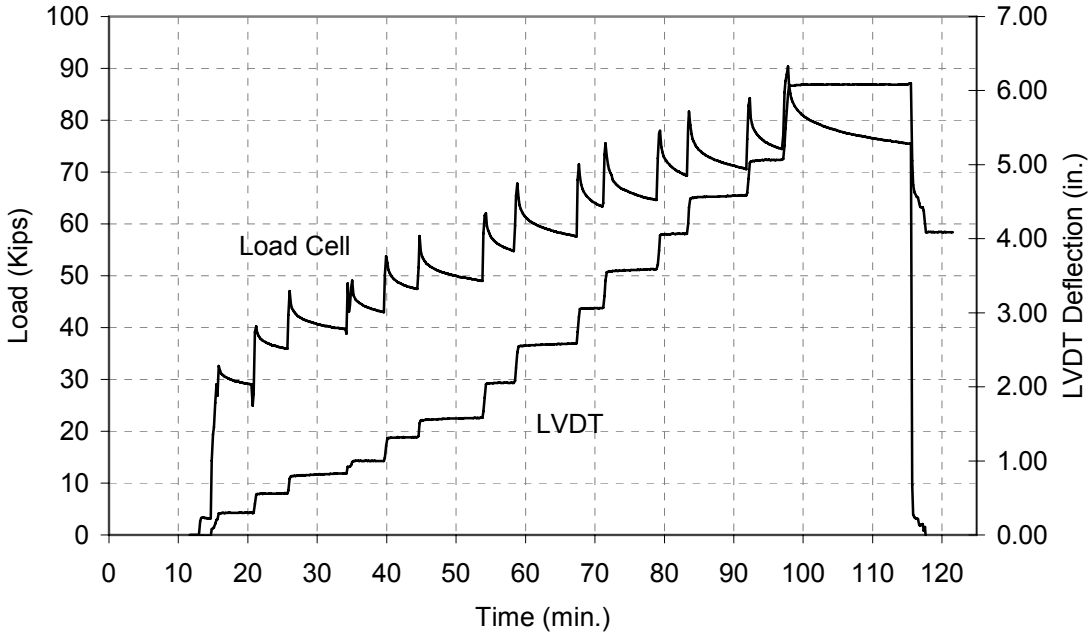

Figure 4.2.1 Shaft B load and deflection vs. time

Figure 4.2.2 shows the results from the load versus deflection of the shaft at three different times after the loading was locked off for each particular step. As the deflection was increased from one step to another there was a peak in the load. This peak load

occurred right before the deflection was held constant. The load 2.5 minutes from the time of this peak was then reported. This was always during the holding portion of any load step. The final load vs. deflection curve on Figure 4.2.2 is the residual load. This load was a local minimum for each loading step. Similar graphs for all other shafts can be found in the Appendix.

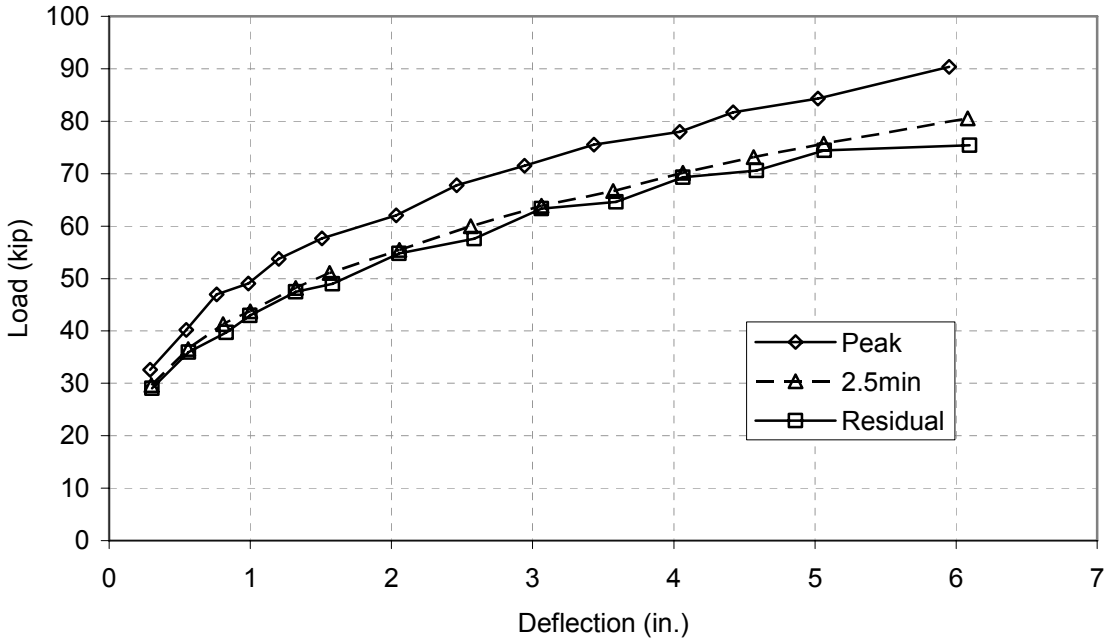

Figure 4.2.2 Shaft B peak, 2.5 minute, and residual load vs. deflection

Figure 4.2.3, 4.3.4, and 4.2.5 show the peak, 2.5min., and residual loads vs. deflection for all of the individual shafts. As expected the shafts that have the furthest distance from the facing also have the highest load and modulus. Shaft A has the lowest load, and also shows some signs of inconsistency. At one loading step for Shaft A the load drops with increasing deflection. This was because the shaft continued moving ¼ inch past the holding point, and then was brought back to the intended position. This caused a reduction in load.

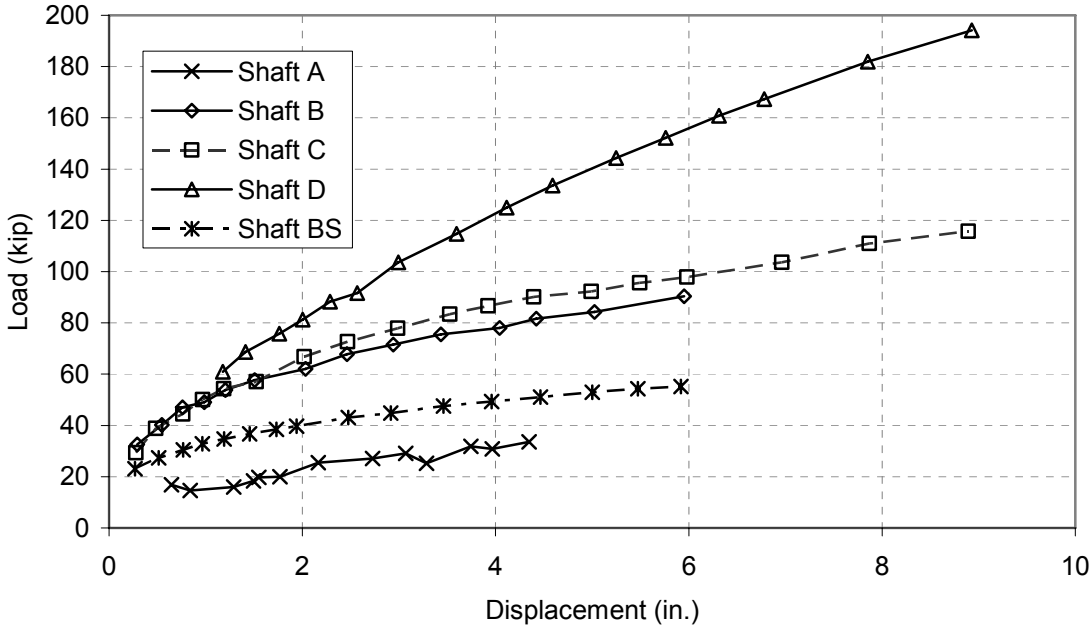

Figure 4.2.3 Peak load vs. deflection for all single shafts

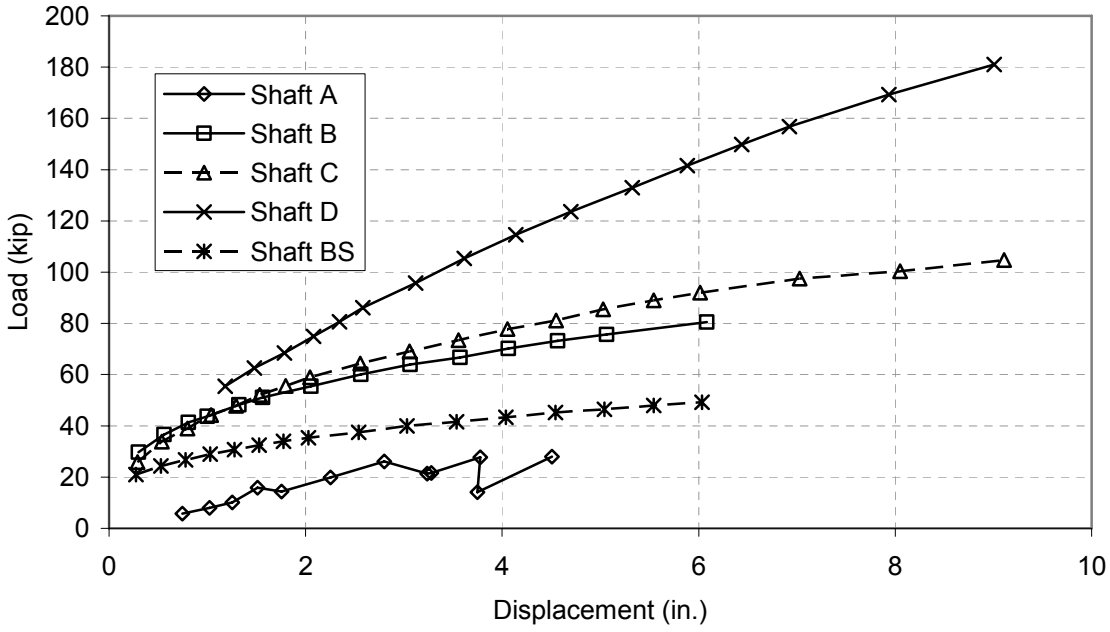

Figure 4.2.4 Load at 2.5 minutes vs. deflection for all single shafts

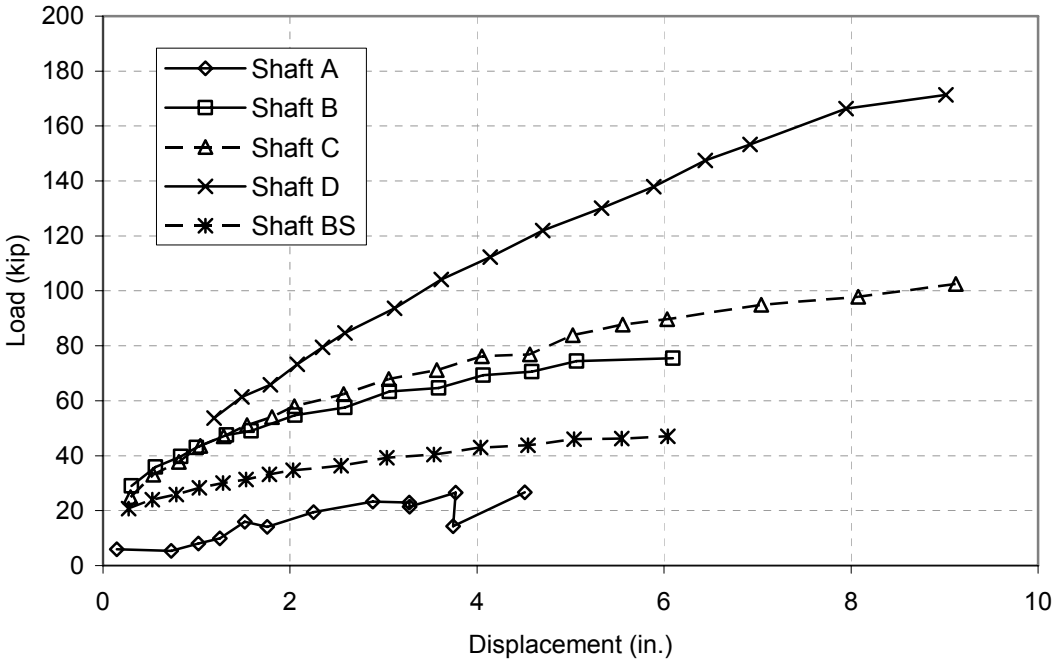

Figure 4.2.5 Residual load vs. displacement for all single shafts

Figure 4.2.6 is the same plot of peak, 2.5 min. and residual load vs. deflection for the center shaft in the group (BG2). Due to use of the loading beam it was apparent that some slack would be present in the system with respect to the shafts on either side of the group. This slack was estimated from the x-intercept of the loading curves and subtracted from the deflection. The original positions of the curves are shown with a drawn line presented in figure 4.2.6. In this figure its clear that there was some slack in the loading system. Because of the slack in Shaft BG2 the outside shafts would have deflected and estimated 0.15 inch before load was applied to the center shaft BG2. If there was no influence from BG1 and BG3 on the soil/grid near BG2 there would be no inaccuracies. If there was any influence from neighboring shafts this would be a conservative estimate. Due to movement of the reference beam a correction to the LVDTs had to be made. This correction was calculated by comparing movement of the

LVDTs associated with the hydraulic cylinders and the measured movement of the loading beam. The difference was the movement of the reference beam.

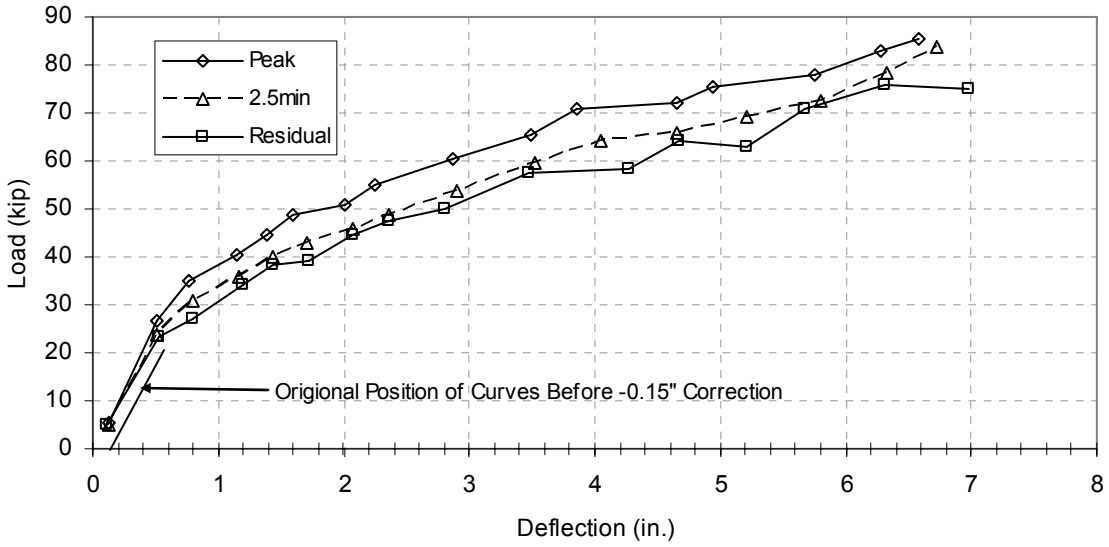

Figure 4.2.6 Shaft BG2 peak, 2.5 minute, and residual load vs. deflection

Figures 4.2.7, 4.2.8, and 4.2.9 are plots of peak, 2.5 minutes, and residual load respectively vs. time for all shafts two diameters from the wall. These shafts are the single shaft (B), each of the group shafts (BG1, BG2, and BG3), and the short shaft (BS). All of the group curves are very near to each other and as expected the weakest shaft is shaft BS, which is embedded 15 feet instead of a full depth of 20 feet like all other shafts. Shaft B is the strongest and the 3 shafts in the group had results in a tight range between B and BS. There is some reduction in strength due to influence from nearby shafts. Data for displacement in excess of 6 inches is of questionable accuracy due to loading misalignments, and frictional resistance of the loading beam.

Tables that relate load vs. deflection for peak and residual load are shown in table 4.2.1 and 4.2.2 respectively. The first displacement increment measured for shaft D was 1.2 inches, the load values for displacements less then 1 inch were not estimated. Also

Shaft A's loading was suspect for the initial points as the loading procedure was still being worked out, so there is some uncertainty associated with the early data for Shaft A. The values from Table 4.2.2 were plotted in Figure 4.2.10. These values were then analyzed and four curves were fit corresponding to the four different shaft deflections given. Looking at the plotted points from Table 4.2.2 the residual load values for a shaft spaced 108 inches (3 shaft diameters, Shaft C) appear lower then expected. This could be due to the influence of the nearby wing wall which had less reinforcement in the upper portion of the wall. The theoretical point that could carry no load would be a shaft directly next to the wall facing or 18 inches from the center of the shaft to the back of the wall facing.

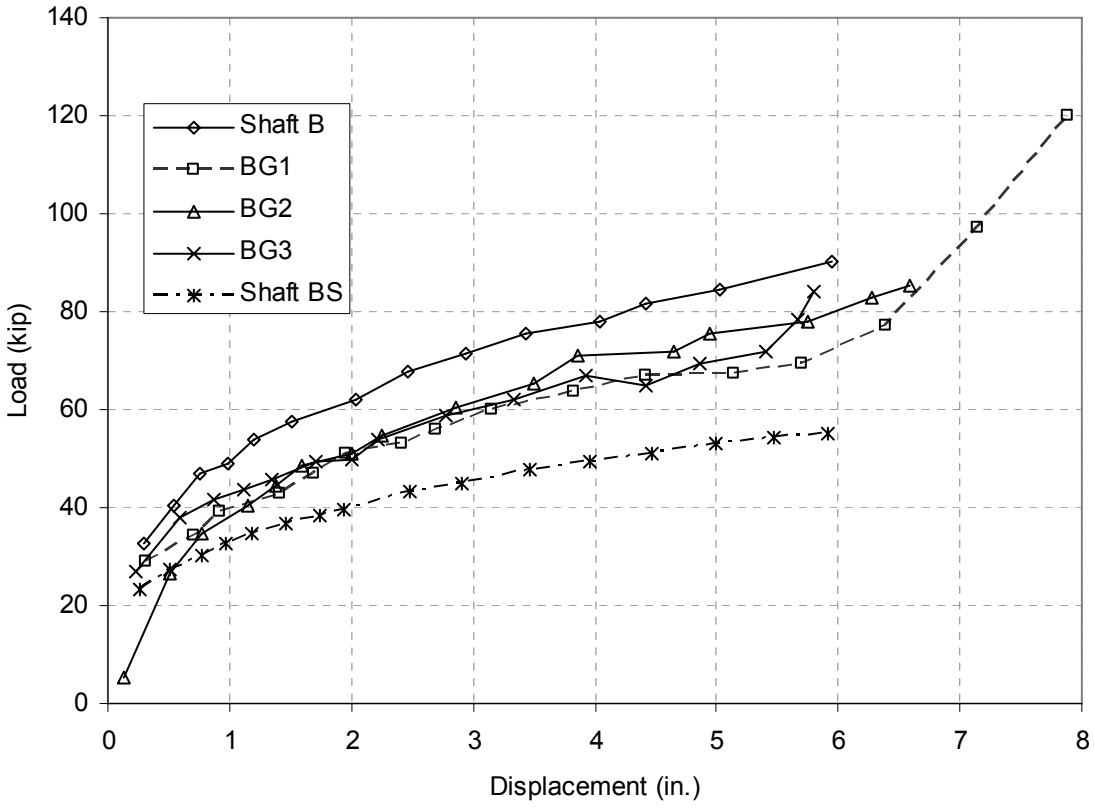

Figure 4.2.7 Peak load vs. displacement for shafts two diameters from the facing

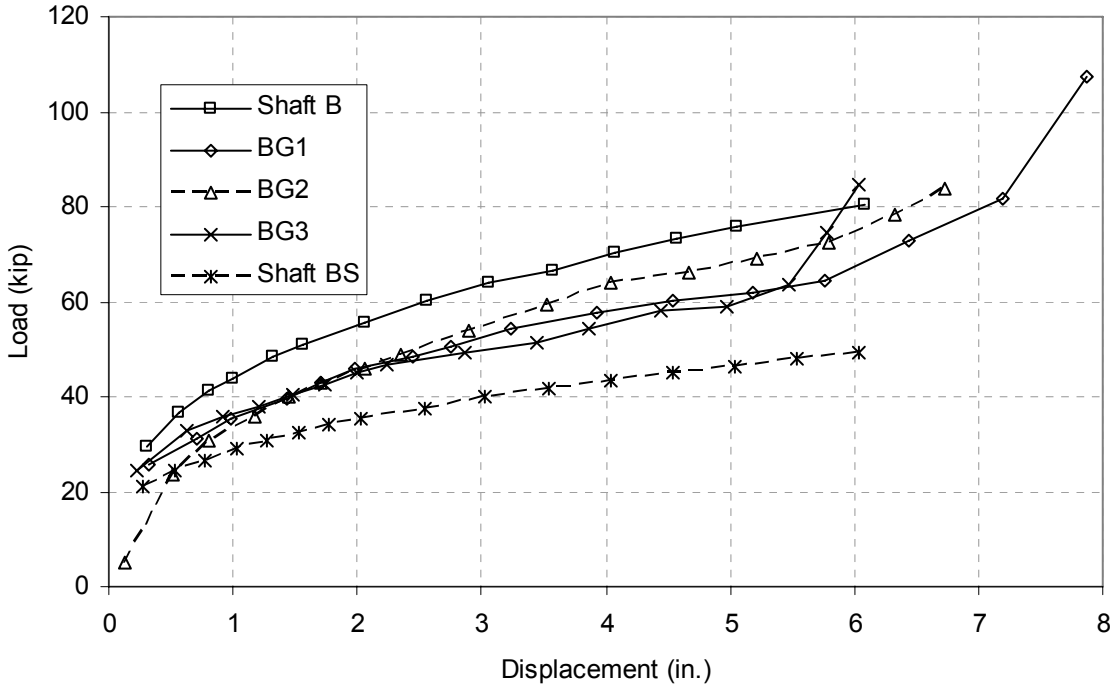

Figure 4.2.8 Load at 2.5 min. vs. displacement for shafts two diameters from the facing

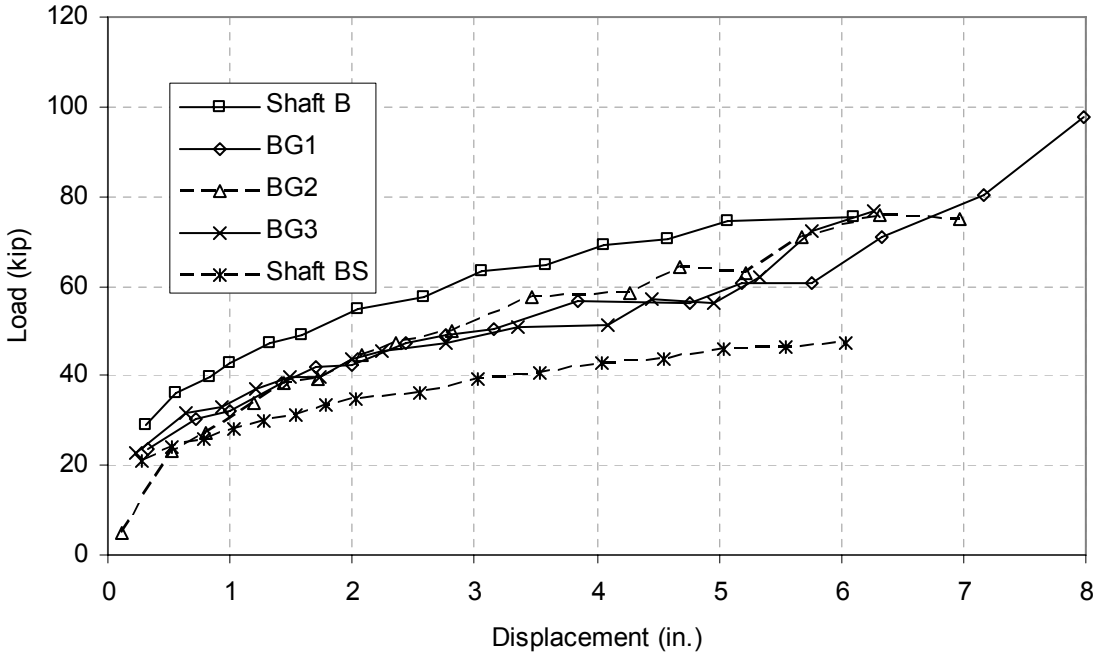

Figure 4.2.9 Residual load vs. displacement for shafts two diameters from the facing

Table 4.2.1 Peak Load vs. Displacement for all Shafts

Shaft	Dist. From Facing (in.)	Peak Load (kip)					
Displacement		0.5"	0.75"	1"	2"	4"	Ultimate
A	36	-	14	15	23	32	34
BS	72 (15' Length)	27	30	33	40	49	55
BG2	72 (15 Spacing)	27	35	39	53	70	85
B	72	40	47	50	62	77	90
C	108	39	44	50	66	87	116
D	144	-	-	55	81	120	194

Table 4.2.2 Residual Load vs. Displacement for all Shafts

Shaft	Dist. From Facing (in.)	Residual Load (kip)					
Displacement		0.5"	0.75"	1"	2"	4"	Ultimate
A	36	5.3	5.3	8	17	27	27
BS	72 (15' Length)	24	26	28	35	41	47
BG2	72 (15 Spacing)	25	28	30	43	58	75
B	72	36	40	44	55	69	75
C	108	34	39	44	58	76	102
D	144	-	-	50	74	110	171

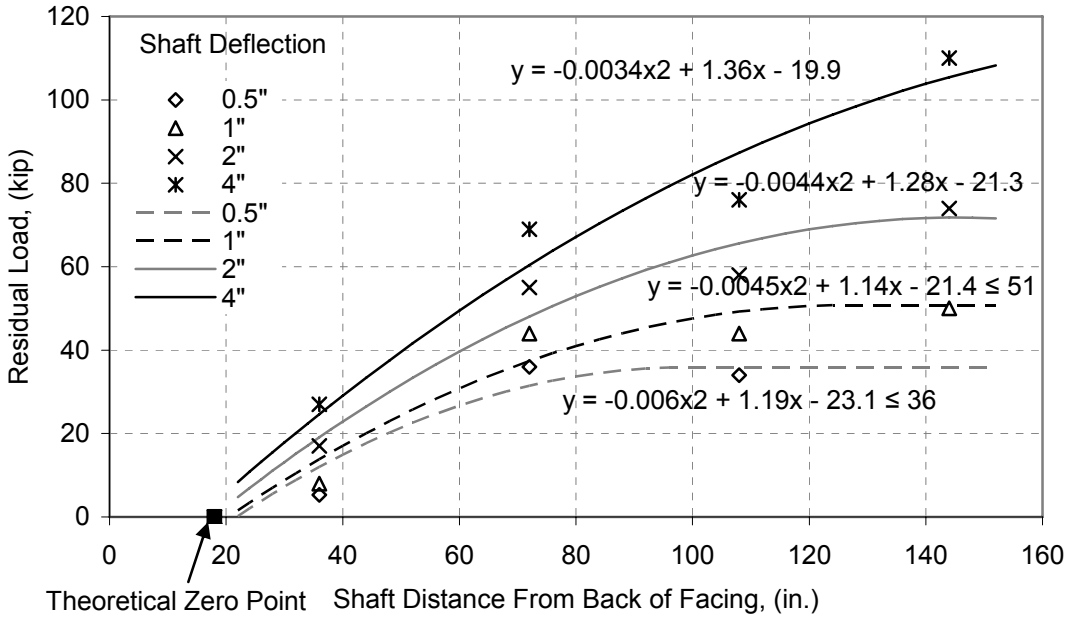

Figure 4.2.10 Plot of distance from wall facing vs. residual load for values in Table 4.2.2 and curves fit with corresponding equations.

4.3 Wall Deflections

Wall deflections were measured using photogametry as described in chapter 3. The results will be reported and analyzed in the next pages. Figure 4.3.1 shows the peak load vs. deflections of the wall facing for the targets that are mounted on the centerline of Shaft A, as well as the shaft itself. Due to the loading problem with Shaft A discussed earlier, this particular plot contains more fluctuations than other plots. As expected the shaft moved more than the top of the wall and the top of the wall moved more than the bottom. Figure 4.3.2 shows the deflection of targets for Shaft A along the horizontal axis at an elevation of 17.7 feet, as well as the shaft deflection. As expected the shaft moves more then the target at the centerline of the shaft, and wall movement decreased with distance from the centerline. Figure 4.3.3 shows the deflection of the facing at the shaft centerline for each load step. The Y-axis shows elevation of the target, and the X-axis shows the deflection of the targets. From this figure an interesting bulge at 17.7feet was found showing that there was increased movement at an elevation below the top. This indicates that the wall is not just tipping over, but is actually moving horizontally depending on the lateral pressure placed on it. Figure 4.3.4 shows the deflection of the facing in the horizontal direction at an elevation of 17.7 feet for each displacement increment. The behavior was as expected with much more movement near the centerline of the shaft and less movement as the horizontal distance increased. This figure shows that significant deflections of the wall were limited to within six feet of the centerline of loading for Shaft A. The influence distance in the horizontal direction was determined from Figure 4.3.4.

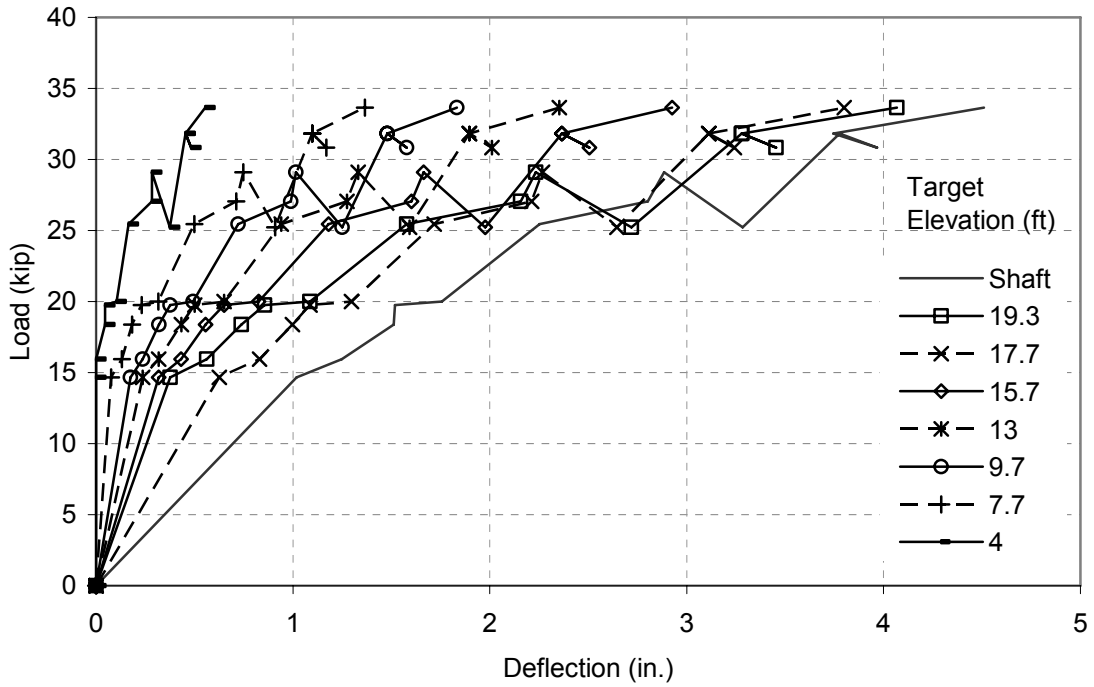

Figure 4.3.1 Shaft A centerline deflections

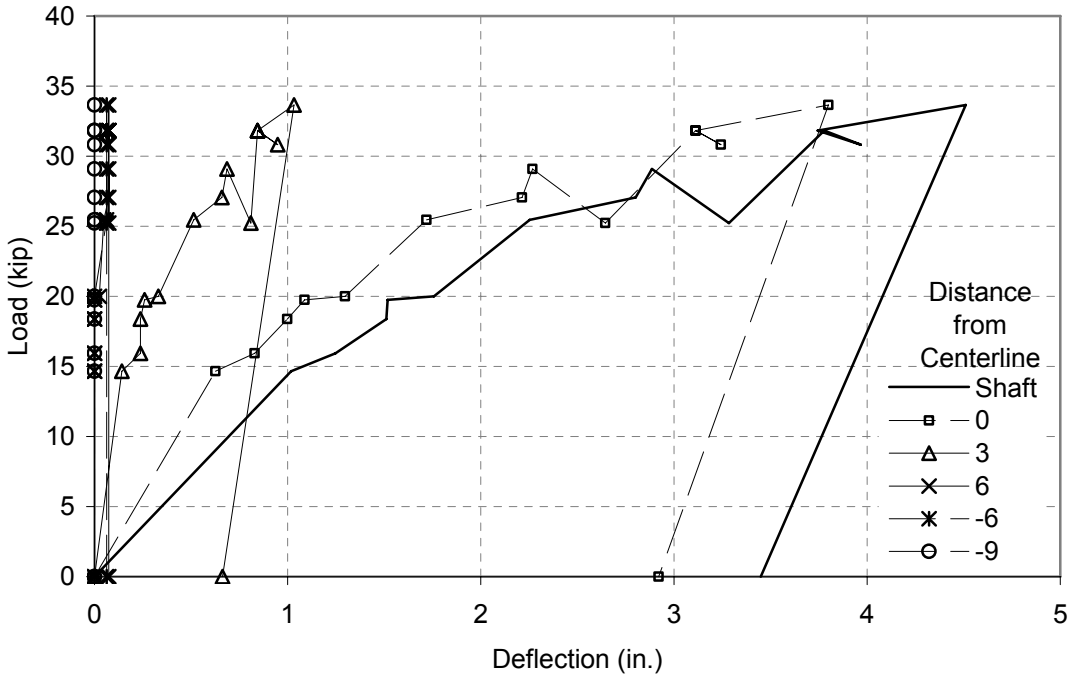

Figure 4.3.2 Shaft A deflection in horizontal direction el. 17.7 feet

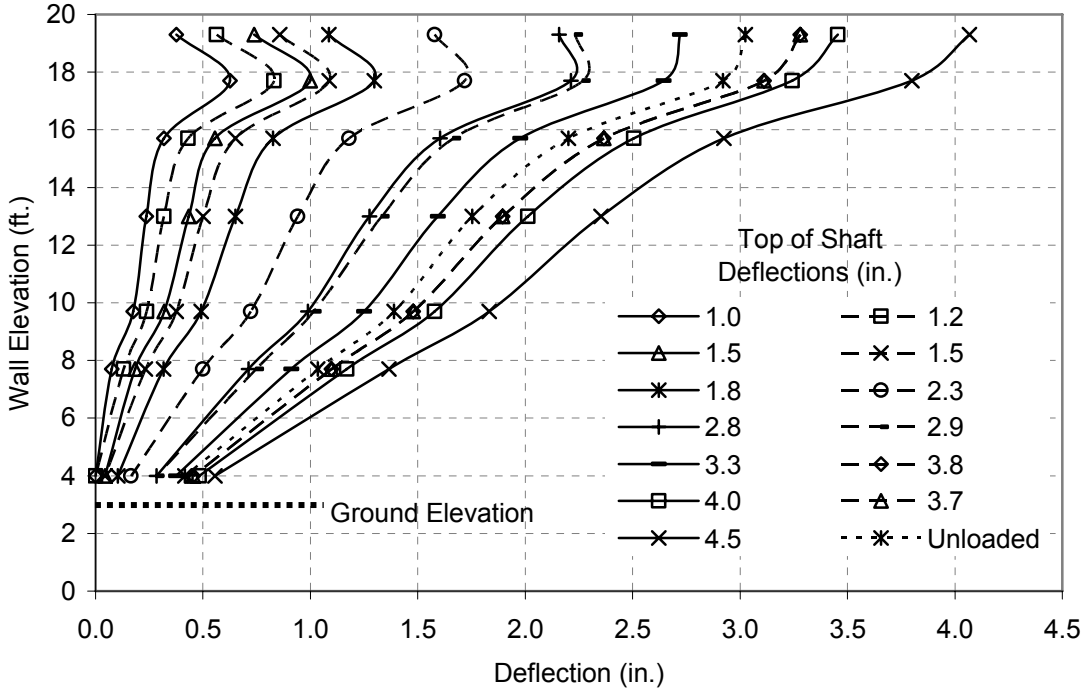

Figure 4.3.3 Shaft A incremental centerline vertical deflection of wall face

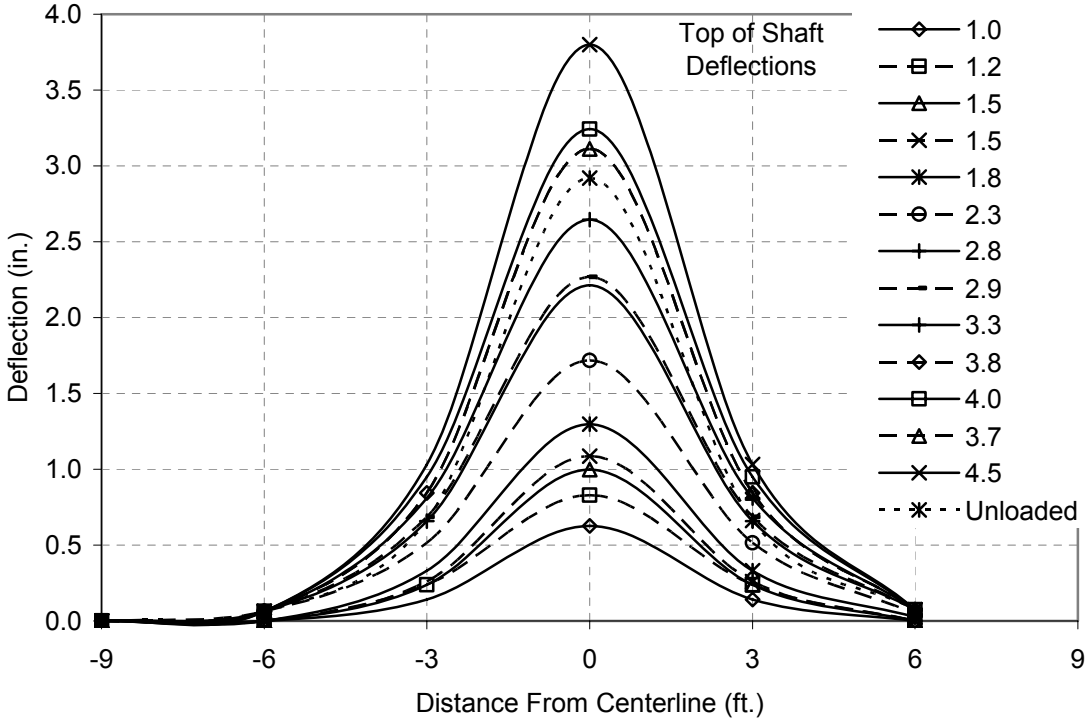

Figure 4.3.4 Shaft A incremental horizontal deflection el. 17.7 feet

A similar sequence of graphs for Shaft B are presented in Figures 4.3.5 to 4.3.8. An interesting aspect of Figure 4.3.5 is there was very little movement of the facing at initial shaft movements. With increasing shaft movement the wall movement, as a percentage of shaft movement, also increased. The deflection at the top two points, elevation 19.3 and 17.7 was very similar. These behaviors were found for all of the shafts. Figure 4.3.8 shows that significant deflections of the wall were limited to within nine feet of the centerline of loading for Shaft B.

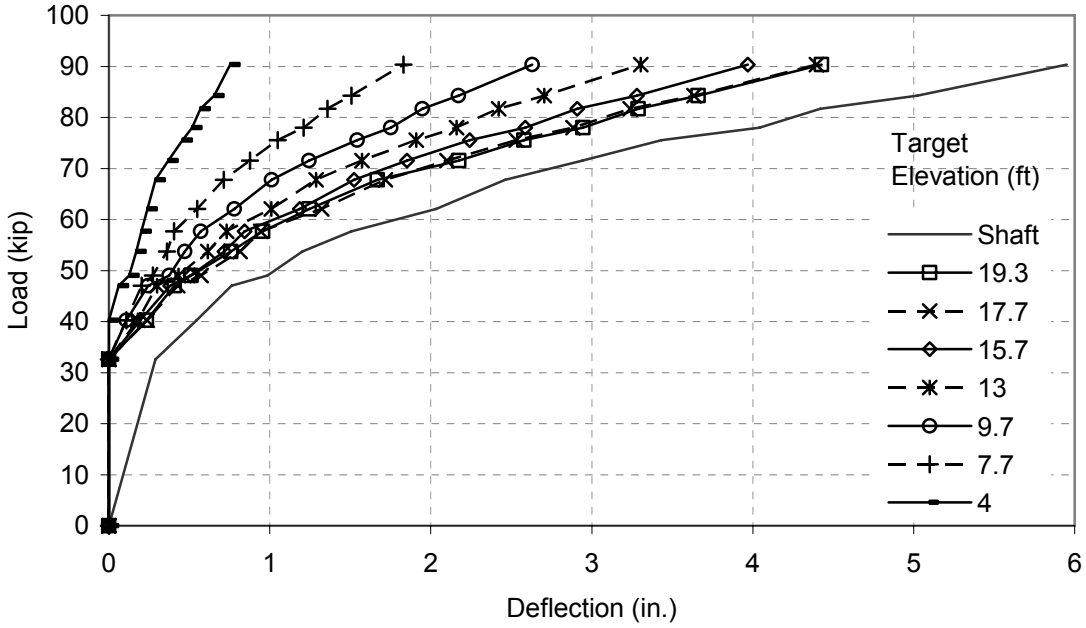

Figure 4.3.5 Shaft B centerline deflections

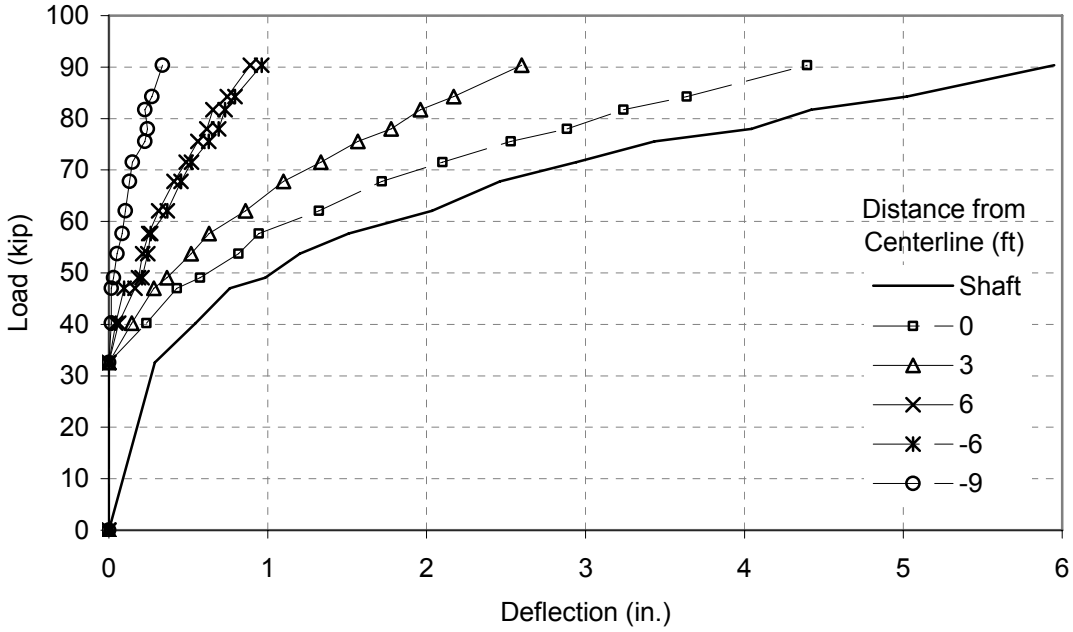

Figure 4.3.6 Shaft B deflection in horizontal direction el. 17.7 feet

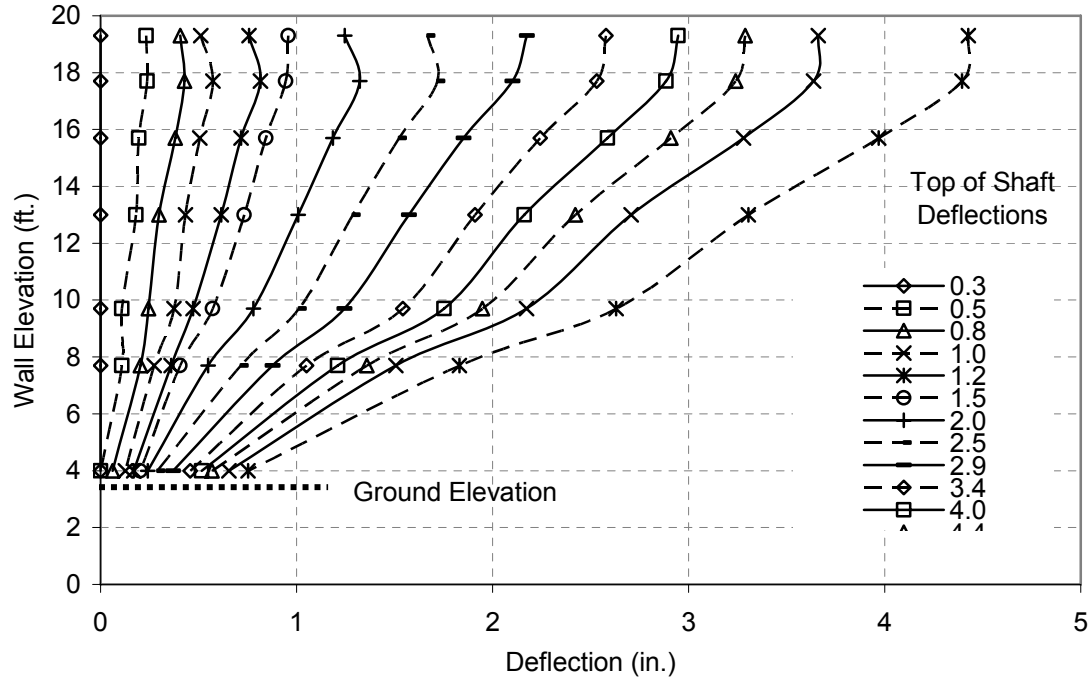

Figure 4.3.7 Shaft B incremental centerline vertical deflection of wall face

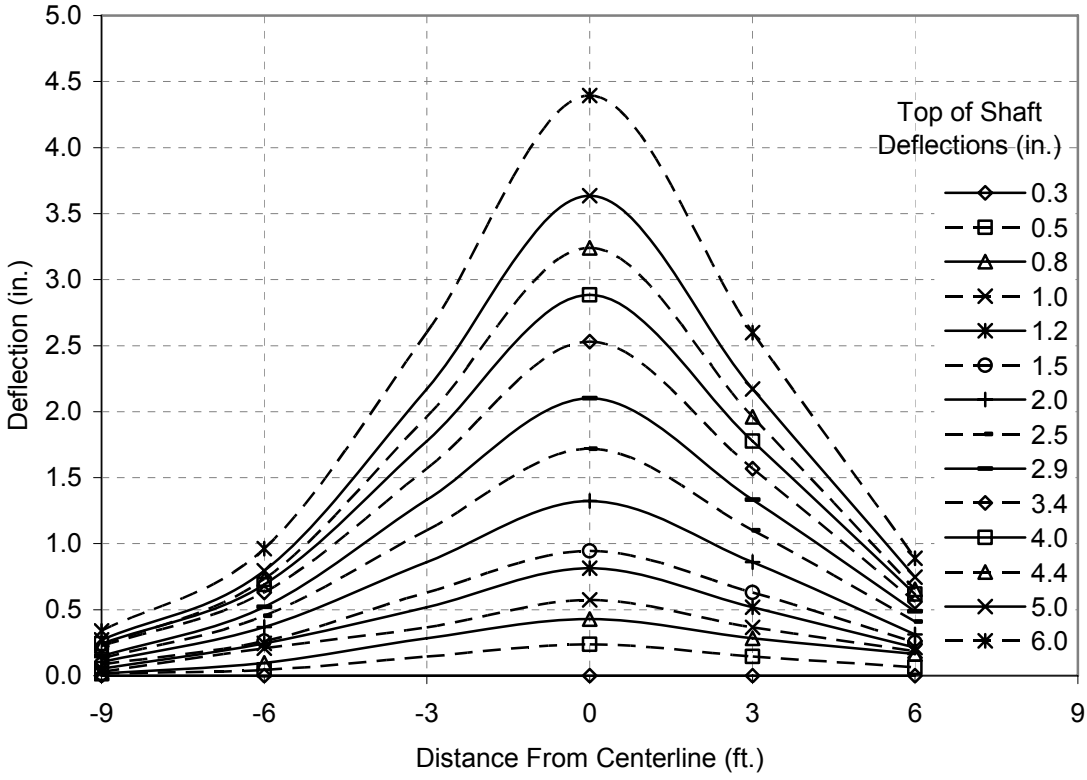

Figure 4.3.8 Shaft B incremental horizontal deflection el. 17.7 feet

Graphs for Shaft BS are shown in Figures 4.3.9 – 4.3.13. Deflections of the wall facing in the horizontal direction were very similar to Shaft B. Significant wall movements were limited to within nine feet of the centerline. Loads were on average two thirds of Shaft B for similar movements. Figure 4.3.11 shows that below the bottom of the shaft (five feet elevation) there was little facing deflection.

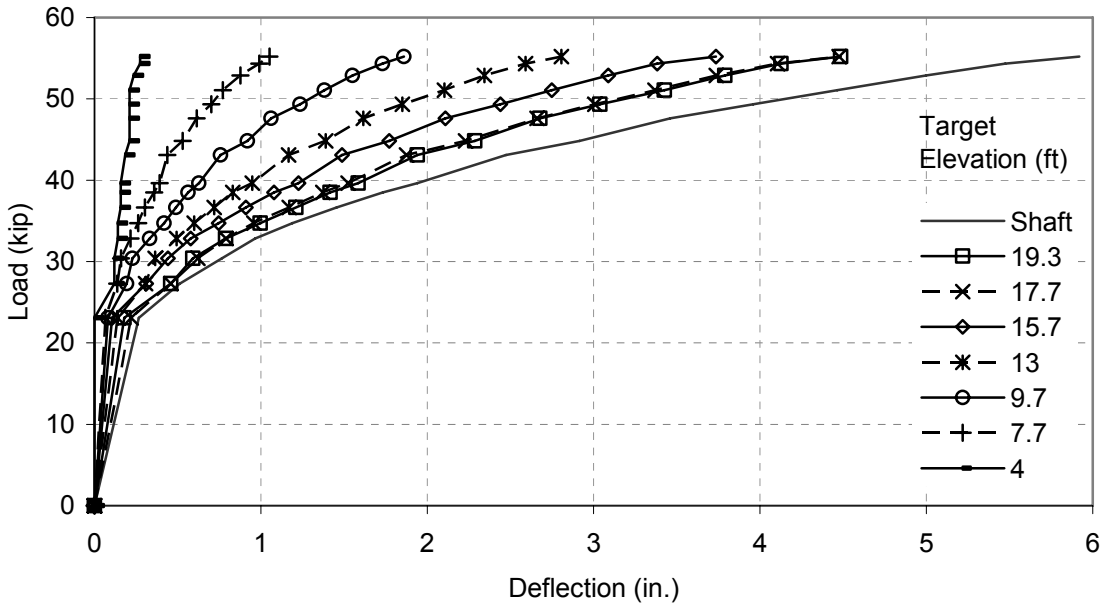

Figure 4.3.9 Shaft BS centerline deflections

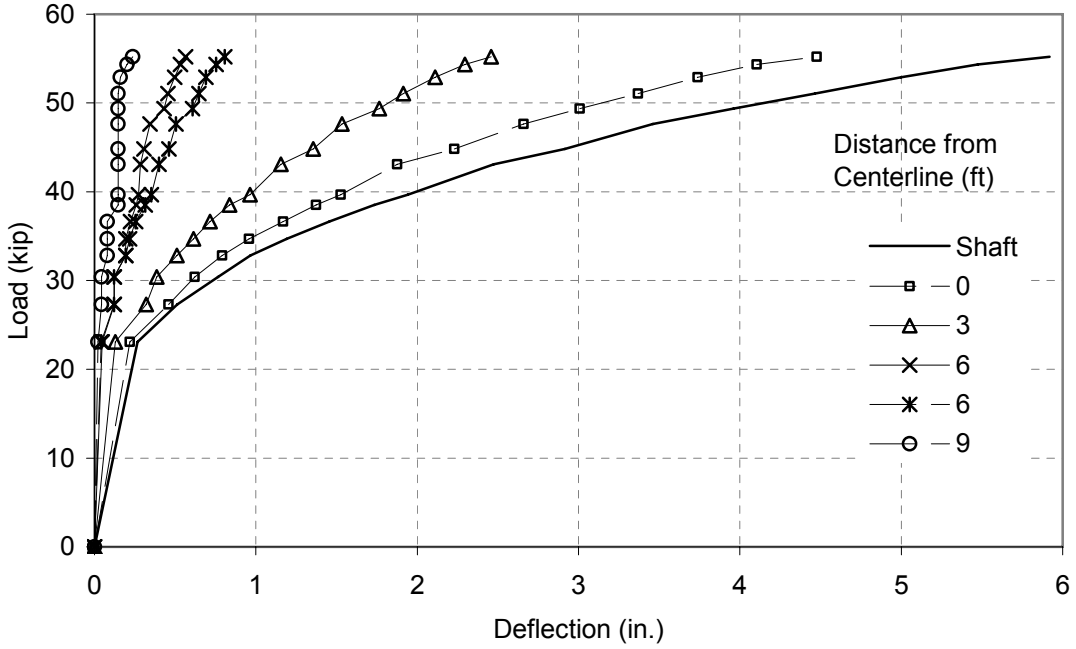

Figure 4.3.10 Shaft BS deflection in horizontal direction el. 17.7 feet

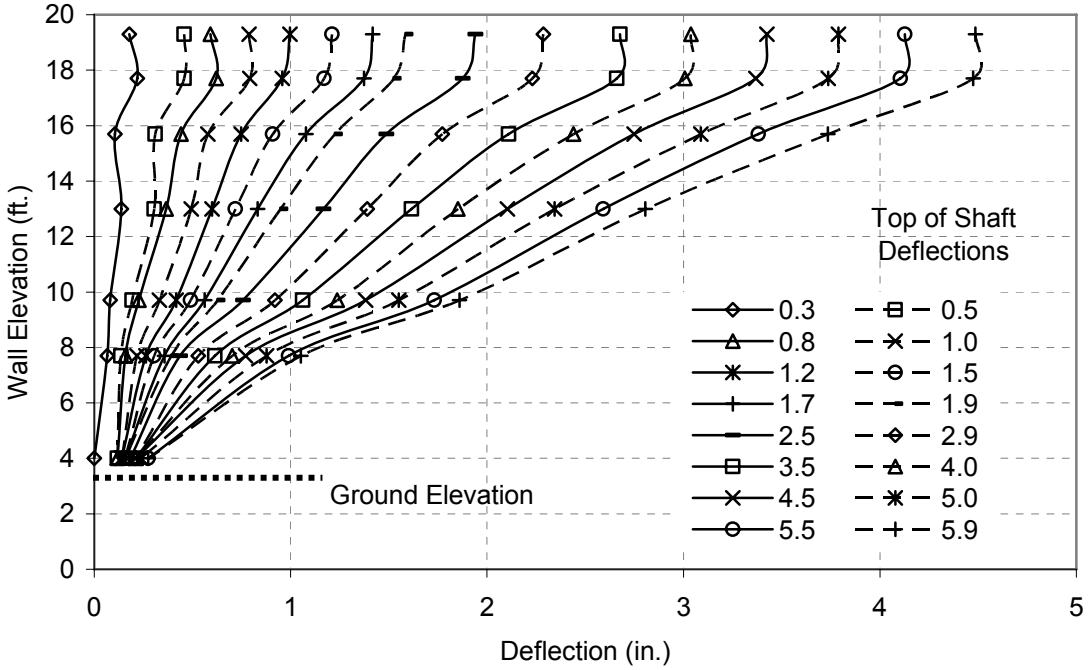

Figure 4.3.11 Shaft BS incremental centerline vertical deflection of wall face

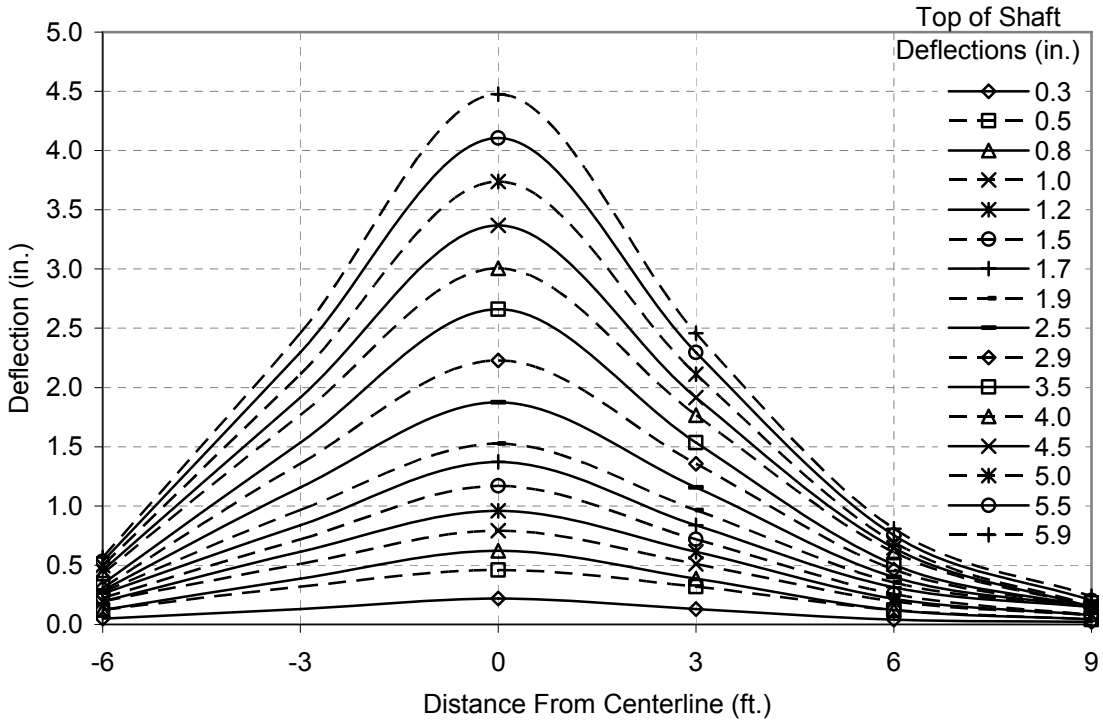

Figure 4.3.12 Shaft BS incremental horizontal deflection el. 17.7 feet

Shaft C (Figures 4.3.13 – 4.3.16) had a slightly different target layout due to alternating blocks. All of the targets were shifted up eight inches or one block layer, and the top target was not installed. The shaft was deflected 2.5 inches further than all other tests with the exception of Shaft D, which was deflected to a similar number of nine inches. Figure 4.3.16 shows significant deflections of the wall in the horizontal direction extended beyond nine feet. This shaft begins to show some deviation of the maximum wall deflection from the maximum shaft movement. Shaft D (Figure 4.3.17) shows this deviation to a larger extent.

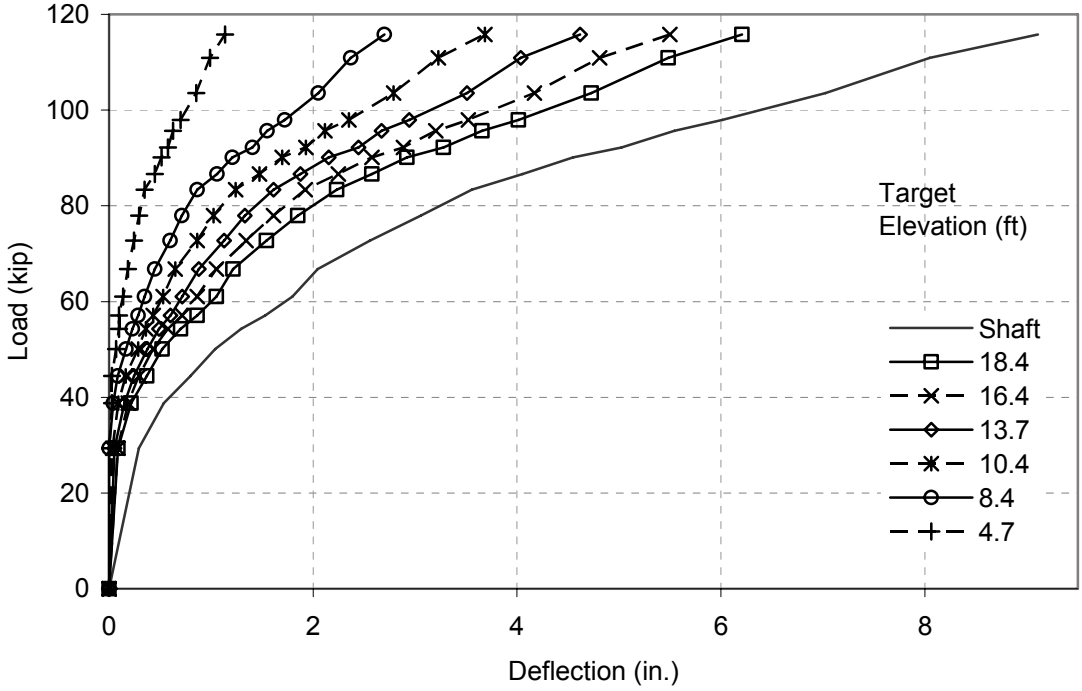

Figure 4.3.13 Shaft C centerline deflections

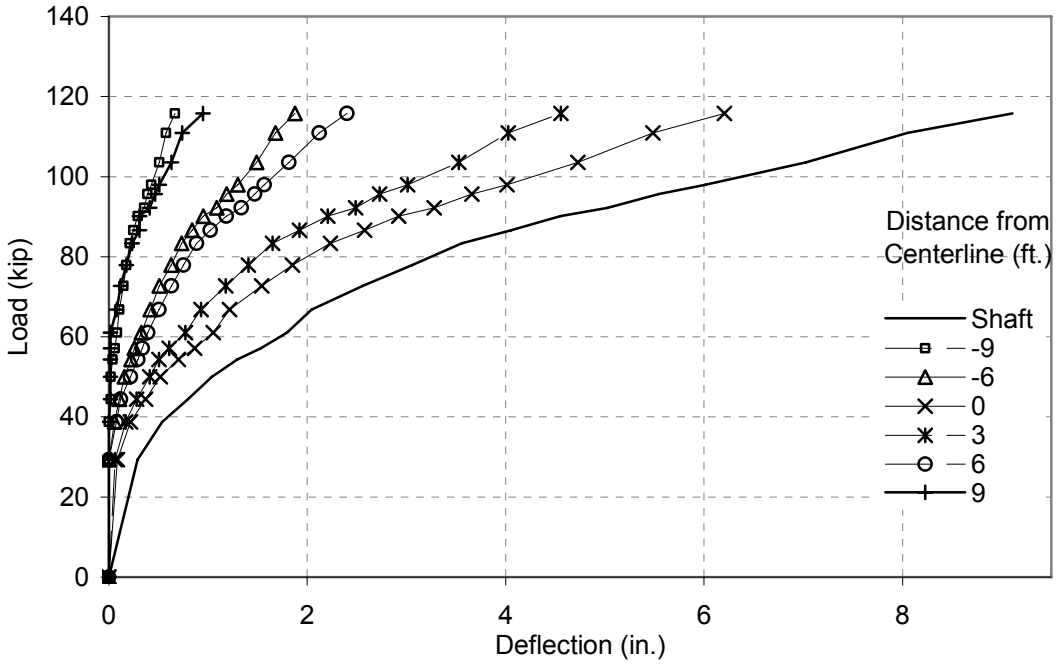

Figure 4.3.14 Shaft C deflection in horizontal direction el. 18.4 feet

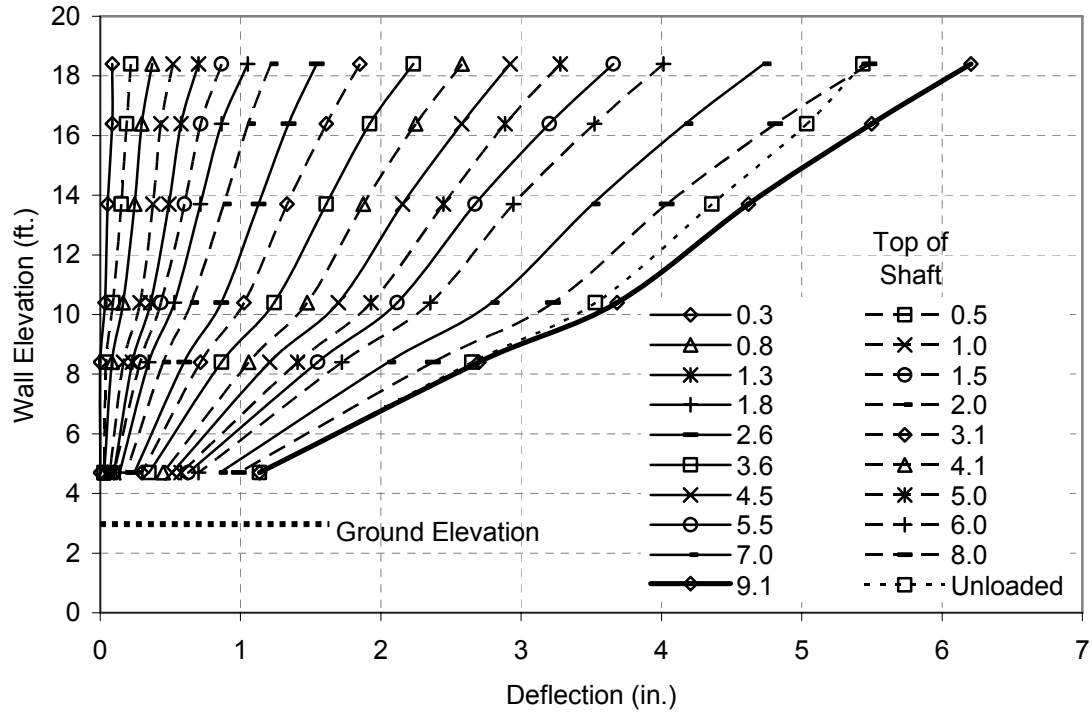

Figure 4.3.15 Shaft C incremental centerline vertical deflection of wall face

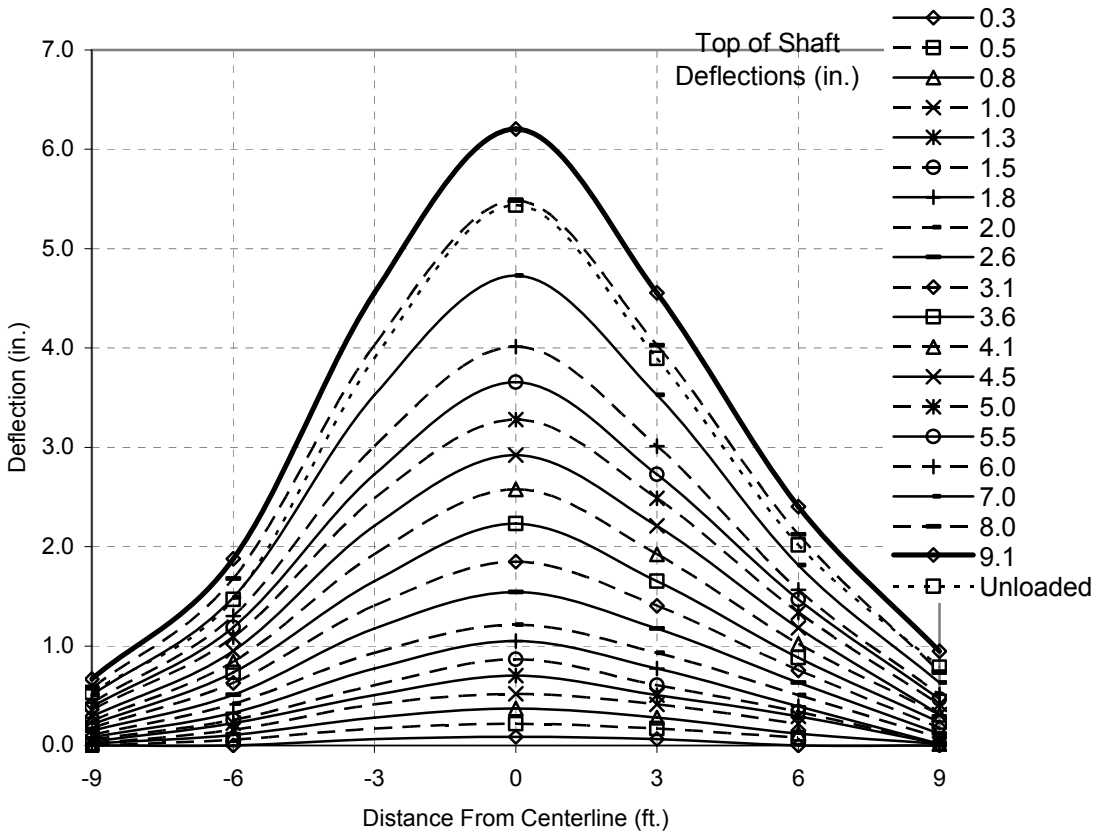

Figure 4.3.16 Shaft C incremental horizontal deflection el. 18.4 feet

Shaft D (Figures 4.3.17 – 4.3.20) was four diameters from the wall facing and therefore the farthest shaft from the wall facing to be tested. The increased distance was reflected in the increased area of influence. Figure 4.3.20 shows that significant deflections of the wall were limited to within 12 feet of the centerline of loading for Shaft D. The deflected shape of the wall facing was much more gradual then for shafts that were closer to the wall facing.

Slip joints were installed half way between test sections to isolate movement of shafts. As seen in wall facing deflections for Shaft D (Figure 4.3.20), movement was not isolated to the test section well, however because of the testing sequence this is not believed to have affected the test results. This should not have affected neighboring

shafts as test D was the only test were movement was observed much beyond the slip joints. Since this test was performed last there was no influence on other tests.

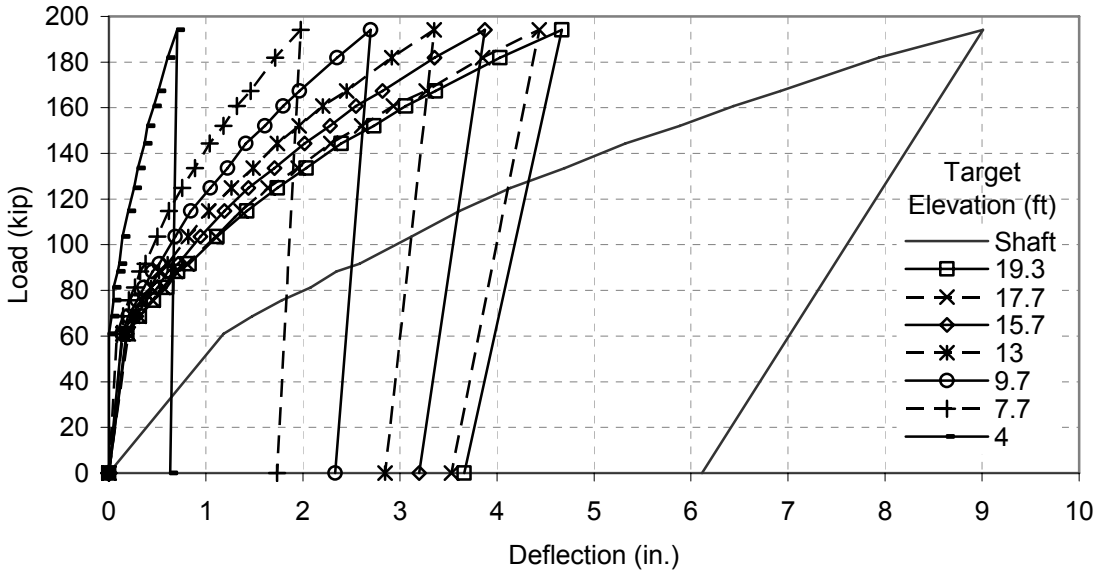

Figure 4.3.17 Shaft D centerline deflections

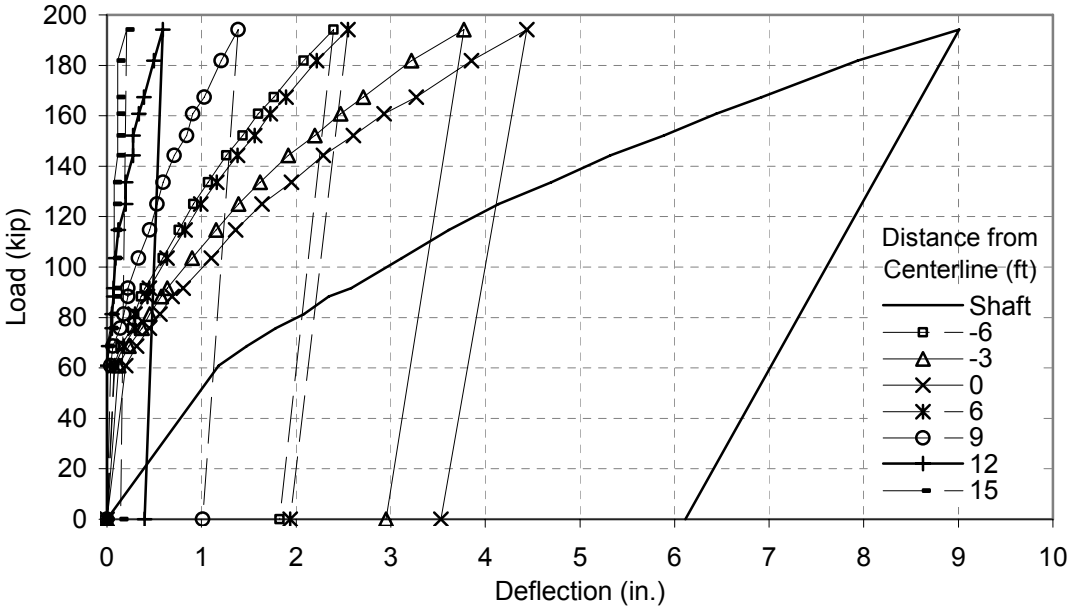

Figure 4.3.18 Shaft D deflection in horizontal direction el. 17.7 feet

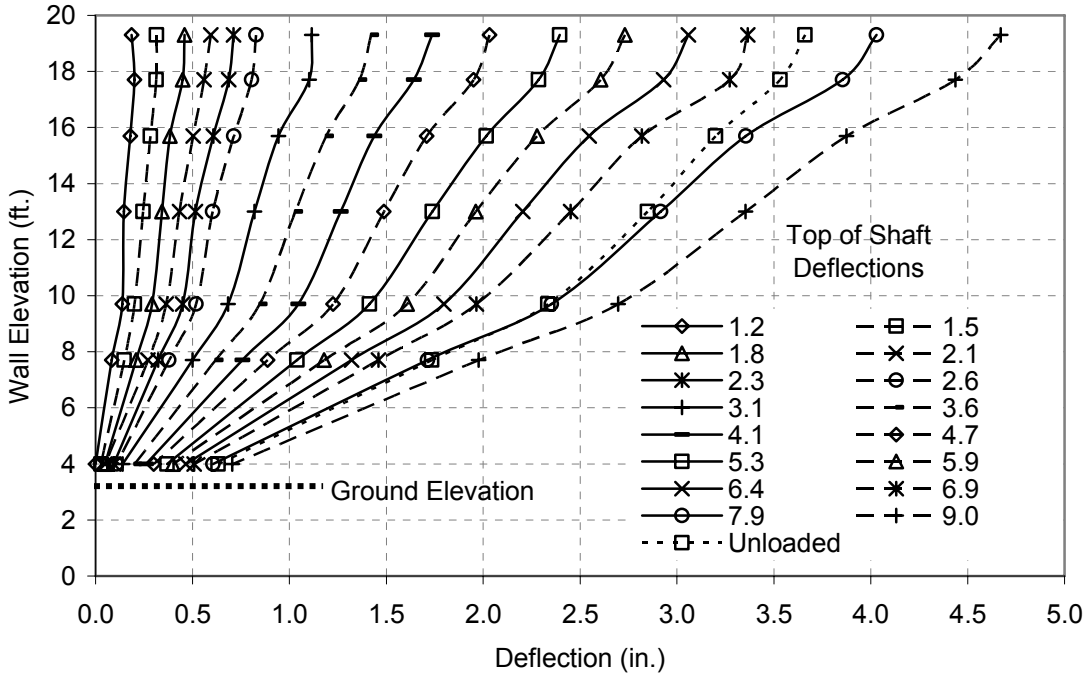

Figure 4.3.19 Shaft D incremental centerline vertical deflection of wall face

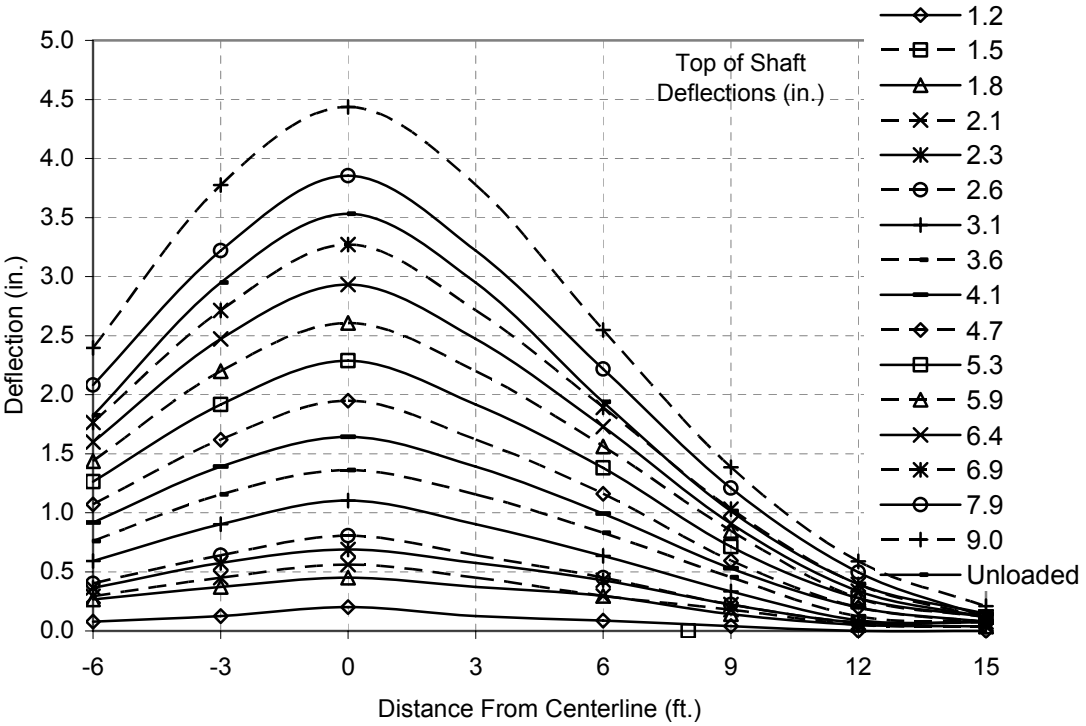

Figure 4.3.20 Shaft D incremental horizontal deflection el. 17.7 feet

Graphs of Shaft BG2 are shown in Figures 4.3.21 – 4.3.24. These graphs are very similar to those for Shaft B. One main difference is the deflections from the neighboring shafts (BG1 and BG3) influenced the horizontal deflections of Shaft BG2. This influence can be seen in Figure 4.3.24 at distances of nine feet significant wall deflections occurred, which did not happen when Shaft B was tested. The horizontal deflections of the entire group test are shown in Figure 4.3.25. This figure clearly shows the influence or nearby shafts. The slack in loading BG2 is noticeable at the wall facing also. The incremental horizontal deflection of Shaft B and BG2 were superimposed and shown in Figure 4.3.26. This figure shows the differences in group loading versus single shaft loading.

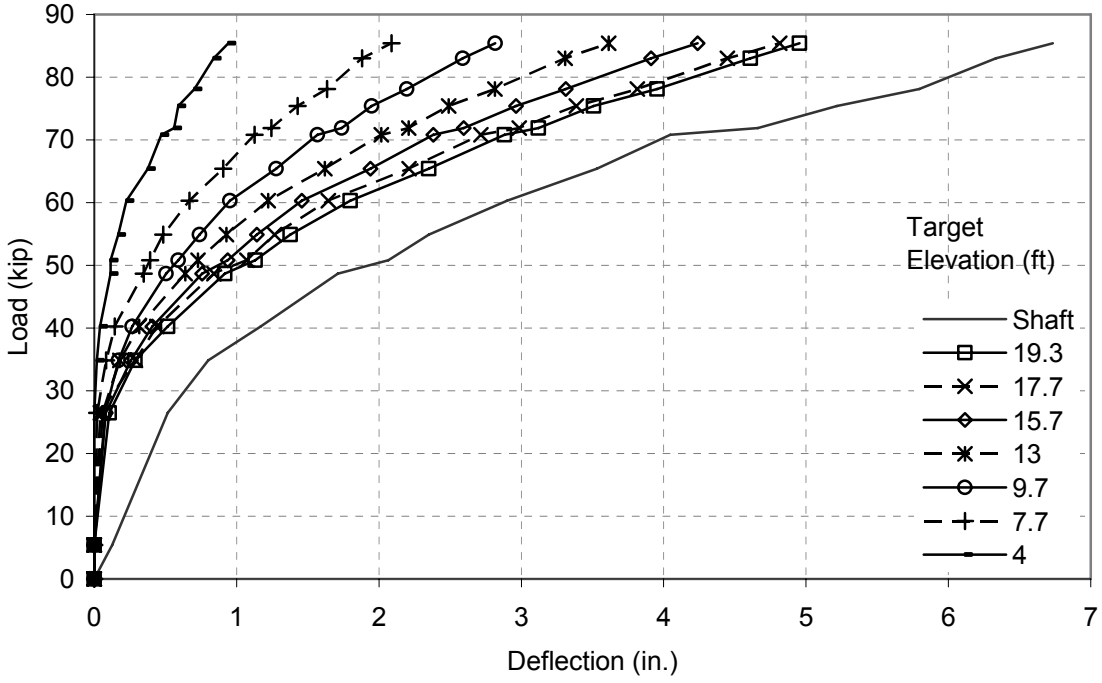

Figure 4.3.21 Shaft BG2 centerline deflections

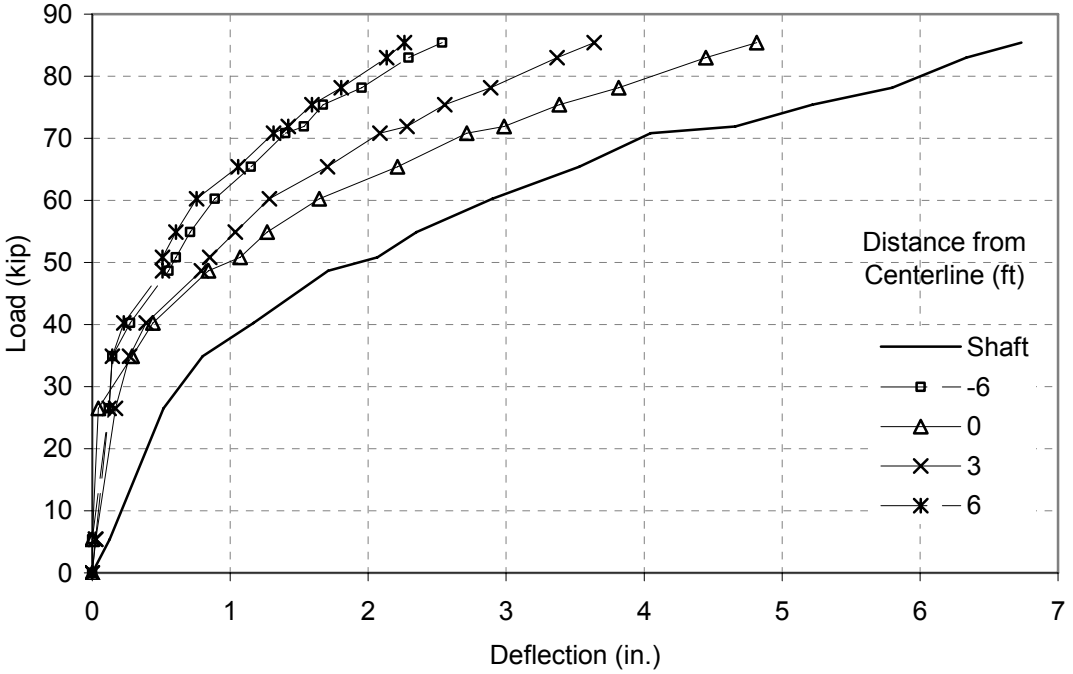

Figure 4.3.22 Shaft BG2 deflection in horizontal direction el. 17.7 feet

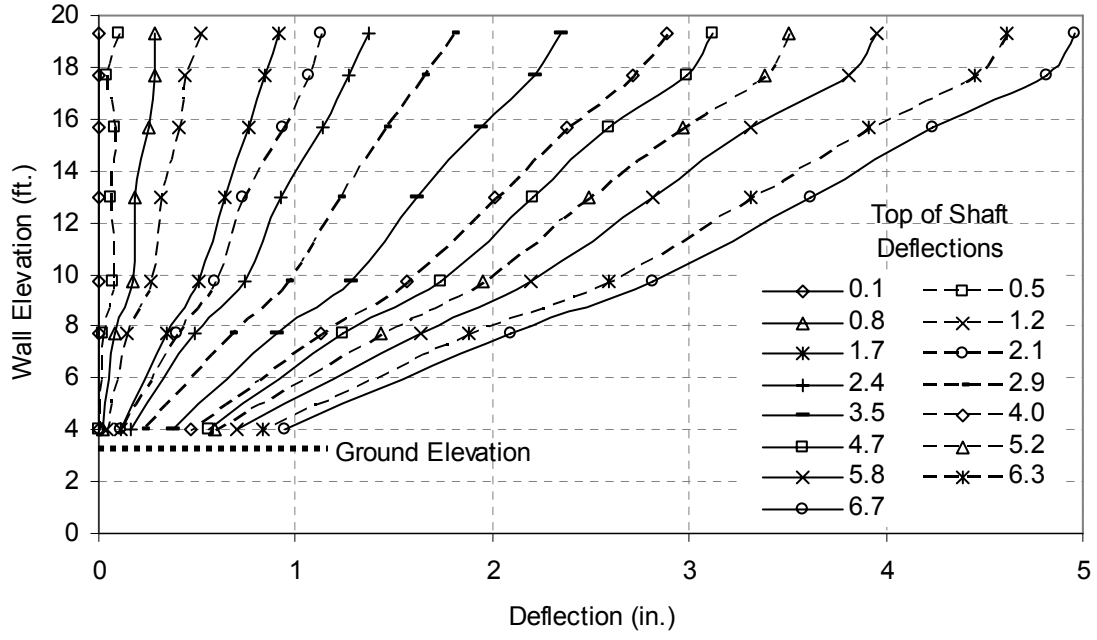

Figure 4.3.23 BG2 incremental centerline vertical deflection of wall face

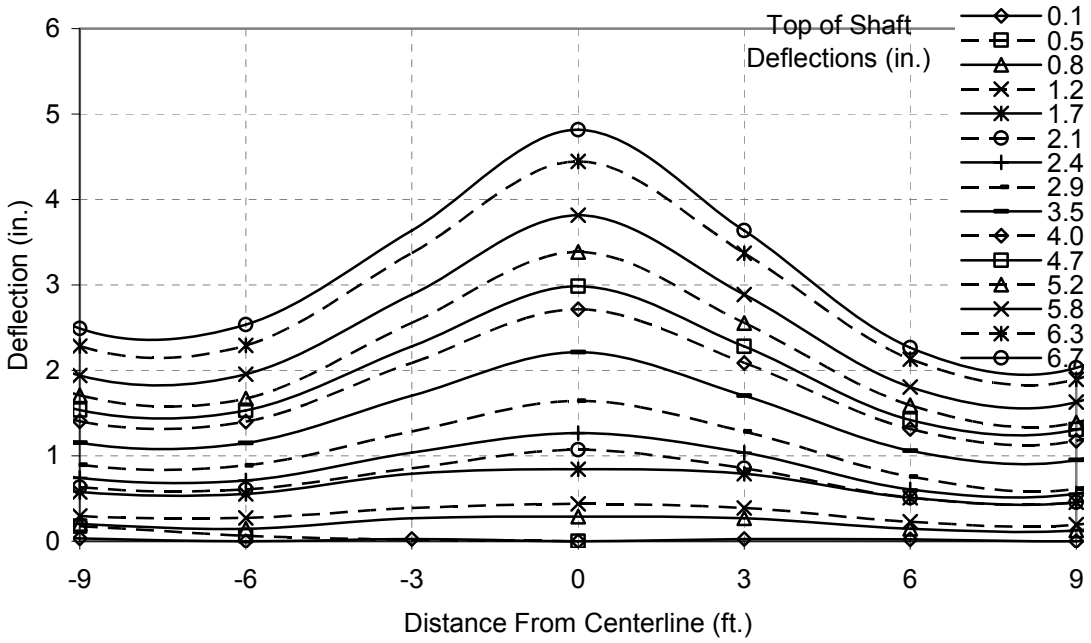

Figure 4.3.24 Shaft BG2 incremental horizontal deflection el. 17.7 feet (portion of Figure 4.3.25)

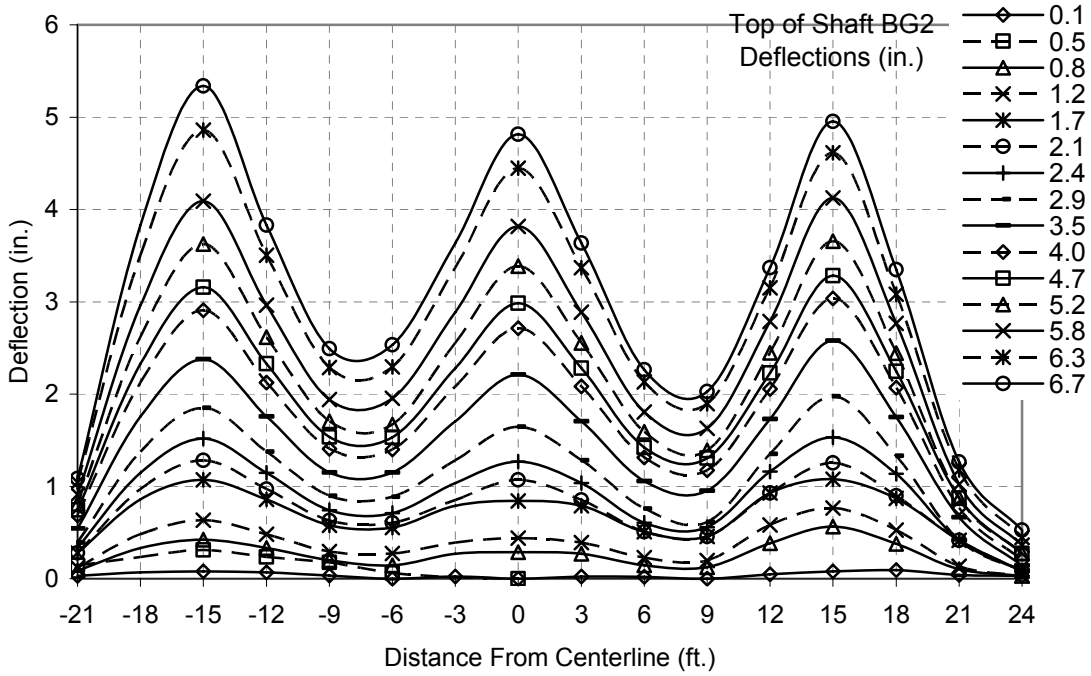

Figure 4.3.25 Shafts BG incremental horizontal deflection el. 17.7 feet

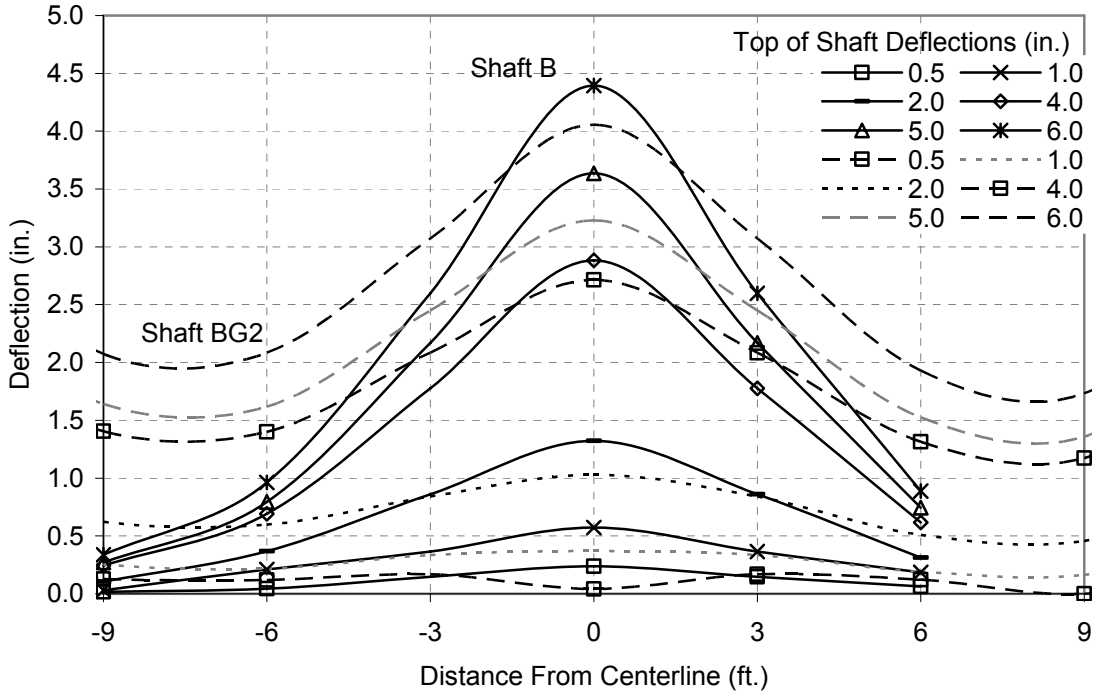

Figure 4.3.26 Shafts BG2 and B incremental horizontal deflection at elevation 17.7 feet

The other two shafts tested in the group (BG1 and BG3) are shown are shown in Figures 4.3.27 – 4.3.32. They performed in a similar way to BG2. As discussed earlier the last two loads associated with shafts BG1 and BG3 are conspicuously high and are only shown for completeness. The accuracy of the photogrammetric analysis is dependant on the distance to the targets. As a result the accuracy of BG1 is greater then BG2 which is greater then BG3. This is only mentioned for completeness because the results compare very well with each other.

Figure 4.3.33 and 4.3.34 show the peak and residual load respectively versus maximum wall deflection. This information is summarized in Tables 4.3.1 and 4.3.2.

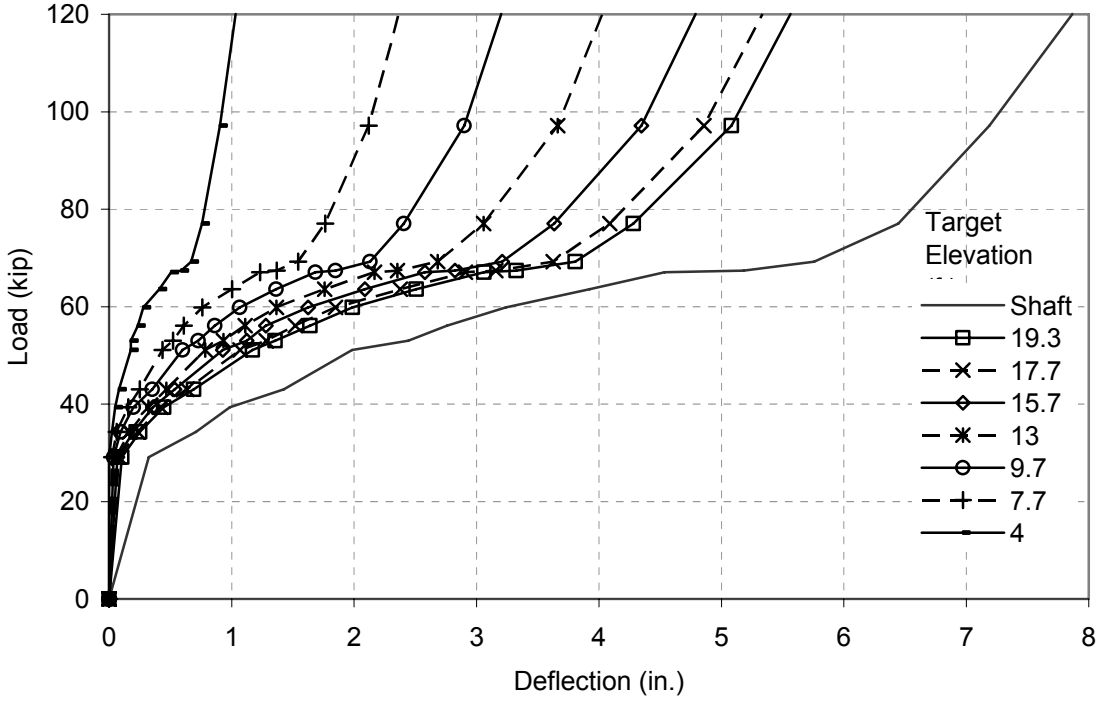

Figure 4.3.27 Shaft BG1 centerline deflections

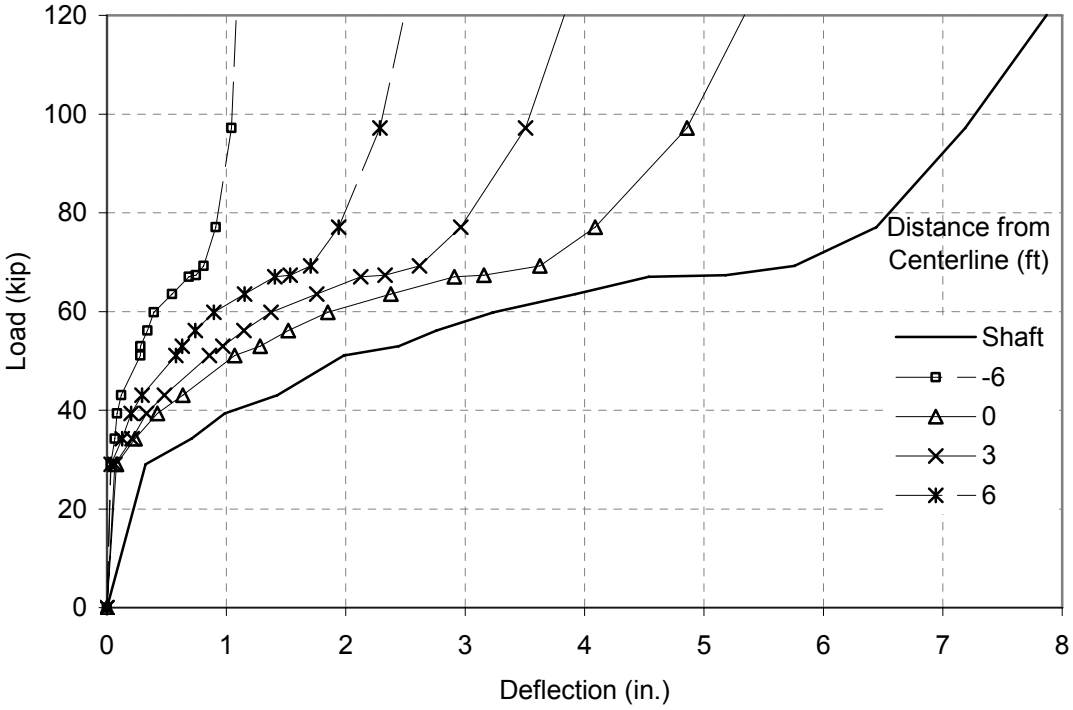

Figure 4.3.28 Shaft BG1 deflection in horizontal direction el. 17.7 feet

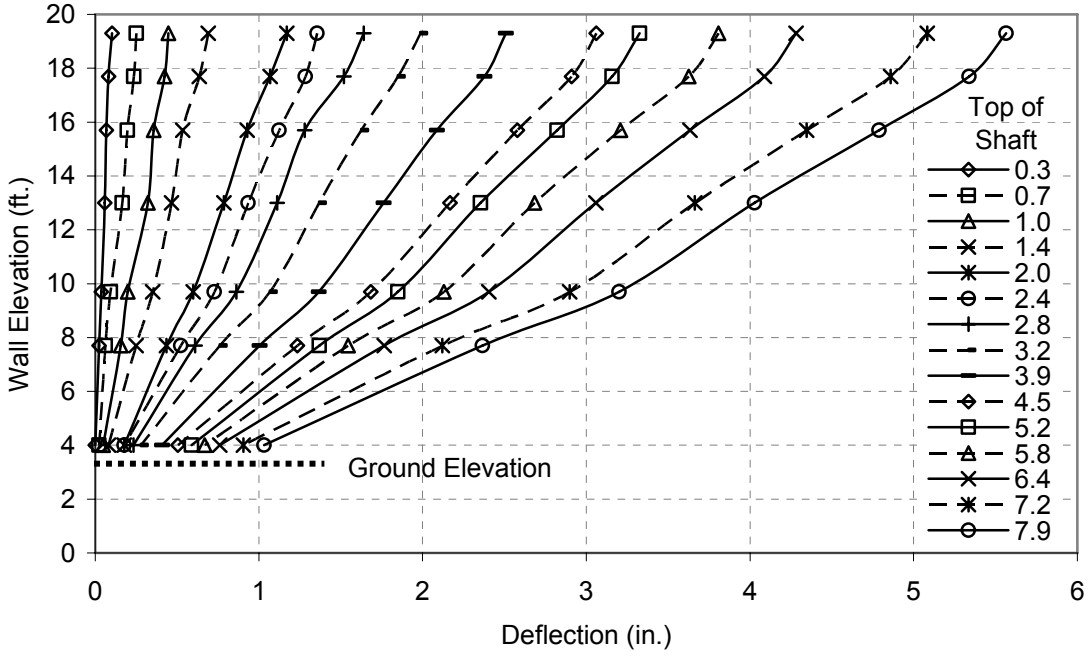

Figure 4.3.29 Shaft BG1 incremental centerline vertical deflection of wall face

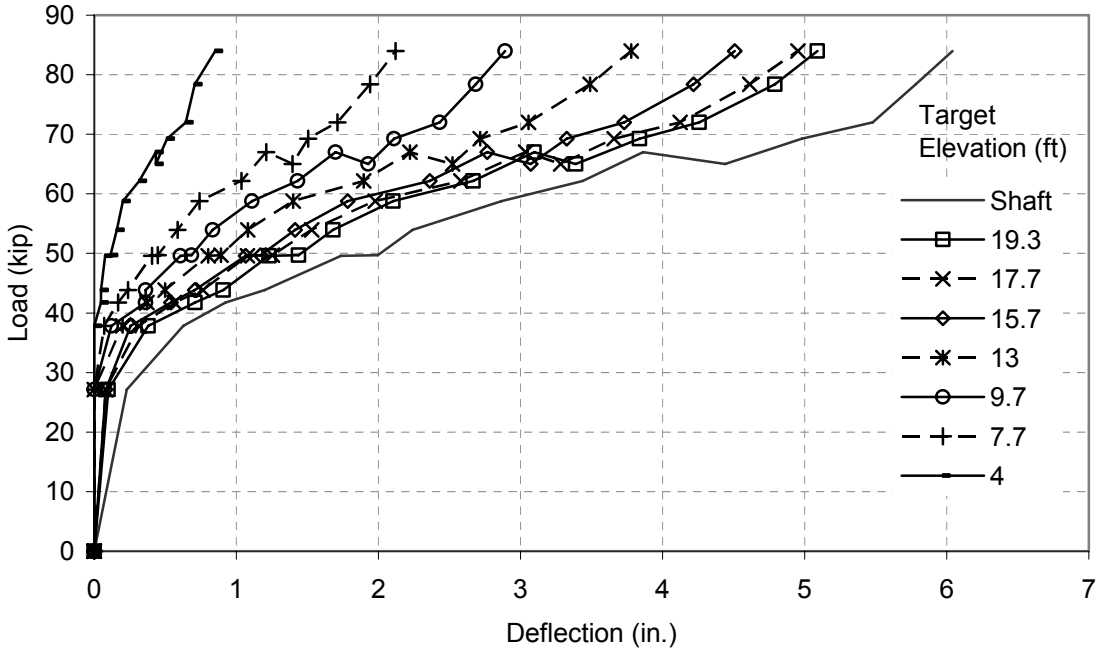

Figure 4.3.30 Shaft BG3 centerline deflections

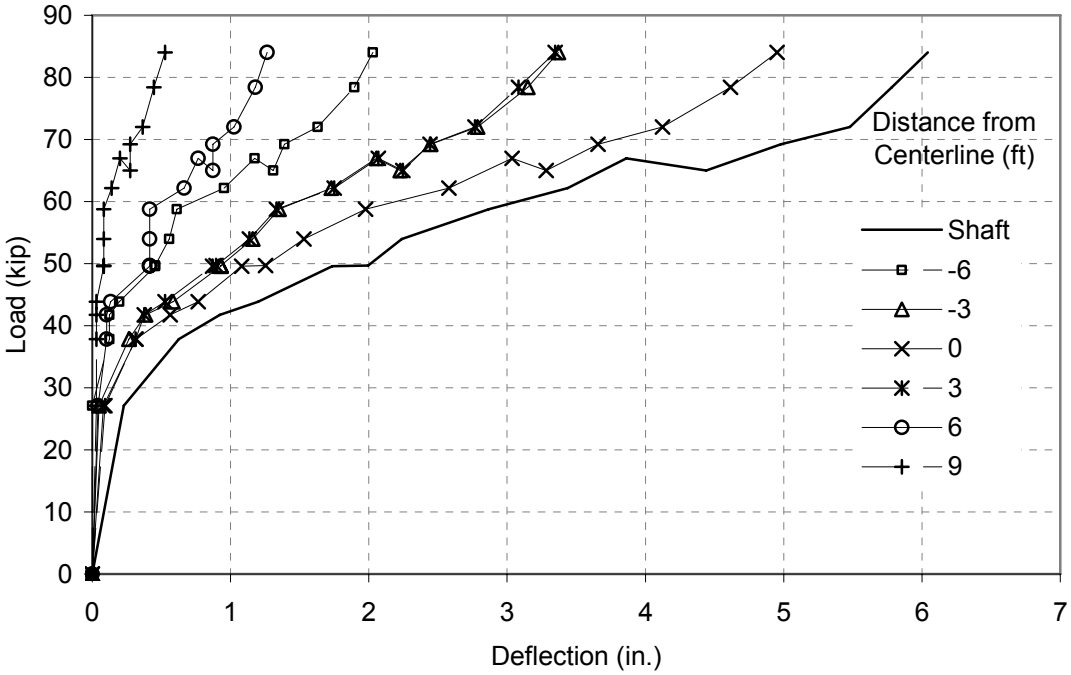

Figure 4.3.31 Shaft BG3 deflection in horizontal direction el. 17.7 feet

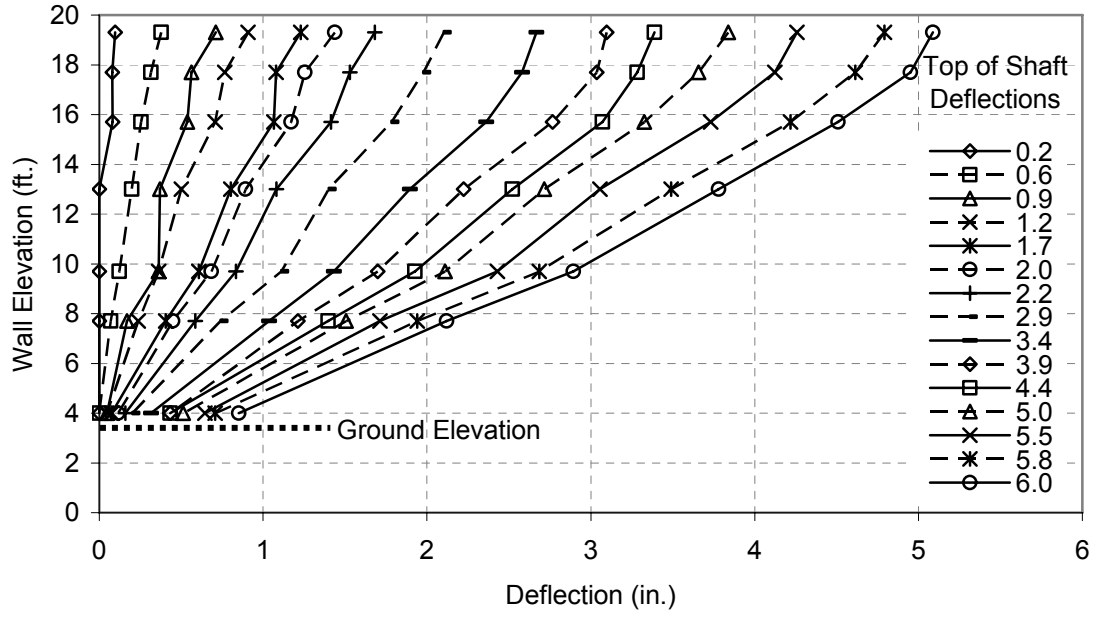

Figure 4.3.32 Shaft BG3 incremental centerline vertical deflection of wall face

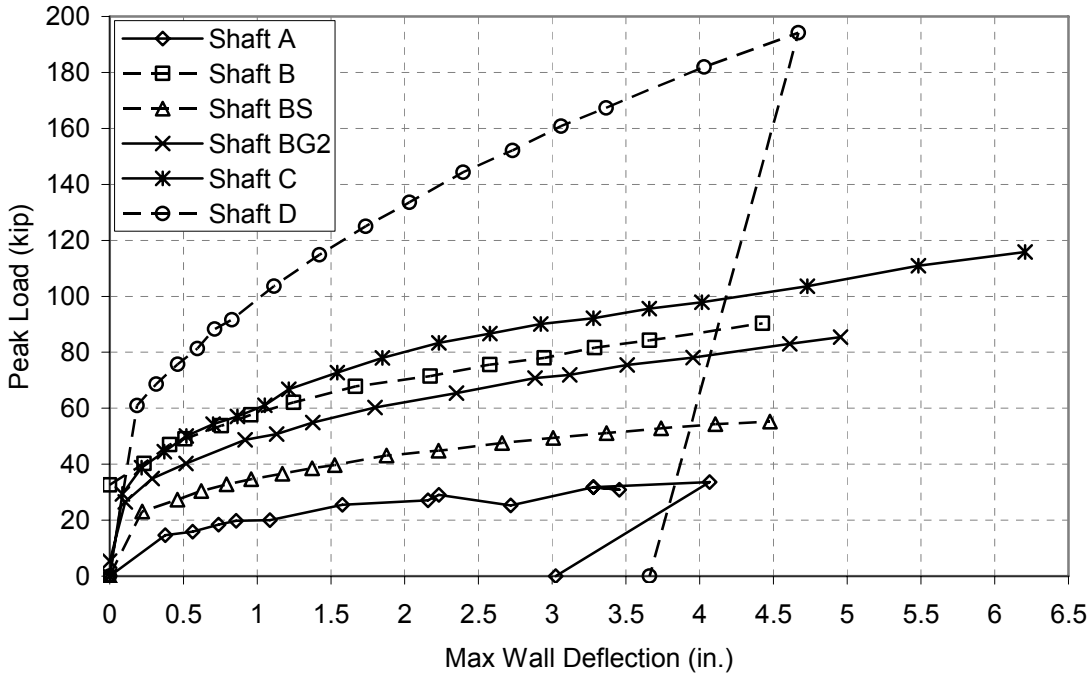

Figure 4.3.33 Peak load vs. maximum wall deflection for all shafts

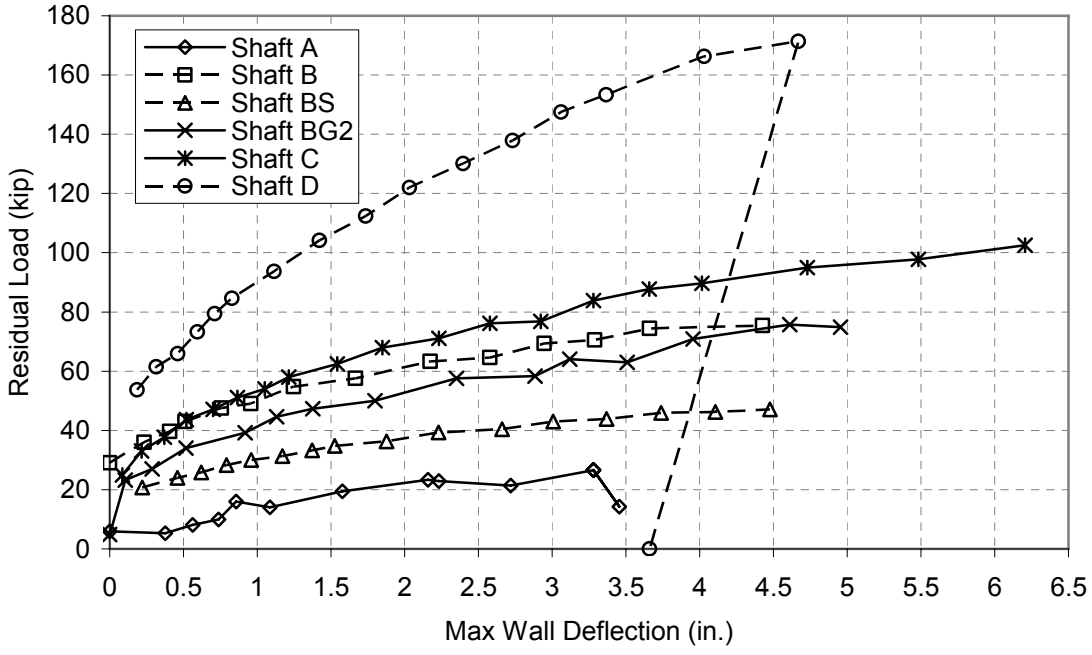

Figure 4.3.34 Residual load vs. maximum wall deflection for all shafts

Table 4.3.1 Peak Load vs. Maximum Wall Deflection

Shaft	Dist. From Facing (in.)	Peak Load (kip)					
Maximum Wall Deflection		0.5"	0.75"	1"	2"	4"	Ultimate
A	36	12	15	18	26	33	33
BS	72 (15' Length)	28	33	35	43	53	55
BG2	72 (15 Spacing)	40	45	50	62	78	85
B	72	48	54	58	70	87	90
C	108	50	55	60	80	98	116
D	144	77	88	99	134	182	194

Table 4.3.2 Residual Load vs. Maximum Wall Deflection

Shaft	Dist. From Facing (in.)	Residual Load (kip)					
Maximum Wall Deflection		0.5"	0.75"	1"	2"	4"	Ultimate
A	36	8	10	15	22	-	27
BS	72 (15' Length)	24	29	31	37	46	47
BG2	72 (15 Spacing)	34	37	41	43	41	46
B	72	43	48	50	61	75	76
C	108	43	49	52	69	90	102
D	144	78	82	90	122	166	171

4.4 Pressure Cell Data

Three pressure cells were installed in front of each shaft at elevations of 7.7, 13.7, and 17.7 feet. This made for a total of 24 cells. Of those, 21 were mounted in a recession within a concrete block using nonshrink grout. Pressure cells mounted in this way were tested and confirmed to provide reliable results. The block and pressure cell were placed against the back of the wall facing in front of the shafts. Three were not encased in concrete, instead they were filled with aggregate behind the pressure cell. Both methods used a sand bag in front of the pressure cell to prevent puncture of the membrane. Those pressure cells not mounted to concrete blocks are located in front of Shaft A at 7.7 feet and Shaft BG3 at elevation 13.7 feet and 17.7 feet. Figure 4.4.1 shows a plot of Shaft A's three pressure cells, the load on that shaft, and the shaft deflection. The pressure at

the beginning of the test was set to zero so this plot shows change in pressure from the start of the test. To read, find a point that is of interest. Load, lateral pressure, and shaft movement for that point of interest can be found by holding the time constant and reading the desired value off the axis. Load and pressure share the same axis and scale. If reading load then the unit is kip. If reading pressure the units are pounds per square foot. Shaft deflection is based on LVDT readings at two feet above the surface. The right axis reads deflection in inches.

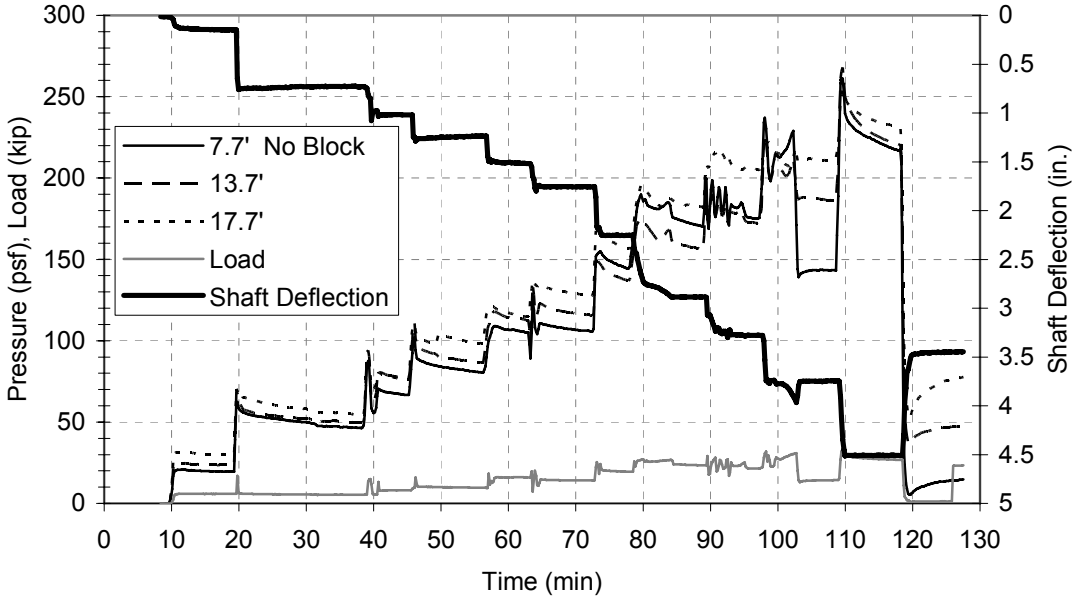

Figure 4.4.1 Shaft A pressure cells, load, and deflection of the shaft

Figure 4.4.2 shows the same plot for Shaft B. Compared to Shaft A the loads, and pressures drop off much faster. At different pressure cell elevations there is also some deviation of pressure increase. The pressure at 13.7, and 7.7 feet elevations increase more then the pressure cell at 17.7 feet elevation. This can be seen for Shafts BG1 and BG3 (Figure 4.4.4 and 4.4.5). The behavior could be a result of vertical confinement

being lower for the upper cell, or it could be due to wall rotation in the upper half of the wall reducing horizontal confinement.

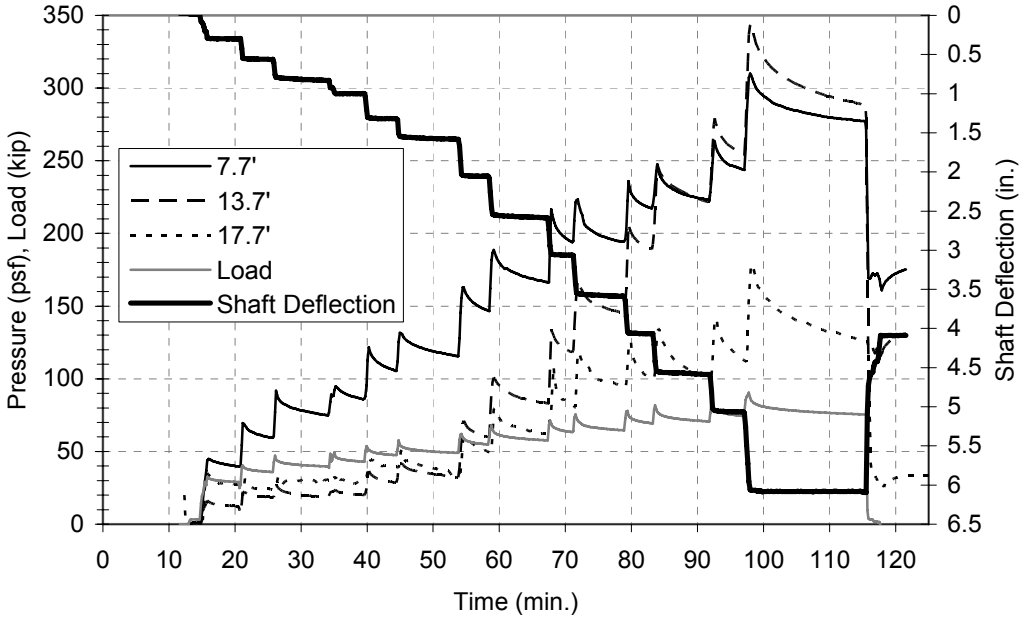

Figure 4.4.2 Shaft B pressure cells, load, and deflection of the shaft

Figures 4.4.3 and 4.4.4 show Shafts BG2 and BG3. BG3 is shown because it contained pressure cells that were not encased in concrete. The values of the pressure cells that were encased in concrete are very comparable to those who were not encased. Behavior in both shafts was similar to Shaft B.

Shaft BS pressure changes can be found in Figure 4.4.5. The effect of the decrease in length of five feet can be seen in this figure also. Here the upper cell detected the greatest increase in pressure and the lower cell detected the least increase in pressure. This is a considerably different behavior then for Shaft B. The value of pressure at the upper location is very comparable to Shaft B, both being near 200 psf at six inches of deflection.

Shaft C and D behaved in a very similar way. Figure 4.4.6 shows Shaft C. Cells for both Shaft C and D at the lowest (7.7') elevation experienced a similar maximum pressure at eight inches of deflection. Both shafts show an intermediate pressure at the middle (13.7') elevation, and the highest pressure cell measured the lowest pressure change.

Figure 4.4.7 shows shaft D. This graph shows pressure falling during the test for the highest pressure cell at elevation 17.7 feet. This is either a failure of the cell, or it shows that pressure at lower elevations caused the wall facing to rotate out producing a net decrease in pressure on the upper cell.

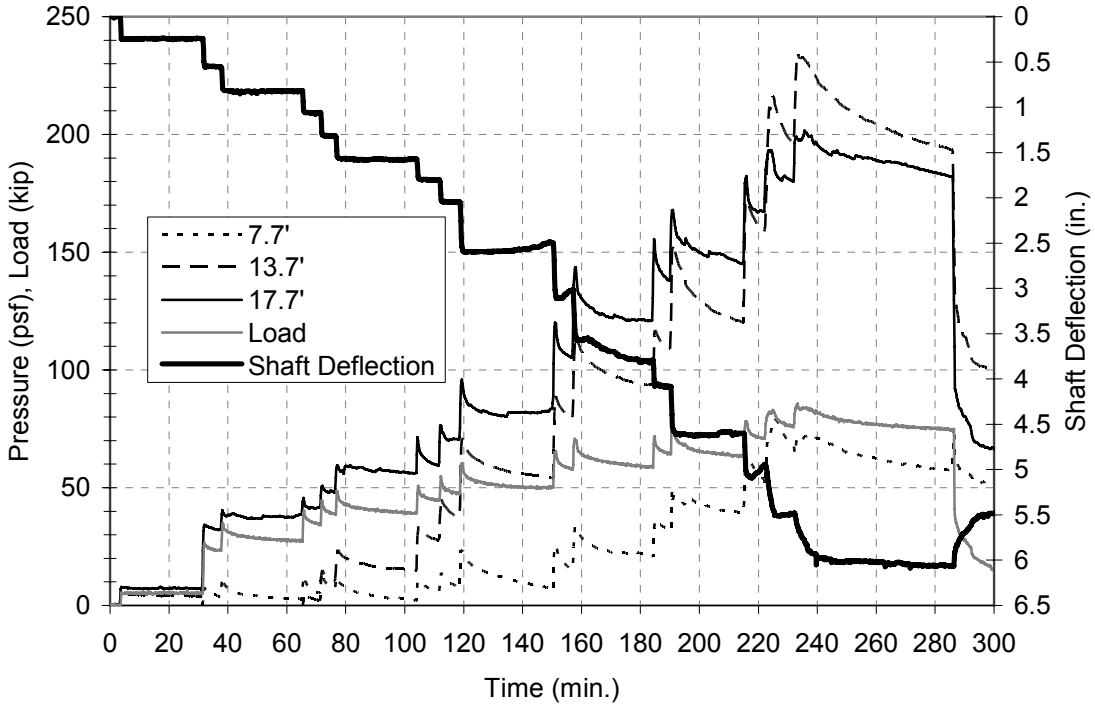

Figure 4.4.3 Shaft BG2 pressure cells, load, and deflection of the shaft

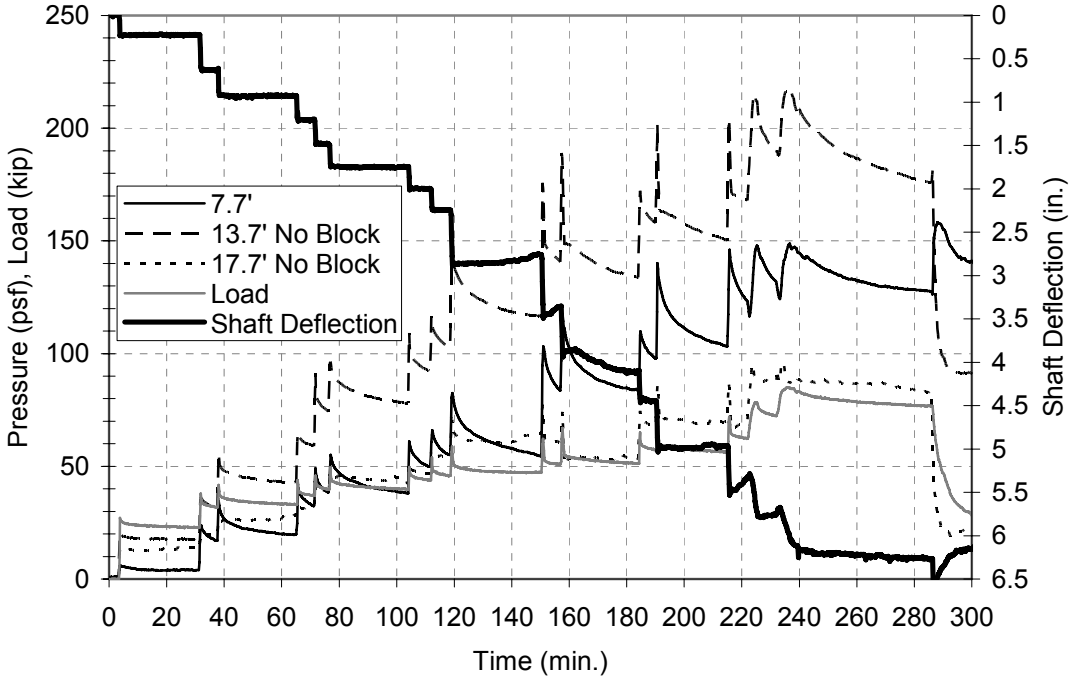

Figure 4.4.4 Shaft BG3 pressure cells, load, and deflection of the shaft

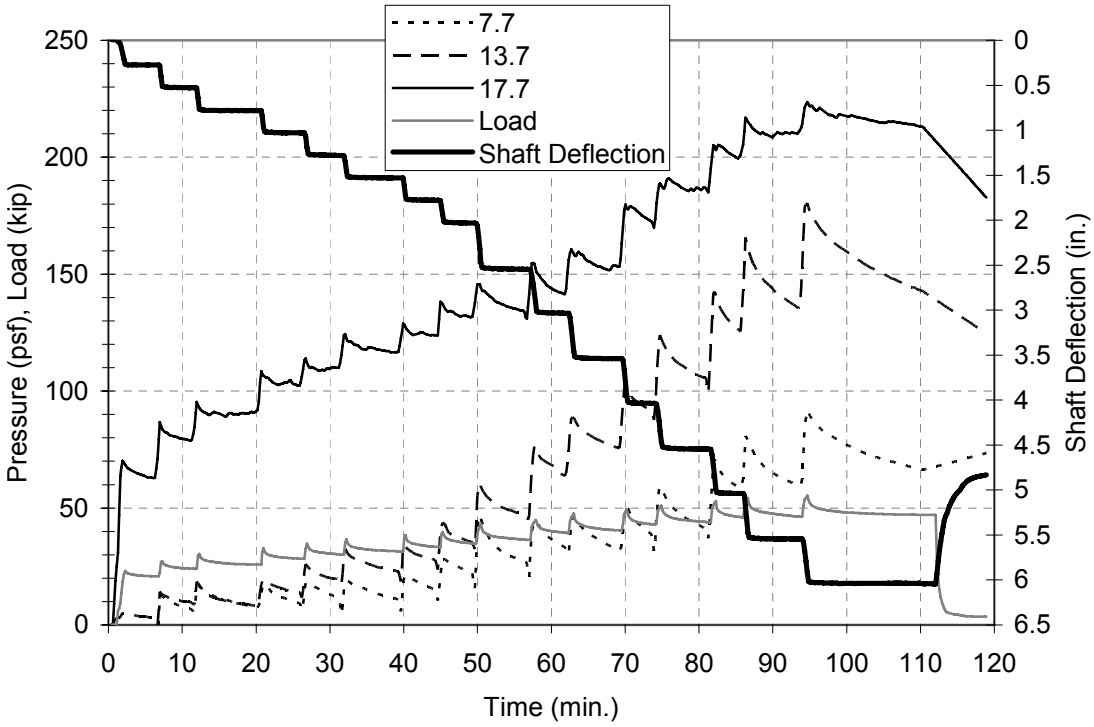

Figure 4.4.5 Shaft BS pressure cells, load, and deflection of the shaft

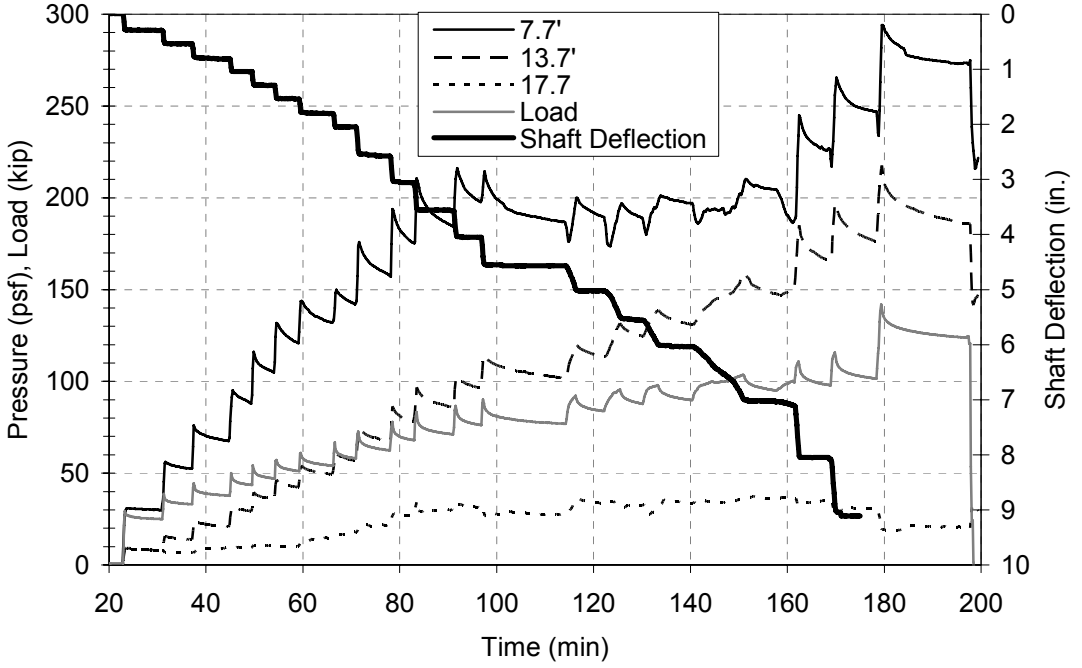

Figure 4.4.6 Shaft C pressure cells, load, and deflection of the shaft

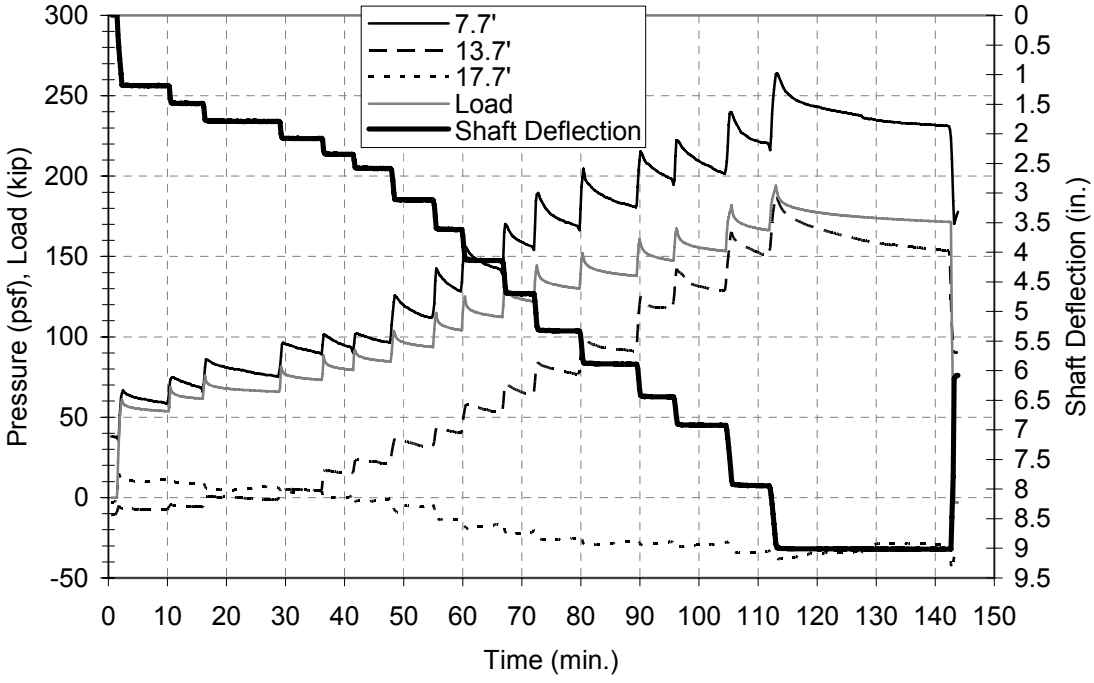

Figure 4.4.7 Shaft D pressure cells, load, and deflection of the shaft

4.5 Surface Observations

The topsoil cover was compacted and relatively dry at the time of testing. This topsoil cracked during the testing process, and these cracks are documented in the next pages. During testing all shafts had cracks form behind the shafts due to caving and from the sides at a diagonal toward the wall facing as a result of shaft movement. Figure 4.5.1 shows typical cracks that formed directly behind each shaft. Figure 4.5.2 shows typical cracks that formed at a diagonal to the sides of the shaft. During the group test a large crack developed at a distance of between 13.5 feet and 14.5 feet from the back of the wall that ran parallel to the wall face. This is the same location as the end of the reinforced zone. It is believed this crack is a result of sliding of the geogrid toward the wall facing due to failure in pullout (Figure 4.5.3).

After testing of the group was performed, a section of geogrid between two of the shafts was exhumed (Figure 4.5.4). This geogrid was then measured for elongation of the grid. The data from this is presented in Figure 4.5.5.

Figure 4.5.1 Surface cracks due to caving on back of shaft

Figure 4.5.2 Diagonal surface cracks

Figure 4.5.3 Crack developed above the end of reinforcement during group test

Figure 4.5.4 Exhumed geogrid between shafts BG1 and BG2

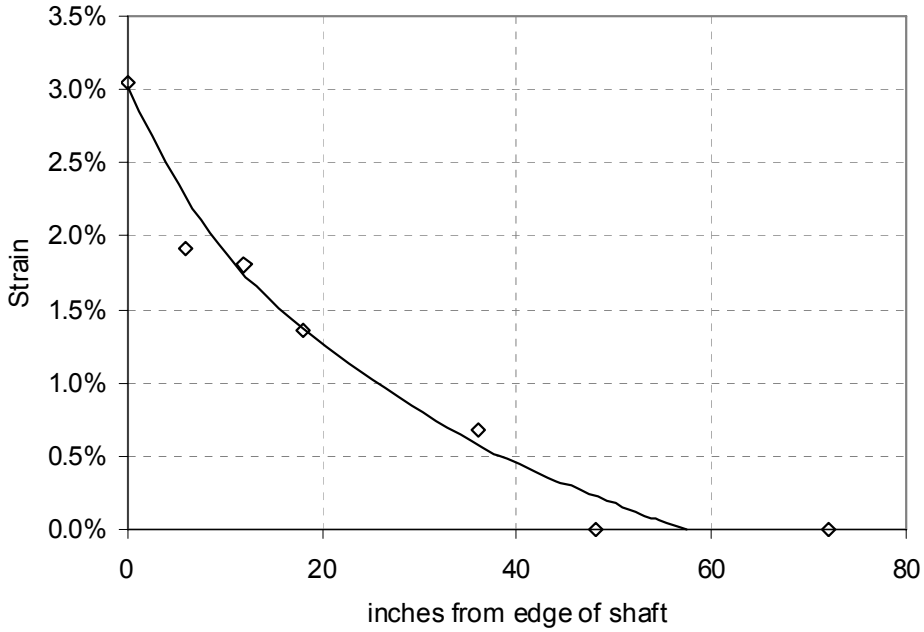

Figure 4.5.5 Strain geogrid layer at 18.7 feet elevation between shafts BG1 and BG2

Chapter 6

Applications, Conclusions and Recommendations

6.1 Expected Wind Load for Sound Walls and other Structures

The Minnesota Department of Transportation estimates a design wind speed of 75 mph for all sound wall type applications. This produces a pressure of 23 psf and load comparable to the loading that was applied to the test Shafts (6500 lb) for a 15 x 15 foot tributary area. A speed of 75 mph is typical for a wall designed in an area with significant cover from near structures, or dense woodlands that is not designed for an extreme event like a tornado. For the same 15x 15 area if the wind speed is increased to 90 mph the pressure and load become 33 psf and 9330 lb. A design wind speed of 90 mph would be used for a wall in an area with little cover from buildings or trees without consideration of an extreme event. For a wind speed of 200 mph, for the same 15 x 15 tributary area, the pressure and load become 163 psf, or 46,000 lb (MnDOT). An extreme event by definition is rare so the application of a wind speed of 200mph would indicate that the structure must perform in all but the most extreme events. The following sections contain recommendations for design and future testing given these loading conditions and state conclusions developed from the tests performed.

6.2.1 Allowable Deflection

Due to the geometry of the facing blocks and the irregularity of the surface, the aesthetics of the wall system were only slightly harmed. The deflection of the wall was only evident from the top of the wall looking down, or from the side looking at the profile. The deflection that could be seen was only visible upon close inspection. This indicates that only large deflections would be objectionable if aesthetics were of

particular interest or concern. Figures 6.2.1 – 6.2.4 show pictures of the deflected wall facing as a result of the group of three shafts that were tested (BG1, BG2, BG3). Figure 6.2.1 is highlighted by the noon sun. This is the only time that deflection of the wall facing is noticeable looking directly at the wall as shown in Figure 6.2.2. The deflection can be seen from the top of the wall looking down the side (Figure 6.2.3), but is much less noticeable from below the wall looking at the profile (Figure 6.2.4).

Figure 6.2.1 Final facing deflection of the group of test shafts noon (5.3 inches, max facing movment)

Figure 6.2.2 Final facing deflection of the group of test shafts afternoon (5.3 inches, max facing movement)

Figure 6.2.3 Profile of final wall deflection for group of test shafts

Figure 6.2.4 Side view of group wall facing final deflection

6.3 Shaft Strength

The three shaft variables affecting strength that were evaluated during these tests are distance from the wall facing, depth of shaft, and the influence of neighboring shafts.

6.3.1 Strength Based on Distance From the Wall Facing

This discussion is based on a length of shaft of 20 feet and a shaft diameter of 36 inches. Design loads that are based on either 75 or 90 mph winds rather then 200 mph

will be experienced more often during the life of the structure. As a result, reductions in allowable design load will be needed to account for the repeated nature of loading. Therefore two different sets of design values are provided based on different factors of safety. The first is based on a strength reduction of 2, or one half of the test load, associated with structures that are designed to withstand an extreme event. The strength reduction of 3 will be used for structures that are designed to withstand a large storm. If designing for the extreme event, other events must be checked due to the higher factor of safety associated with those more recurrent smaller events. Table 6.3.1 shows the ultimate residual load for a test shafts divided by the strength reduction factor of 2 or 3 depending on the design case. These values of loading are based on the ultimate residual lateral load that the shaft can resist. This is due to the length of time that a wind speed can be sustained. If the load were an impact load the peak load measured would be more appropriate.

6.3.2 Strength Based on Length of Shaft

At this time if a shaft must be designed to be 15 feet instead of 20 feet then a recommendation can only be made for a 36 inch diameter shaft that is 72 inches, two shaft diameters, from the wall facing. (Table 6.3.1)

6.3.3 Influence of Neighboring Shafts (Group Effect) on Ultimate Strength

Study of the influence of neighboring shafts was only conducted on the shafts that were 72 inches, or two diameters, from the wall facing. The influence area is described as the area with a wall deflection greater then 10 percent of the maximum wall facing deflection. These results are tabulated in Table 6.3.1. See Figure 6.3.1 for spacing other

then those in Table 6.3.1. When designing a shaft spacing of 15 feet, and distance from the wall facing of 72 inches use values obtained from the Group tests.

Table 6.3.1 Distance from Wall Facing vs. Allowable Lateral Load and Influence Length

Test Shaft ID	Distance (in.) Center of shaft to Back of Wall Facing	Measured Residual Load (kip)	Allowable Lateral Load (kip) Factor of Safety 2	3	Required Shaft Spacing (ft) To avoid Influence
A	36	27	13.5	9.0	10
B	72	75	37.5	25.0	17
BS	72 (15' Length)	47	23.5	15.7	17
BG2	72 (15 Spacing)	75	37.5	25.0	-
C	108	102	51.0	34.0	20
D	144	171	85.5	57.0	26

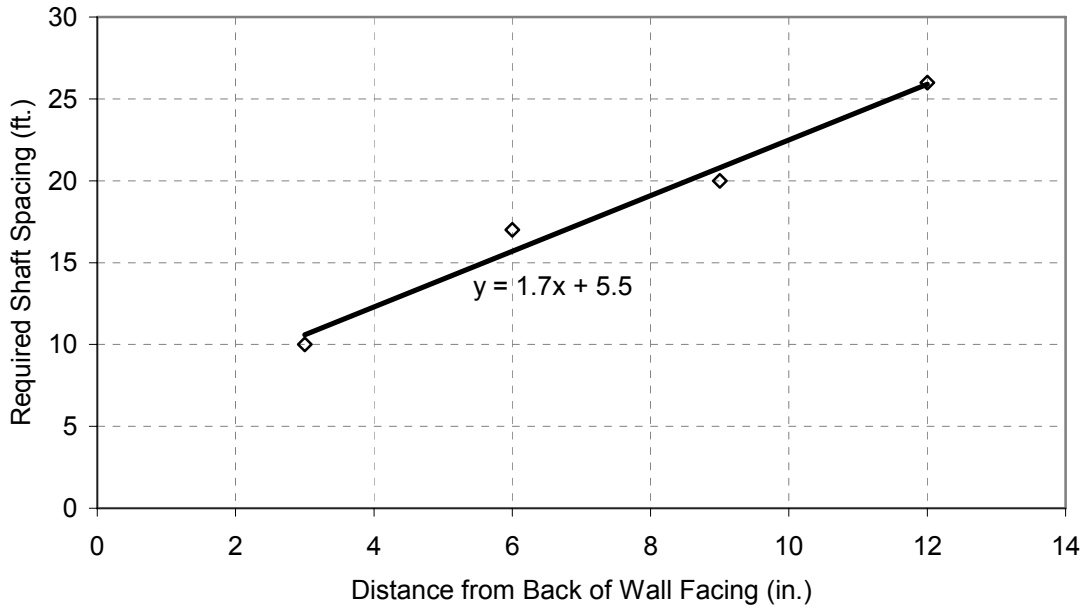

Figure 6.3.1 Distance from back of wall vs. required spacing to avoid influence from neighboring shafts.

6.4 Service Limit State Recommendations

Limitations on deflection of the shafts or the wall facing will often control the design. Therefore design values of allowable load for a particular deflection are presented in this section. These values are based on the residual load that was generated

during testing that is associated with the deflection of interest. Table 4.2.2 shows residual load for each shaft configuration at different shaft deflections. Shafts were assumed to pivot at the base of the shaft and there was no bending of the shaft. Table 4.3.2 shows residual load for each shaft configuration at different maximum wall facing deflections. For deflections at locations other then the location of maximum wall deflection, figures from section 4.3 should be used to determine the residual load that would produce the deflection in question.

Table 4.2.2 Residual Load vs. Shaft Movement

Shaft	Dist. From Facing (in.)	Residual Load (kip)					
Displacement		0.5"	0.75"	1"	2"	4"	Ultimate
A	36	5.3	5.3	8	17	27	27
BS	72 (15' Length)	24	26	28	35	41	47
BG2	72 (15 Spacing)	25	28	30	43	58	75
B	72	36	40	44	55	69	75
C	108	34	39	44	58	76	102
D	144	-	-	50	74	110	171

Table 4.3.2 Residual Load vs. Maximum Wall Deflection

Shaft	Dist. From Facing (in.)	Residual Load (kip)					
Maximum Wall Deflection		0.5"	0.75"	1"	2"	4"	Ultimate
A	36	8	10	15	22	-	27
BS	72 (15' Length)	24	29	31	37	46	47
BG2	72 (15 Spacing)	34	37	41	43	41	46
B	72	43	48	50	61	75	76
C	108	43	49	52	69	90	102
D	144	78	82	90	122	166	171

6.5 Recommendations For Further Research

Future testing and analysis should be conducted to expand the application of this type of design. Cyclic loading was not considered and a strength reduction should be considered if cyclic loading is present. More testing should be considered to estimate the

influence the effect of different backfill material, types of geogrid, facing type, and different reinforcement geometries. The effect of different spacings could also be evaluated for other shaft distances from the facing. Another option, in addition to full scale testing, to determine these variables would be to use numerical modeling. Modeling may be used to simulate the testing that was performed and then modified to determine the effects of varying aspects of the design.

References:

1. FHWA, "Mechanically Stabilized Earth Walls and Reinforced Soil Slopes – Design and construction Guidelines," August 1997. FHWA-SA-96-071.

2. Anderson, Peter L., "Increased Use of MSE Abutments," International Bridge Conference 2005 IBC-05-10. The Reinforced Earth Company, North Reading, MA.

3. Tensar Earth Technologies, "Demonstration of Pile Driving through the HDPE Geogrid Reinforced Soil Fill of Full-Height Precast Concrete Panel Faced, Mechanically Stabilized Earth Wall," 2001 Report, Colorado E-470 Project.

4. Johnson, Rebecca, "Soil Characterization and P-Y Curve Development for LOESS."

5. Minnesota Department of Transportation, "Noise Analysis: Guidelines for the Evaluation of Noise Barrier Designs" Office of Environmental Services.

6. FHWA, "Design and Construction of Driven Pile Foundations", November 1998. FHWA-HI-97-013.

7. KDOT "KDOT Project: RE-0446-01 Grading Cross Section", March 2007.

8. Tensar Earth Technologies, Inc. "Construction Drawings: I-435 and Leavenworth Rd Interchange", April 2007.

Appendix

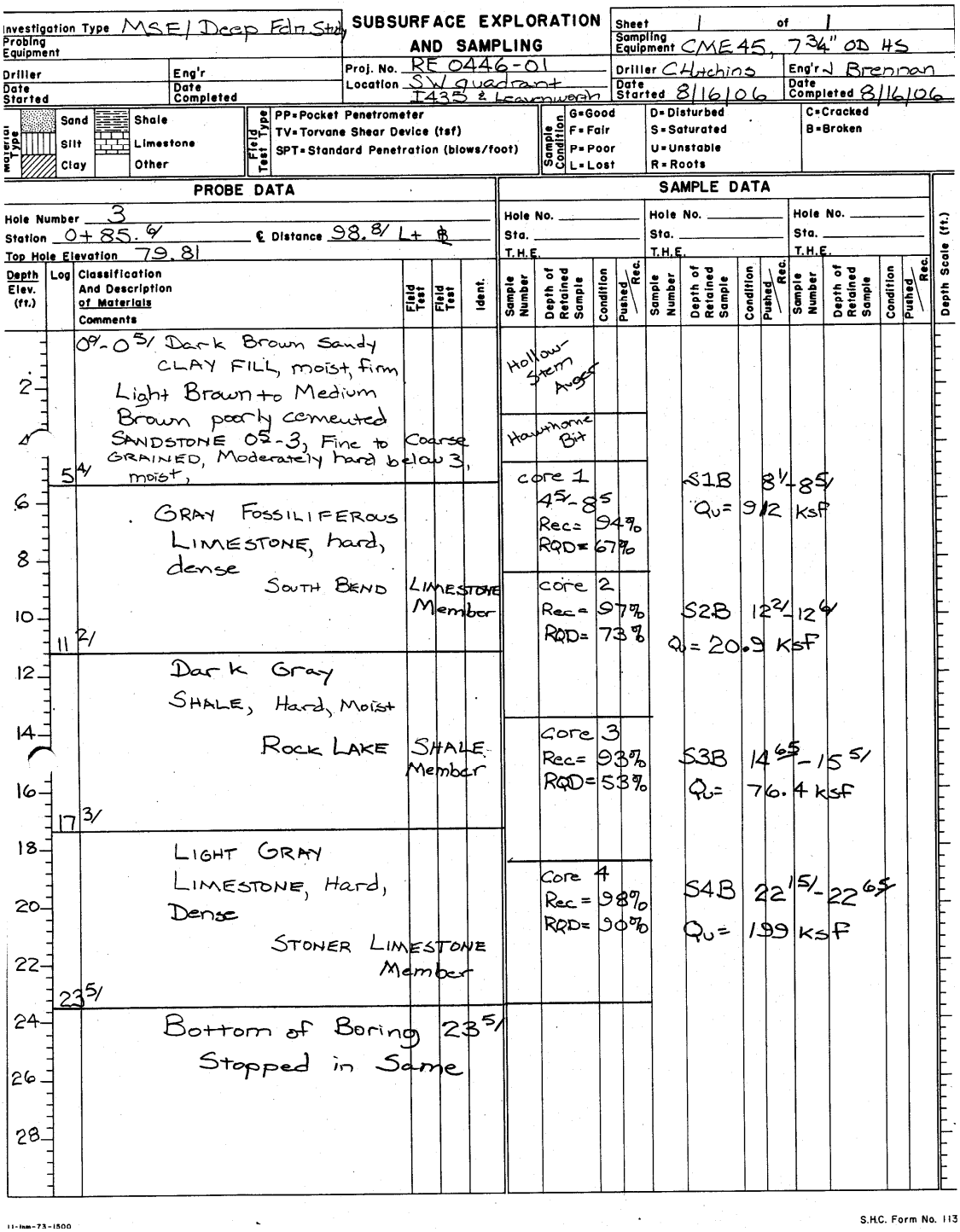

Figure A.1 Typical Boring Log

Table A.1 Test Results for Rock Samples

Sample No.	Station	Offset (FT)	Depth (FT)	Description	Unconfined. Compression Qu (psf)	Elastic Modulus E (psf)	Dry Density γ_d (pcf)	Moisture Percent w %
S1A	1+80.3	102.3 Lt	5.2-6.25	Lt gray limestone	997000	171000000	163	1.4
S2A	1+80.3	102.3 Lt	9.3-10.1	Dk gray shale	26900	1450000	125	14.6
S3A	1+80.3	102.3 Lt	13.5-14.2	Dk gray shale	*	*	136	1.4
S1B	0+85.6	98.8 Lt	8.1-8.5	Lt gray limestone	912000	95400000	160	1.7
S2B	0+85.6	98.8 Lt	12.2-12.6	Dk gray shale	20900	2780000	138	6.2
S3B	0+85.6	98.8 Lt	14.65-15.5	Dk gray shale	76400	1890000	135	8.5
S4B	0+85.6	98.8 Lt	18.5-23.5	Lt gray limestone	199000	53900000	149	4.5

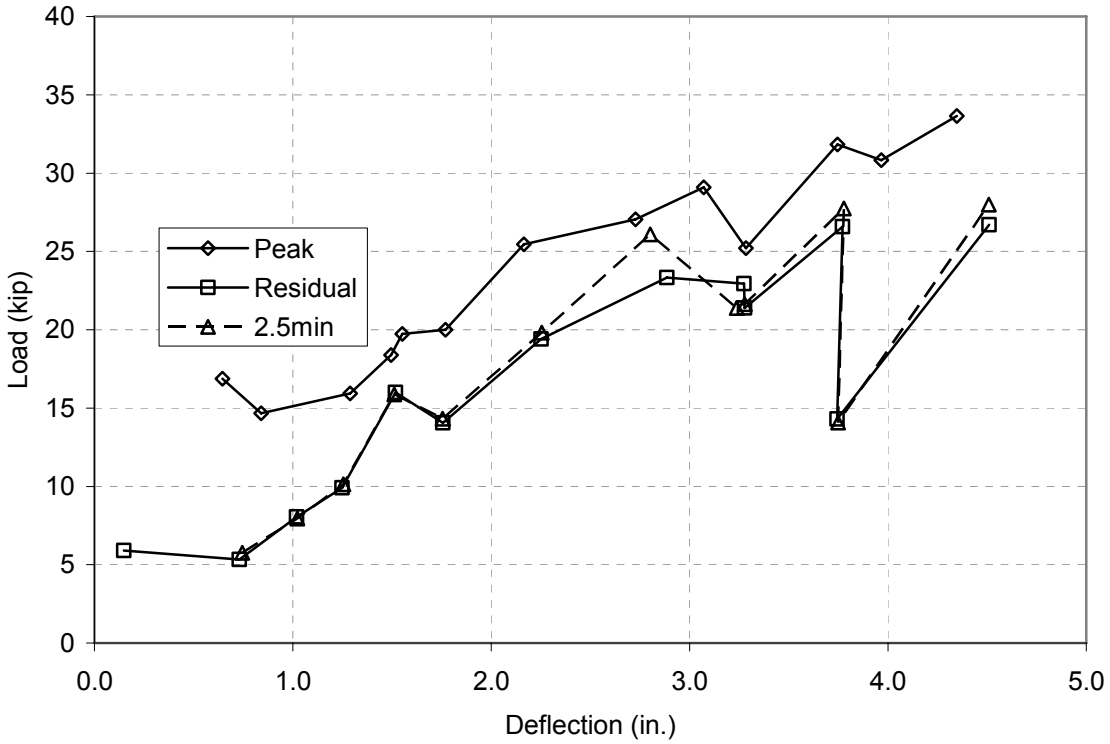

Figure A.2 Shaft A Peak, 2.5min, and Residual Load vs. Deflection

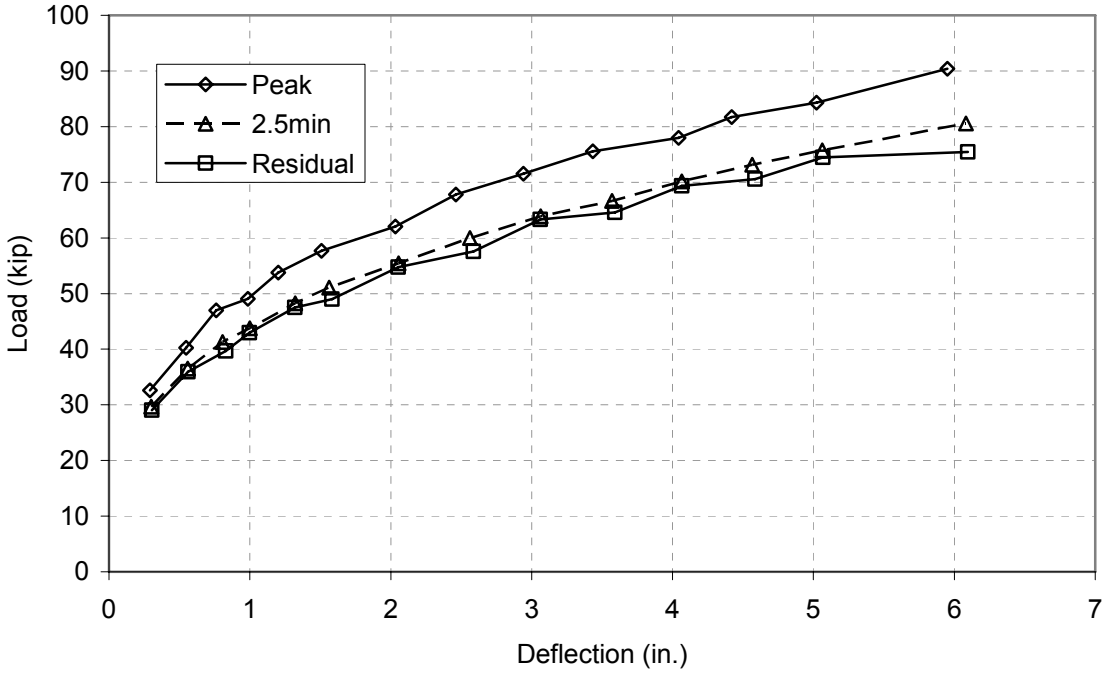

Figure A.3 Shaft B Peak, 2.5min, and Residual Load vs. Deflection

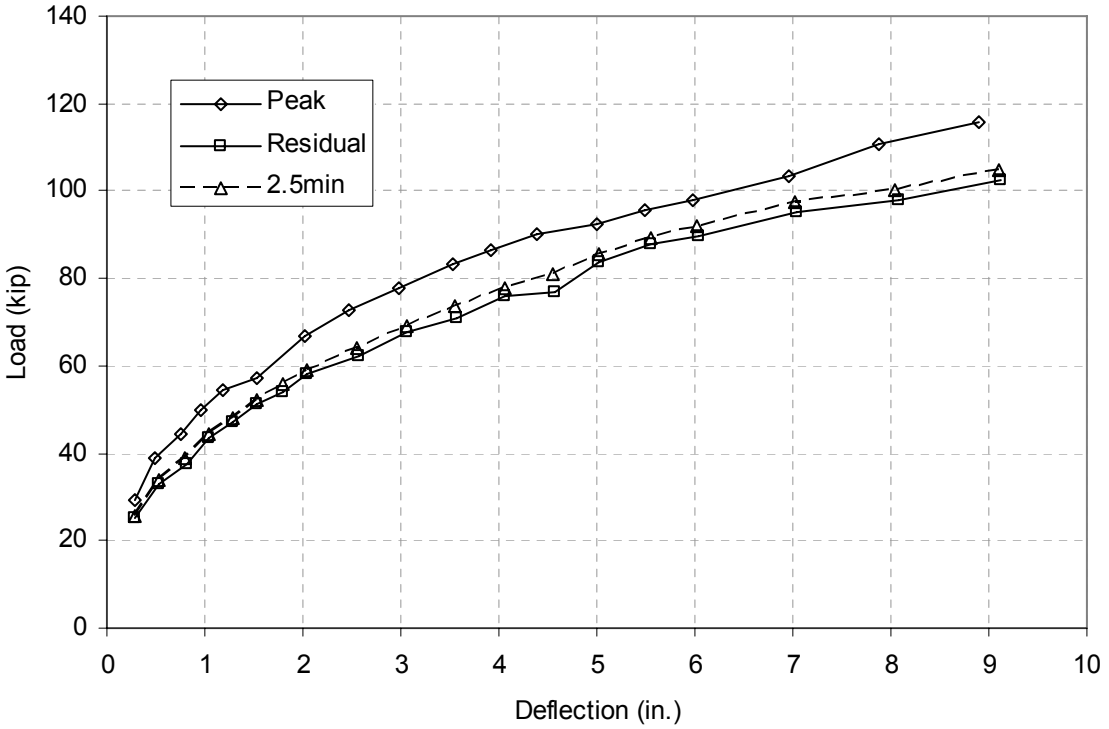

Figure A.4 Shaft C Peak, 2.5min, and Residual Load vs. Deflection

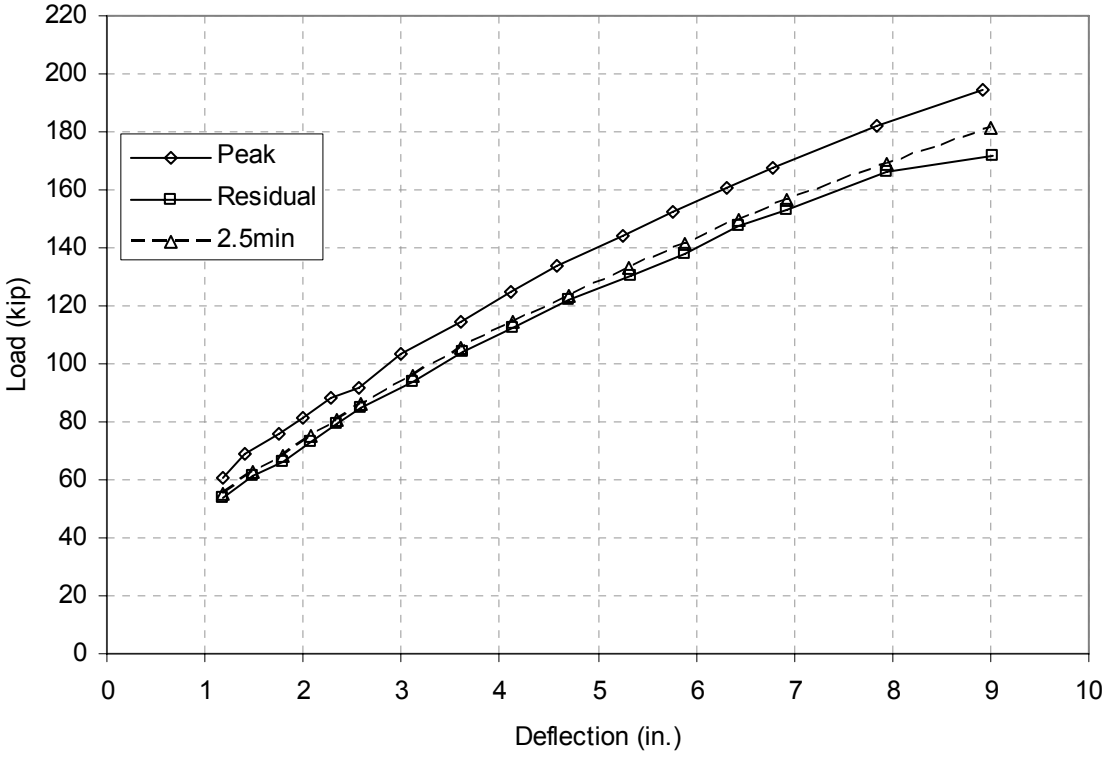

Figure A.5 Shaft D Peak, 2.5min, and Residual Load vs. Deflection

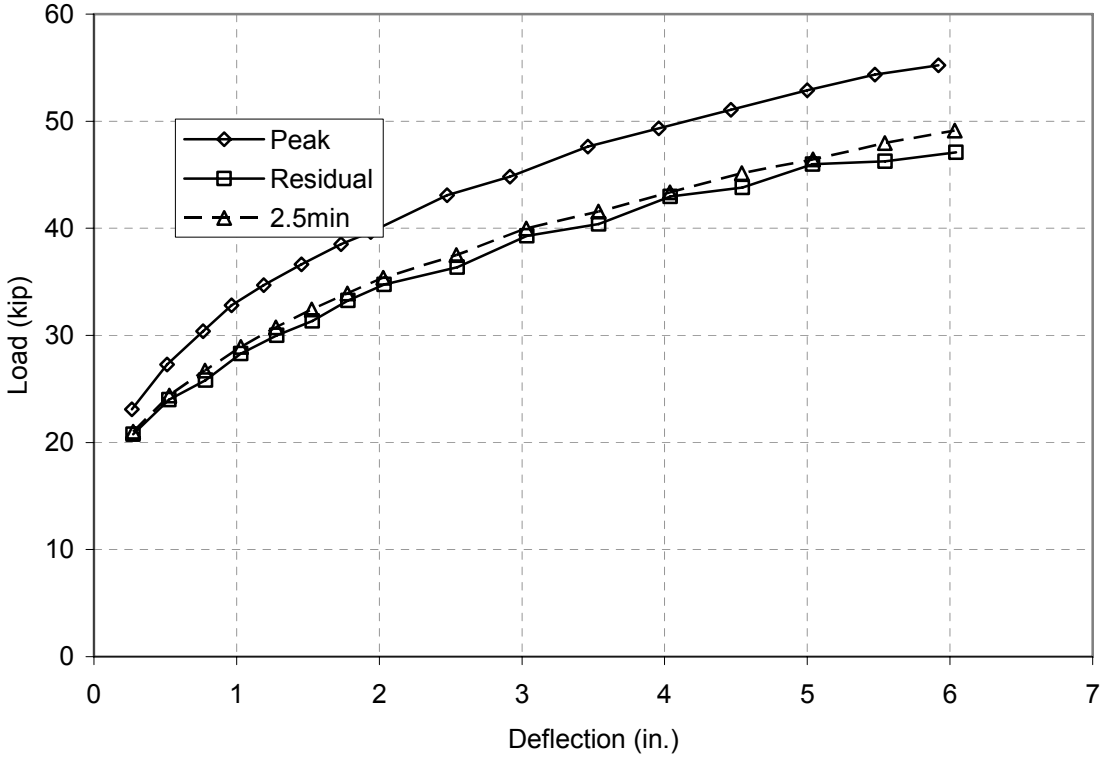

Figure A.6 Shaft BS Peak, 2.5min, and Residual Load vs. Deflection

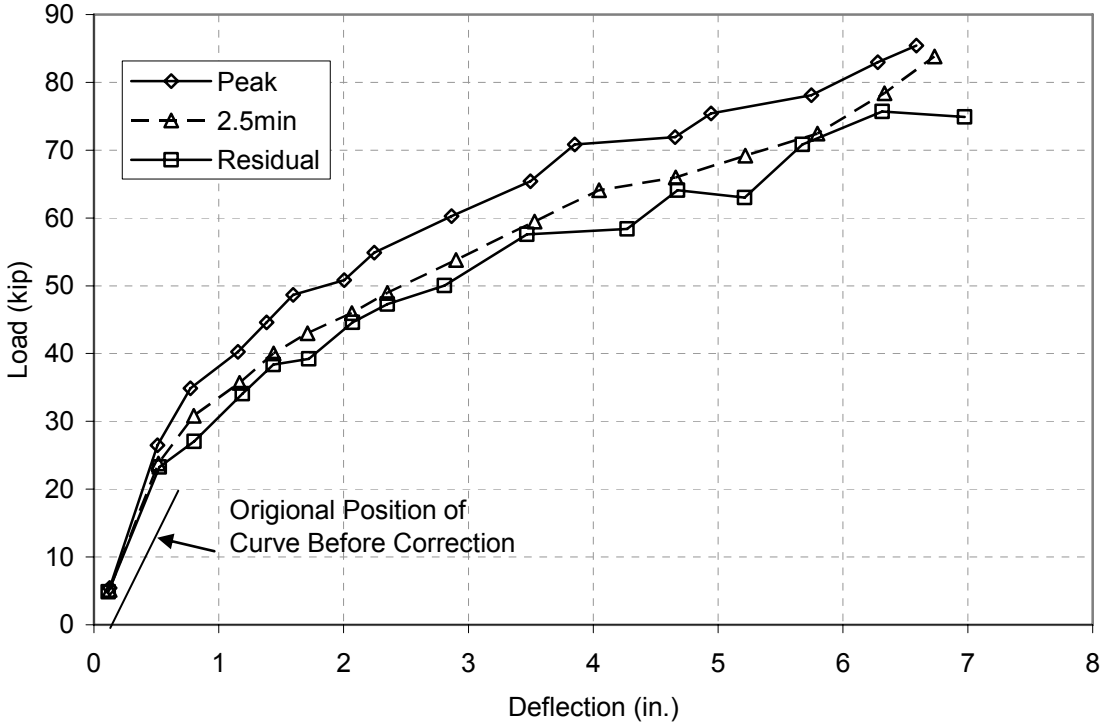

Figure A.7 Shaft BG2 Peak, 2.5min, and Residual Load vs. Deflection

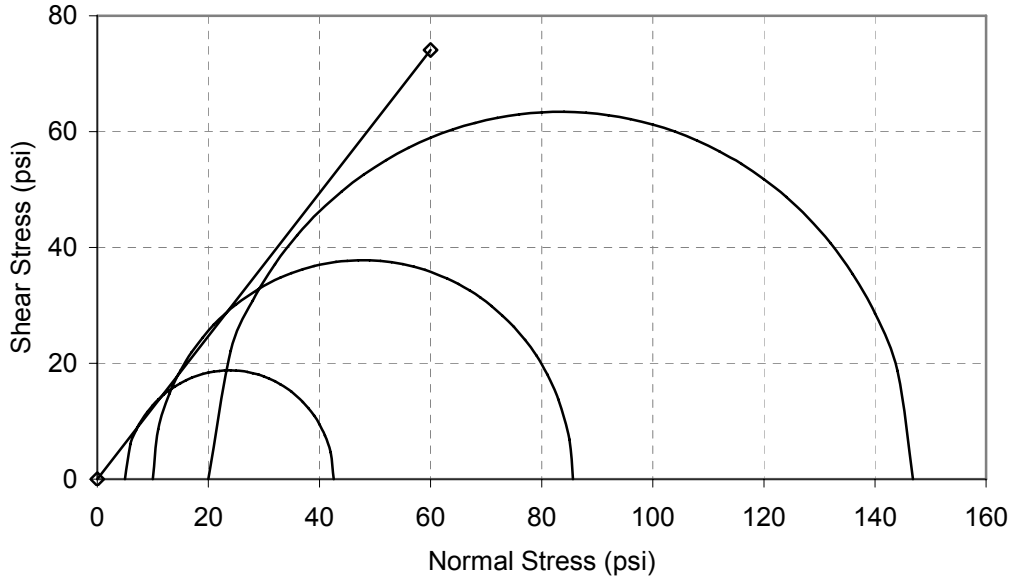

Figure A.8 Mohr's circle at failure for 5, 10, and 20 psi cell pressure

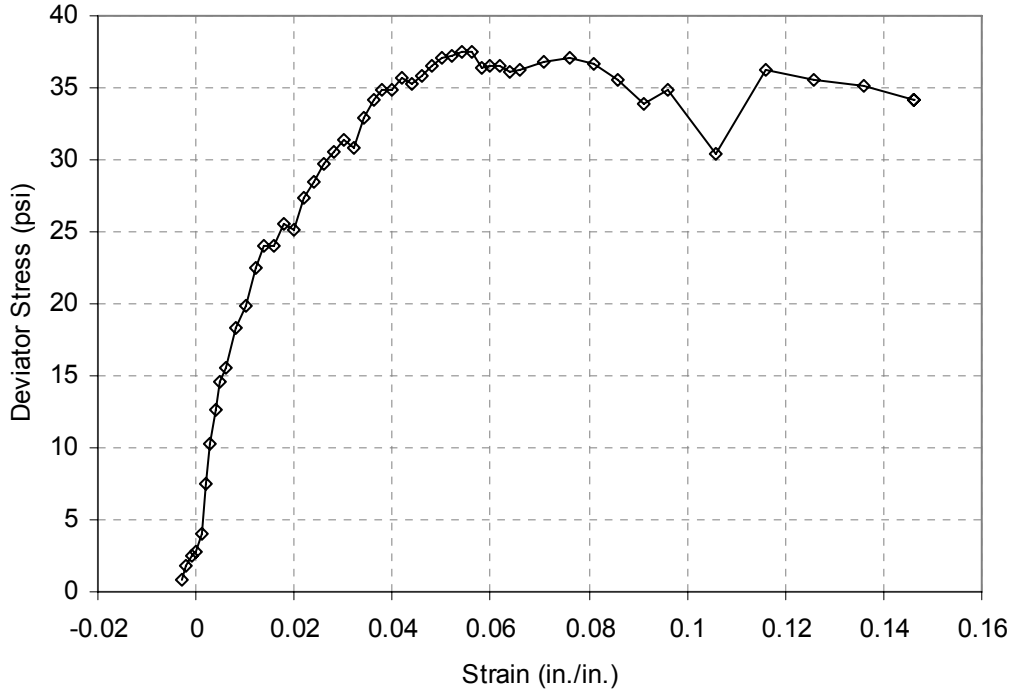

Figure A.9 Tri-axial plot 5psi cell pressure

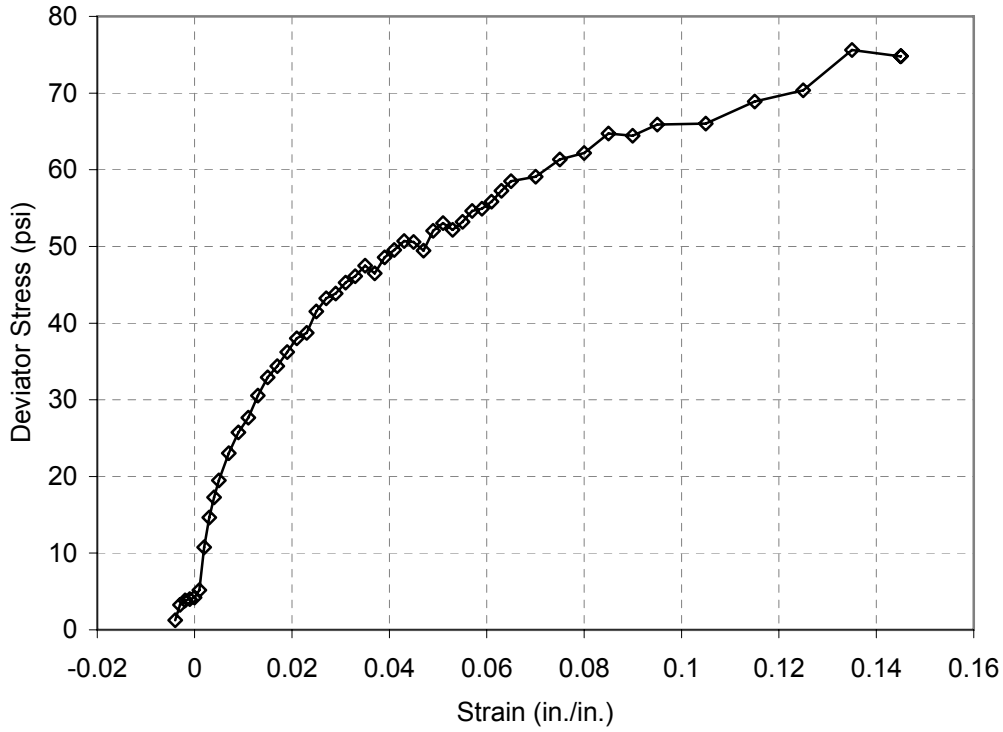

Figure A.10 Tri-axial plot 10psi cell pressure

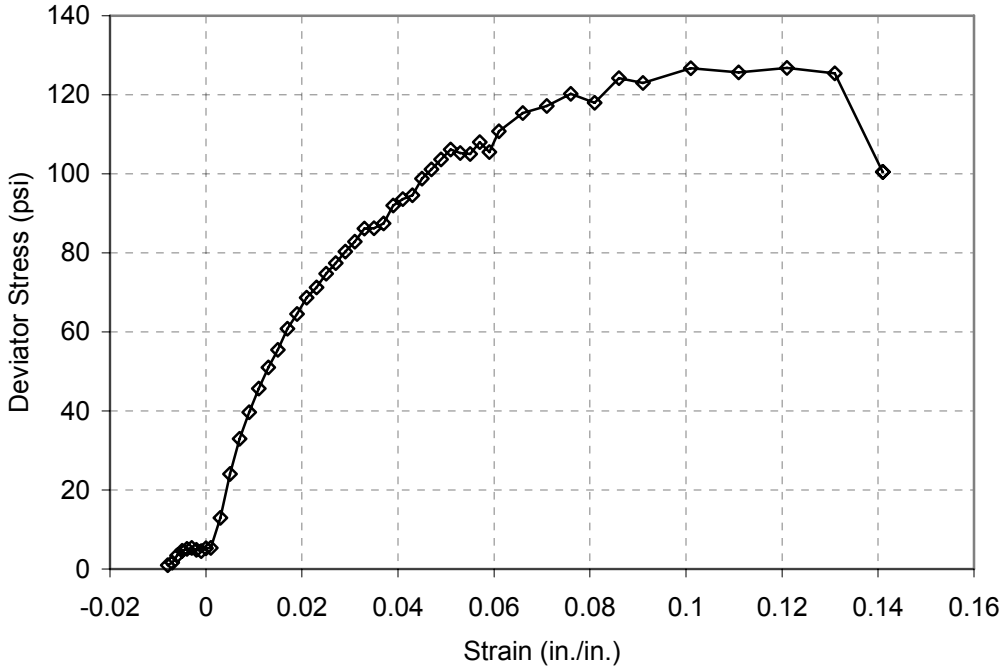

Figure A.11 Tri-axial plot 20psi cell pressure

Table A. 1 Concrete Cylinder List

RE-0446-01 ACT 230. MSEW/DEEP FOUNDATIONS INTERACTION STUDY - I-435 & LEAVENWORTH ROAD					
DATE	**SHAFTS**	**SLUMP (in.)**	**TEMP. (°F)**	**Strength (psi)**	**Date**
7/19/2007	R1	7 3/4	82	4,902	8/16/2007
7/19/2007	R1			5,888	11/8/2007
7/19/2007	R1			5,637	11/8/2007
7/20/2007	N SHAFT	7 1/2	89	0	
7/20/2007	N SHAFT			7,588	8/20/2007
7/20/2007	N SHAFT			0	
7/20/2007	S SHAFT			0	
7/20/2007	S SHAFT			7,020	8/20/2007
7/20/2007	S SHAFT			0	
7/24/2007	R2 & R5	8	86	3,562	8/20/2007
7/24/2007	R2 & R5			7,471	11/9/2007
7/24/2007	R2 & R5			7,665	11/9/2007
7/25/2007	R6	8	85	7,121	11/14/2007
7/25/2007	R6			6,779	11/28/2007
7/25/2007	R6			5,937	8/24/2007
7/25/2007	R3 & R4	8 3/4	86	6,889	11/14/2007
7/25/2007	R3 & R4			7,018	11/14/2007
7/25/2007	R3 & R4			6,227	8/24/2007

Concrete Cylinder List (cont.)

10/4/2007	C & R5	8	80	5,773	11/14/2007
10/4/2007	C & R5			5,203	11/1/2007
10/4/2007	C & R5			5,215	11/1/2007
10/4/2007	BS & R5	9	76	6,066	11/9/2007
10/4/2007	BS & R5			5,460	11/1/2007
10/4/2007	BS & R5			5,795	11/1/2007
10/4/2007	R6	8 1/2	78	5,231	11/1/2007
10/4/2007	R6			5,363	11/1/2007
10/4/2007	R6			6,016	11/9/2007
10/5/2007	BG3 & R4	8	82	6,349	11/2/2007
10/5/2007	BG3 & R4			6,554	11/14/2007
10/5/2007	BG3 & R4			6,384	11/2/2007
10/5/2007	A & D	9 1/2	80	5,619	11/2/2007
10/5/2007	A & D			6,183	11/2/2007
10/5/2007	A & D			6,501	11/8/2007
10/5/2007	R4 & BG2	10 1/4	80	5,326	11/2/2007
10/5/2007	R4 & BG2			5,633	11/2/2007
10/5/2007	R4 & BG2			6,290	11/14/2007
10/5/2007	D & R1	8 3/4	81	6,594	11/2/2007
10/5/2007	D & R1			6,947	11/8/2007
10/5/2007	D & R1			6,405	11/2/2007
10/5/2007	BG2	8 1/4	81	7,141	11/14/2007
10/5/2007	BG2			6,569	11/2/2007
10/5/2007	BG2			7,011	11/2/2007
10/9/2007	BG1 & R3	7 1/2	80	6,853	11/6/2007
10/9/2007	BG1 & R3			7,177	11/6/2007
10/9/2007	BG1 & R3			7,139	11/14/2007
10/9/2007	B & R3	10	78	7,279	11/6/2007
10/9/2007	B & R3			6,739	11/6/2007
10/9/2007	B & R3			7,521	11/8/2007
10/9/2007	R3 & R2	9	82	7,632	11/6/2007
10/9/2007	R3 & R2			7,861	11/6/2007
10/9/2007	R3 &R2			8,108	11/8/2007
10/9/2007	R2	7	81	7,380	11/6/2007
10/9/2007	R2			7,475	11/6/2007